Science Advances
AAAS

advances.sciencemag.org/cgi/content/full/5/3/eaav0316/DC1

Supplementary Materials for

Newly developed reversible MAO-B inhibitor circumvents the shortcomings of irreversible inhibitors in Alzheimer's disease

Jong-Hyun Park, Yeon Ha Ju, Ji Won Choi, Hyo Jung Song, Bo Ko Jang, Junsung Woo, Heejung Chun, Hyeon Jeong Kim, Su Jeong Shin, Oleg Yarishkin, Seonmi Jo, Mijeong Park, Seul Ki Yeon, Siwon Kim, Jeongyeon Kim, Min-Ho Nam, Ashwini M. Londhe, Jina Kim, Sung Jin Cho, Suengmok Cho, Changho Lee, Sung Yeoun Hwang, Sang Wook Kim, Soo-Jin Oh, Jeiwon Cho, Ae Nim Pae, C. Justin Lee*, Ki Duk Park*

*Corresponding author. Email: cjl@kist.re.kr (C.J.L.); kdpark@kist.re.kr (K.D.P.)

Published 20 March 2019, *Sci. Adv.* **5**, eaav0316 (2018)
DOI: 10.1126/sciadv.aav0316

This PDF file includes:

Supplementary Results

Reversibility test

To investigate the reversibility of KDS2010 MAO-B inhibition, we measured MAO-B inhibition after three separate washes. First, the inhibitory activities of 1 μM KDS2010 and 1 μM selegiline, an irreversible MAO-B inhibitor, were examined. Both compounds inhibited human MAO-B (hMAO-B) activity by over 90%. Next, an aliquot of the enzyme solution containing 1 μM of compound was washed using an effective centrifugation ultrafiltration method. After 3 repeat washes of the KDS2010 sample, 82% of the hMAO-B enzymatic activity was recovered, indicating that KDS2010 is a reversible inhibitor. However, enzymatic activity was not recovered in the assay performed with selegiline (Fig. 2E).

Mode of MAO-B inhibition of KDS2010

To examine the mode of MAO-B inhibition, substrate-dependent kinetic experiments were performed, and both the corresponding progression curves and the Lineweaver–Burk plots were generated. The Michaelis–Menten kinetic parameters, Michaelis constant (K_m) and maximal velocity (V_{max}) of hMAO-B inhibition were determined in the presence and absence of KDS2010. The Lineweaver–Burk plot for different concentration of KDS2010 was linear and intersected at the *y*-axis. Using Sigma plot®, V_{max}, K_m and inhibition constant (K_i) were calculated (V_{max} = 3.303e^{+7}, K_m = 1.02e^{-4} and K_i = 2.48e^{-9}). These results indicate that KDS2010 is a competitive MAO-B inhibitor (Figure S3).

Molecular modeling

We performed a molecular docking study to investigate the KDS2010 binding site on hMAO-B. Fig. 2G shows an overlay of the KDS2010 binding pose inside the hMAO-B protein with that of selegiline, which covalently binds to FAD. KDS2010 had a very compact binding pose with a glide score of -10.611 kcal/mol. The fluorine atom formed one halogen bond with PRO102 (Fig. 2G, middle). KDS2010 formed two hydrogen bonds with GLN206. In the hydrophobic region of the binding cavity, the central benzene ring of KDS2010 was engaged through π-sulfur interaction with CYS172 and π-π T-shaped interactions with TYR326, which is the "gating" residue in the MAO-B inhibitor binding site.

The binding mode of KDS2010 was compared to that of selegiline (Fig. 2G, right). The alkyne group of selegiline formed a covalent bond with FAD, and the phenyl group was fixed in position inside the inhibitor binding site by two π-type interactions with TYR326 and CYS172.
We also have shown 3D and 2D interactions of Selegiline, KDS2010, and KDS0014 (Fig. S5). Figures in the main article (Fig. 2) rendered by pymol software. 2D and 3D-zoomed figures of interactions were prepared using Discovery Studio 2018 Software. KDS0014 has a slightly lower docking score of -9.820 kcal/mol but has a similar interactions with KDA2010. Hydrogen bond interactions with GLN206, pi-sulfur contact with CYS172, pi-pi-static interactions with TYR326, and pi-alkyl contacts with ILE199, ILE171 are similar to KDS2010.
Overall KDS2010 possibly occupied the same binding cavity as selegiline but formed more compact reversible interactions with important residues according to the molecular modeling results.

In vitro and *in vivo* Absorption, Distribution, Metabolism and Excretion/Toxicity (ADME/Tox) studies

To determine whether KDS2010 has good drug-like properties for clinical candidate, we performed various *in vitro* and *in vivo* ADME/Tox tests. First, KDS2010 showed favorable metabolic stabilities against 4 selected liver microsomal enzymes (human, dog, rat, and mouse), with 92%, 61%, 60% and 66% of the parent compound remaining after 30 min of incubation, respectively. Plasma stabilities of KDS2010 in both human and rat were also excellent, with 98% and 95% of the parent compound remaining after 120 min of incubation, respectively (table S2). In the CYP inhibition test, the KDS2010 IC_{50} values against 5 tested isotypes (1A2, 2C9, 2C19, 2D6, and 3A4) were over 10 μM, indicating that KDS2010 is not likely to cause adverse effects by means of drug-drug interactions (table S2). In the *in vivo* toxicity studies, no significant toxicities were observed after oral administration of either a single dose tested up to 1,000 mg/kg body weight or 14 consecutive doses tested up to 200 mg/kg/day. Therefore, the No Observed Adverse Effect Level (NOAEL) for KDS 2010 was > 1,000 mg/kg and > 200 mg/kg/day for single dose and 14-day repeated doses, respectively (table S2). In addition, in a hERG channel binding assay, KDS2010 exerted low inhibitory effects against hERG, an important cardiac ion channel, indicating that it is unlikely to cause human cardiotoxicity.

In vivo Pharmacokinetics/Blood-Brain Barrier (PK/BBB) study

We investigated *in vivo* PK of KDS2010 and observed an excellent PK profile with a favorable half-life ($t_{1/2}$ = 3.3±0.2 h), high drug exposure in the blood after oral administration (C_{max} = 952.1±80.3), and excellent bioavailability (F = 123%). The total drug concentration in the brain 2 h after oral administration (10 mg/kg body weight) was very high (6,716.3±260.6 ng/g) and the brain-to-plasma total drug concentration ratio (brain total drug concentration/plasm total drug concentration, B/P; 2h after oral administration) was 9.2, indicating that KDS2010 is a suitable CNS drug (table S3).

Supplementary Materials and Methods

Kinetic studies of MAO-B inhibition

To examine the interaction mode of KDS2010, the type of enzyme inhibition was determined by using Michaelis-Menten kinetic experiments. The detailed MAO-B enzyme assay is described in the online methods. Briefly, the catalytic rates of human MAO-B enzyme were measured at six different concentrations of the benzylamine substrate (0.063, 0.125, 0.25, 0.5, 1 and 2 mM) in the absence or in the presence of four different concentrations of KDS2010 (0.1, 0.3, 1, 3 and 10 nM). The corresponding progression curves and the Lineweaver-Burk plots were generated using Sigma plot®. In addition, the maximal velocity (V_{max}), Michaelis constant (K_m) and inhibition constant (K_i) were calculated.

Pharmacokinetic study

Rats (Sprague-Dawlery) were purchased from Koatech (Korea), and maintained in a specific pathogen-free facility (Laboratory Animal Center, Daegu-Gyeongbuk Medical Innovation Foundation, Korea). Rats (250-300 g) at 7-week of age were fasted for 16 h and used in the pharmacokinetic experiments. Control blood was collected from the jugular vein prior to KDS2010 administration. For oral administration, four rats were treated with a suspension of KDS2010 in 10% DMSO, 15% water, and 75% PEG400 at a dose of 10 mg/kg via oral gavage. For intravenous administration, KDS2010 was injected at a dose of 1 mg/kg via the caudal vein. Dosing volume of KDS2010 was 600 μL for oral and 200 μL for intravenous administration. Blood from the jugular vein was collected in heparinized tubes at 0.08, 0.25, 0.5, 1, 2, 4, 6 and 8 h after compound administration. The plasma was isolated from the blood samples by centrifugation at 12,000 rpm for 15 min. Then, 20 μL of plasma was mixed with 80 μL of acetonitrile (Sigma) containing internal standard and centrifuged at 14,000 rpm for 5 min. The plasma supernatants were collected and loaded into triple quadrupole LC-MS/MS (Triple Quad 5500, Applied Biosystems) to measure the KDS2010 serum concentration. The standard curve range was 5 to 1000 ng/mL and the lower limit of quantification of measurements was 5 ng/mL. Pharmacokinetic parameters were analyzed by non-compartmental analysis using Phoenix WinNolin version 6.4 (Pharsight).

To determine the brain-to-plasma ratio (B/P), brains obtained from rats 2 h after oral administration (10 mg/kg) were washed three times with PBS to remove blood and homogenized in 4 volumes per brain weight of PBS. In total, 20 μL of brain homogenate was added to 80 μL acetonitrile and the mixture was centrifuged at 14,000 rpm for 5 min. The supernatant was analyzed using the method described above to determine the brain KDS2010 concentration.

***In vivo* toxicity**

In vivo toxicity studies were performed by Medicilon (Medicilon Preclincal Research LLC.). For single dose tests, the rats (Sprague Dawley, *n*=10/group) were administered KDS2010 at 250, 500, 1000 or 2000 mg/kg via oral gavage and changes in mortality, body weight, and food consumption were monitored for 14 days. For the repeated dose test, the rats (*n*=20/group) were given KDS2010 at 50, 100 and 200 mg/kg/day for 14 consecutive days via oral gavage and sacrificed on day 15th for pathological assessments. The volume for each administration was 10 mL/kg/day.

***In vitro* assays for CYP inhibition**

The luminescence assay using the P450-Glo screening systems (Promega) was used to determine is KDS2010 inhibits CYP. The luminogenic inhibition assays were performed following the protocols from Promega Corp. (Technical Bulletin, P450-Glo Assays, Promega Corp., 2009). Briefly, a CYP enzyme and an appropriate substrate were combined in potassium phosphate (KPO_4) buffer (100 mM, pH 7.4) with or without KDS2010, and the reaction was initiated by adding an NADPH regenerating system (containing $NADP^+$, glucose-6-phosphate, magnesium chloride ($MgCl_2$) and glucose-6-phosphate dehydrogenase). After incubation at 37 °C for 10-30 min (different incubation time depending on the isotype), the reconstituted luciferin detection reagent was added to stop the reaction and produce the luminescent signal. After 20 min of incubation to stabilize the signal, luminescence was detected using microplate reader (SpectraMax®i3, Molecular Devices) and the values were reported as relative light unit (RLU).

Assessment of metabolic stability

To assess the stability of KDS2010 against human liver microsomes, reaction mixture (120 μL) consisting of 1 μM KDS2010, human liver microsomal fractions (0.5 mg/mL,

Corning®UltraPool™ HLM150), NADPH-regenerating system (10 mM glucose-6-phosphate, 0.2 U/ml glucose-6-phosphate dehydrogenase and 9.2 mM $MgCl_2$), and 100 mM potassium phosphate (pH 7.4) was pre-incubated for 5 min at 37 °C. The reaction was initiated by addition of NADPH (1.2 mM). At 0 and 30 min, samples (50 μL) were taken from the reaction mixture, combined with acetonitrile (50 μL), and centrifuged at 10,000×g for 10 min. The supernatants were analyzed by LC/MS/MS to detect the remaining KDS2010.

To assess the stability of KDS2010 against plasma enzymes, human plasma (198 μL Sigma-Aldrich) was pre-incubated for 5 min at 37 °C and then 2 μL of KDS2010 (100 μM, final concentration 1 μM) was added. At 0, 15 and 30 min, samples (50 μL) were taken from the reaction mixture, combined with acetonitrile (50 μL), and centrifuged at 10,000×g for 5 min. The supernatants were analyzed by LC/MS/MS to detect the remaining KDS2010. The percentage of the parent compound remaining was calculated by comparing peak areas.

hERG channel inhibition assay

hERG channel binding assay was performed using predictor hERG fluorescence polarization assay (#PV5365, Invitrogen) according to the manufacturer's instructions. Briefly, KDS2010 was serially diluted (16 points, 3−fold) and incubated with the reaction mixture containing hERG membrane, fluorescence tracer red dye and fluorescence polarization buffer for 4 h at 25 °C. Fluorescence (Excitation at 530 nm, Emission at 590 nm) was measured using a multi-mode microplate reader (Synergy Neo, Biotek). E-4031 was used as a positive standard (IC_{50} = 10-90 nM).

General Synthetic Method

Melting points were determined in open capillary tubes using a Standford Research Systems melting point apparatus and were uncorrected. Reactions progression was checked using analytical thin-layer chromatography (TLC) plates (#1.05715, Merck) and analyzed with 254 nm and 365 nm ultraviolet light. The reaction mixtures were purified by flash column chromatography using silica gel (#1.09385, Merck). Nuclear magnetic resonance (NMR) spectral data were obtained at either 300 MHz (^1H) or 400 MHz (^1H) and at75 MHz (^{13}C) or 100 MHz (^{13}C) using a BRUKER apparatus. Chemical shifts (δ) were expressed in parts per million (ppm) from Tetramethylsilane (TMS), the internal standard and coupling constants (J) were expressed

in hertz and assigned as follows: s, singlet; d, doublet; t, triplet; q, quartet; AB_q, AB quartet; br, broad. All chemical reagents and solvents were of reagent grade, used without further purification and were purchased from commercial sources. Low-resolution mass spectrometry was performed on a liquid chromatograph mass spectrometer (SHIMADZU Excellence in Science, LCMS-2020). Analytical HPLC was performed using a Waters E2695 system equipped with a SHISEIDO capcell pak C_{18} MG II column (4.6 mm × 150 mm; 5 μm). HPLC data were recorded using the following parameters: 1% acetic acid in H_2O/MeCN, 90/10 → 0/100 in 10 min, +10 min isocratic hold, flow rate of 1.0 mL/min, λ = 254 and 280 nm. Compounds were checked by using TLC, ^1H and ^{13}C NMR and LR-MS. The TLC, NMR, and the analytical data confirmed that the purity of the products was ≥ 95%.

General procedure for the aldehyde compounds (2a–2k) (Method A)

A mixture of 4-bromobenzaldehyde, the desired quantitiy of arylboronic acid (**1a–1k**) (1.3 equiv), tetrakis(triphenylphosphine)palladium(0) (4-8 mol%), and Na_2CO_3 (4.86 equiv) in degassed toluene/H_2O (7/3) was refluxed for 18 h. The reaction mixture was filtered through celite and concentrated *in vacuo*. The resulting residue was dissolved in EtOAc (200 mL), and washed with H_2O (2 × 200 mL). The organic layer was dried with anhydrous Na_2SO_4 and concentrated *in vacuo*. The residue was purified by using column chromatography on silica gel.

General procedure for the free amine compounds (3a–3k) (Method B)

To a solution of L-alaninamide hydrochloride (1.2 equiv, > 95% optical purity) in anhydrous methanol, triethylamine (TEA, 1.5 equiv) was added, and then the desired biphenyl aldehyde (**2a**–**2k**) was added at room temperature. After 2-5 h, the reaction mixture was concentrated *in vacuo*. The residue was dissolved in EtOAc and washed with brine. The organic layer was dried over anhydrous Na_2SO_4, and then sodium cyanoborohydride (4-6 equiv) was added to the reaction mixture at 0°C. The reaction mixture was stirred at room temperature (18 h) and further concentrated *in vacuo*. The residue was dissolved in EtOAc (150 mL) and washed with brine (2 × 150 mL). The organic layer was dried over anhydrous Na_2SO_4 and concentrated *in vacuo*. The residue was purified by using column chromatography on Silica gel.

General procedure for the final KDS compounds (Method C)

Methanesulfonic acid (1.00-1.25 equiv) was added to a solution of amine **3a–3k** (1 equiv) in EtOAc at 50-55°C. After 1 h, the reaction mixture was cooled to room temperature, filtered *in vacuo* and washed with EtOAc. The filter cake was dried, yielding the desired compounds without further purification.

2'-Fluoro-[1,1'-biphenyl]-4-carbaldehyde (2a)

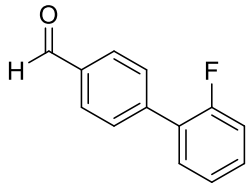

Using Method A, 4-bromobenzaldehyde (1.00 g, 5.40 mmol), 2-fluorophenylboronic acid (**1a**) (0.97 g, 6.92 mmol), tetrakis(triphenylphosphine)palladium(0) (0.25 g, 0.216 mmol) and Na_2CO_3 (2.78 g, 26.3 mmol) in toluene/H_2O (50 mL/7.2 mL) gave **2a** as a white solid (0.26 g, 24%); R_f = 0.65 (n-Hexane/EtOAc 9/1); mp 43–45 °C; ^{1}H NMR (300 MHz, DMSO–d_6) δ 10.07 (s, C(O)**H**), 7.98-8.06 (m, 2Ar**H**), 7.79 (dd, J = 1.6, 8.2 Hz, 2Ar**H**), 7.62 (td, J = 1.7, 7.9 Hz, 1Ar**H**), 7.49–7.55 (m, 1Ar**H**), 7.44–7.49 (m, 2Ar**H**); ^{13}C NMR (100 MHz, $CDCl_3$) δ 191.9 (**C**(O)H), 159. 8 (d, $J_{C–F}$ = 247.7 Hz), 142.0, 135.4, 130.7 (d, $J_{C–F}$ = 14.4 Hz), 130.2 (d, $J_{C–F}$ = 8.3 Hz), 129.8, 129.7 (d, $J_{C–F}$ = 7.5 Hz), 127.8 (q, $J_{C–F}$ = 13.1 Hz), 124.6, 116.3 (d, $J_{C–F}$ = 20.8 Hz) (Ar**C**).

3'-Fluoro-[1,1'-biphenyl]-4-carbaldehyde (2b)

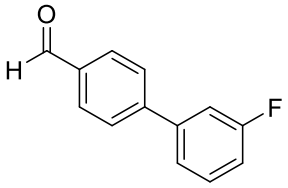

Using Method A, 4-bromobenzaldehyde (2.98 g, 16.09 mmol), 3-fluorophenylboronic acid (**1b**) (3.91 g, 20.60 mmol), tetrakis(triphenylphosphine)palladium(0) (0.74 g, 0.64 mmol) and Na_2CO_3 (8.29 g, 78.2 mmol) in toluene/H_2O (148.9 mL/21.4 mL) gave **2b** as a white solid (2.64 g, 82%); R_f = 0.30 (n-Hexane/EtOAc 15/1); mp 33–35 °C; ^{1}H NMR (400 MHz, DMSO–d_6) δ 10.07 (s, C(O)**H**), 8.01 (d, J = 8.3 Hz, 2Ar**H**), 7.96 (d, J = 8.3 Hz, 2Ar**H**), 7.63–7.67 (m, 2Ar**H**), 7.54–7.59 (m, 1Ar**H**), 7.27–7.31 (m, 1Ar**H**); ^{13}C NMR (75 MHz, DMSO–d_6) 193.0 (**C**(O)H), 163.1 (d, $J_{C–F}$ = 242.4 Hz, **C**F), 144.8 (d, $J_{C–F}$ = 2.2 Hz), 141.6 (d, $J_{C–F}$ = 7.9 Hz), 135.9, 131.4 (d, $J_{C–F}$ =

8.4 Hz), 130.5, 127.9, 123.6 (d, $J_{C–F}$ = 2.6 Hz), 115.7 (d, $J_{C–F}$ = 20.9 Hz), 114.3 (d, $J_{C–F}$ = 22.3 Hz) (Ar**C**).

4'-Fluoro-[1,1'-biphenyl]-4-carbaldehyde (2c)

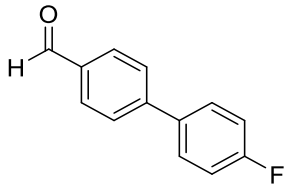

Using Method A, 4-bromobenzaldehyde (1.50 g, 8.11 mmol), 4-fluorophenylboronic acid (**1c**) (1.45 g, 10.38 mmol), tetrakis(triphenylphosphine)palladium(0) (0.75 g, 0.65 mmol) and Na_2CO_3 (4.18 g, 39.40 mmol) in toluene/H_2O (75 mL/10.8 mL) gave **2c** as a white soild (1.51 g, 93%); R_f = 0.25 (n-Hexane/EtOAc 10/1); mp 79–80 °C; ^{1}H NMR (400 MHz, DMSO–d_6) δ 10.05 (s, C(O)**H**), 7.99 (d, J = 8.1 Hz, 2Ar**H**), 7.90 (d, J = 8.1 Hz, 2Ar**H**), 7.84 (d, J = 5.7 Hz, 2Ar**H**), 7.81 (d, J = 5.7 Hz, 2Ar**H**), 7.32–7.37 (m, 2Ar**H**); ^{13}C NMR (75 MHz, $CDCl_3$) δ 191.8 (**C**(O)H), 163.2 (d, $J_{C–F}$ = 246.9 Hz, **C**F), 146.1, 135.9 (d, $J_{C–F}$ = 3.3 Hz), 135.2, 130.3, 129.1 (d, $J_{C–F}$ = 8.2 Hz), 127.5, 116.0 (d, $J_{C–F}$ = 86.1 Hz) (Ar**C**).

2'-Chloro-[1,1'-biphenyl]-4-carbaldehyde (2d)

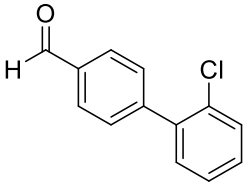

Using method A, , 4-bromobenzaldehyde (3.00 g, 16.21 mmol), 2-chlorophenylboronic acid (**1d**) (3.25 g, 20.75 mmol), tetrakis(triphenylphosphine)palladium(0) (0.75 g, 0.65 mmol) and Na_2CO_3 (8.35 g, 78.8 mmol) in toluene/H_2O (150 mL/21.6 mL) gave **2d** as a white soild (0.39 g, 11%); R_f = 0.20 (n-Hexane/EtOAc 5/1); mp 71–72 °C; ^{1}H NMR (300 MHz, DMSO–d_6) δ 10.08 (s, C(O)**H**), 8.00 (d, J = 7.9 Hz, 2Ar**H**), 7.67 (d, J = 7.9 Hz, 2Ar**H**), 7.58–7.64 (m, 1Ar**H**), 7.44–7.52 (m, 3Ar**H**); ^{13}C NMR (75 MHz, DMSO–d_6) δ 193.1 (**C**(O)H), 145.0, 139.2, 135.8, 131.6, 130.6, 130.5, 1300.4, 129.8, 128.1 (Ar**C**).

3'-Chloro-[1,1'-biphenyl]-4-carbaldehyde (2e)

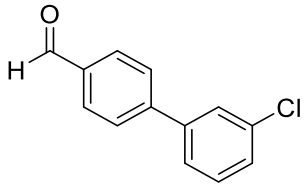

Using Method A, 4-bromobenzaldehyde (0.50 g, 2.7 mmol), 3-chlorophenylboronic acid (**1e**) (0.52 g, 3.24 mmol), tetrakis(triphenylphosphine)palladium(0) (0.12 g, 0.11 mmol) and Na_2CO_3 (1.39 g, 13.13 mmol) in toluene/H_2O (25 mL/3.6 mL) gave **2e** as a white soild (0.49 g, 84%); R_f = 0.25 (n-Hexane/EtOAc 9/1); mp 49–51 °C; ^{1}H NMR (400 MHz, DMSO–d_6) δ 10.07 (s, C(O)**H**), 8.02 (d, J = 8.2 Hz, 2Ar**H**), 7.96 (d, J = 8.2 Hz, 2Ar**H**), 7.85 (s, 1Ar**H**), 7.75 (d, J = 7.3 Hz, 1Ar**H**), 7.57–7.50 (m, 2Ar**H**); ^{13}C NMR (400 MHz, DMSO–d_6) δ 193.1 (**C**(O)H), 144.6, 141.4, 136.0, 134.4, 131.3, 131.3, 130.6, 128.8, 128.0, 127.4, 127.3, 126.3 (Ar**C**).

4'-Chloro-[1,1'-biphenyl]-4-carbaldehyde (2f)

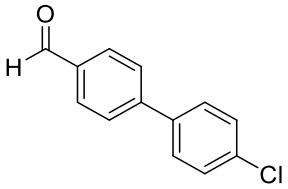

Using Method A, 4-bromobenzaldehyde (3.00 g, 16.21 mmol), 4-chlorophenylboronic acid (**1f**) (3.25 g, 20.75 mmol), tetrakis(triphenylphosphine)palladium(0) (0.75 g, 0.65 mmol) and Na_2CO_3 (8.35 g, 78.8 mmol) in toluene/H_2O (150 mL/21.6 mL) gave **2f** as a white soild (2.73 g, 78%); R_f = 0.35 (n-Hexane/EtOAc 10/1); mp 142–145 °C; ^{1}H NMR (300 MHz, DMSO–d$_6$) δ 10.06 (s, C(O)**H**), 8.01 (d, J = 8.2 Hz, 2Ar**H**), 7.92 (d, J = 8.2 Hz, 2Ar**H**), 7.81 (d, J = 8.5 Hz, 2Ar**H**), 7.56 (d, J = 8.5 Hz, 2Ar**H**); ^{13}C NMR (75 MHz, $CDCl_3$) δ 191.7 (**C**(O)H), 145.8, 138.2, 135.5, 134.8, 130.3, 129.2, 129.1, 128.6, 128.3, 127.9, 127.5 (Ar**C**).

2'-(Trifluoromethyl)-[1,1'-biphenyl]-4-carbaldehyde (2g)

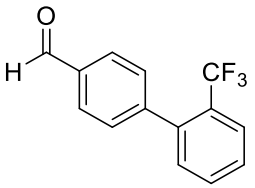

Using Method A, 4-bromobenzaldehyde (3.00 g, 16.22 mmol), 2-(trifluoromethyl) phenylboronic acid (**1g**) (3.94 g, 20.76 mmol), tetrakis(triphenylphosphine)palladium(0) (0.76 g, 0.64 mmol) and Na_2CO_3 (8.36 g, 78.8 mmol) in toluene/H_2O (150 mL/21.6 mL) gave **2g** as a white solid (0.40 g, 10%); R_f = 0.25 (n-Hexane/EtOAc 15/1); mp 77–80 °C; ^{1}H NMR (300 MHz, $CDCl_3$) δ 10.08 (s, C(O)**H**), 7.93 (d, J = 8.3 Hz, 2Ar**H**), 7.78 (d, J = 7.9 Hz, 2Ar**H**), 7.46–7.65 (m, 4Ar**H**), 7.33 (d, J = 7.32 Hz, 1Ar**H**); ^{13}C NMR (75 MHz, DMSO–d_6) δ 193.3 (**C**(O)H), 145.7, 139.9, 136.0, 132.9, 132.2, 130.1, 129.5, 129.1, 127.2 (q, $J_{C–F}$ = 29.4 Hz), 126.7 (q, $J_{C–F}$ = 5.2 Hz), 124.5 (q, $J_{C–F}$ = 272.2 Hz) (Ar**C**).

3'-(Trifluoromethyl)-[1,1'-biphenyl]-4-carbaldehyde (2h)

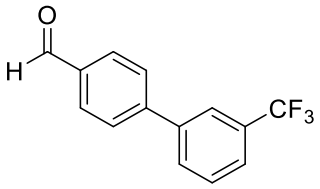

Using Method A, 4-bromobenzaldehyde (0.50 g, 2.70 mmol), 3-(trifluoromethyl) phenylboronic acid (**1h**) (0.67 g, 3.51 mmol), tetrakis(triphenylphosphine)palladium(0) (0.13 g, 0.11 mmol) and Na_2CO_3 (1.43 g, 13.51 mmol) in toluene/H_2O (25 mL/3.6 mL) gave **2h** as a colorless oil (0.61 g, 97%); R_f = 0.20 (n-Hexane/EtOAc 15/1); ^{1}H NMR (400 MHz, DMSO–d_6) δ 10.10 (s, C(O)**H**), 8.00–8.10 (m, 6Ar**H**), 7.73–7.82 (m, 2Ar**H**); ^{13}C NMR (75 MHz, $CDCl_3$) δ 191.8 (**C**(O)H), 145.6, 130.6, 135.8, 131.5 (q, $J_{C–F}$ = 32.2 Hz), 130.7, 130.4, 129.6, 127.9, 125.1 (q, $J_{C–F}$ = 3.8 Hz), 124.2 (q, $J_{C–F}$ = 3.7 Hz), 124.0 (q, $J_{C–F}$ = 270.6 Hz) (Ar**C**).

4'-(Trifluoromethyl)-[1,1'-biphenyl]-4-carbaldehyde (2i)

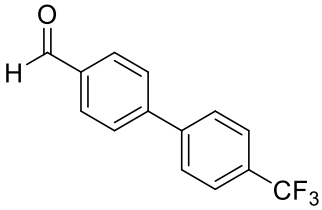

Using Method A, 4-bromobenzaldehyde (1.50 g, 8.11 mmol), 3-(trifluoromethyl) phenylboronic acid (**1i**) (1.97 g, 10.38 mmol), tetrakis(triphenylphosphine)palladium(0) (0.38 g, 0.32 mmol) and Na_2CO_3 (4.18 g, 39.4 mmol) in toluene/H_2O (75 mL/10.8 mL) gave **2i** as a white solid (1.17 g, 58%); R_f = 0.30 (Hexane/EtOAc 10/1); mp 73–74 °C; ^{1}H NMR (300 MHz, $CDCl_3$) δ 10.09 (s,

C(O)**H**), 7.97–8.01 (m, 2Ar**H**), 7.74–7.77 (m, 6Ar**H**); ^{13}C NMR (75 MHz, $CDCl_3$) δ 193.2 (**C**(O)H), 144.6, 143.3, 136.2, 130.7, 129.2 (q, $J_{C–F}$ = 31.7 Hz), 128.4, 128.3, 126.4 (q, $J_{C–F}$ = 3.8 Hz), 124.6 (q, $J_{C–F}$ = 264.0 Hz) (Ar**C**).

3'-(Trifluoromethoxy)-[1,1'-biphenyl]-4-carbaldehyde (2j)

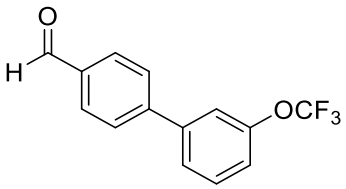

Using Method A, 4-bromobenzaldehyde (2.00 g, 10.8 mmol), 3-(trifluoromethoxy) phenylboronic acid (**1j**) (2.85 g, 13.8 mmol), tetrakis(triphenylphosphine)palladium(0) (0.5 g, 0.43 mmol) and Na_2CO_3 (5.57 g, 52.5 mmol) in toluene/H_2O (100 mL/14.4 mL) gave **2j** as a colorless oil (2.15 g, 75%); R_f = 0.35 (n-Hexane/EtOAc 10/1); ^{1}H NMR (300 MHz, DMSO–d_6) δ 10.08 (s, C(O)**H**), 8.02 (dd, J = 1.9, 6.6 Hz, 2Ar**H**), 7.97 (dd, J = 1.9, 6.6 Hz, 2Ar**H**), 7.81–7.86 (m, 1Ar**H**), 7.76 (s, 1Ar**H**), 7.66 (t, J = 8.0 Hz, 1Ar**H**), 7.42–7.50 (m, 1Ar**H**); ^{13}C NMR (75 MHz, $CDCl_3$) δ 191.8 (**C**(O)H), 149.8 (**C**OCF_3), 145.5, 141.9, 135.8, 130.4, 130.3, 128.7, 125.7, 120.7, 120.5 (q, $J_{C–F}$ = 256.0 Hz), 120.0 (Ar**C**).

4'-(Trifluoromethoxy)-[1,1'-biphenyl]-4-carbaldehyde (2k)

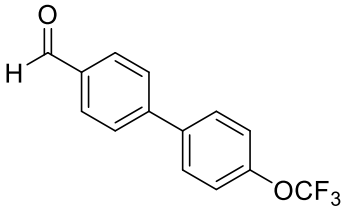

Using Method A, 4-bromobenzaldehyde (0.50 g, 2.70 mmol), 3-methoxyphenylboronic acid (**1k**) (0.71 g, 3.46 mmol), tetrakis(triphenylphosphine)palladium(0) (0.13 g, 0.108 mmol) and Na_2CO_3 (1.39 g, 13.1 mmol) in toluene/H_2O (25 mL/3.6 mL) gave **2k** as a white solid (0.71 g, 98%); R_f = 0.65 (n-Hexane/EtOAc 9/1); mp 31–33 °C; ^{1}H NMR (300 MHz, DMSO–d_6) δ 10.07 (s, C(O)**H**), 7.96–8.05 (m, 2Ar**H**), 7.88–7.95 (m, 4Ar**H**), 7.51 (d, J = 8.0 Hz, 2Ar**H**); ^{13}C NMR (75 MHz, $CDCl_3$) δ 191.7 (**C**(O)H), 149.5266, 145.7, 138.4, 135.5, 130.3, 128.8, 127.7, 121.4, 120.5 (q, $J_{C–F}$ = 256.1 Hz) (Ar**C**).

(*S*)-2-(((2'-Fluoro-[1,1'-biphenyl]-4-yl)methyl)amino)propanamide (3a)

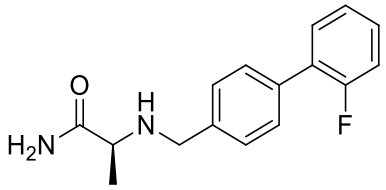

Using method B, L-alaninamide hydrochloride (0.19 g, 1.52 mmol), triethylamine (0.21 mL, 1.52 mmol) **2a** (0.25 g, 1.27 mmol) and sodium cyanoborohydride (0.13 g, 1.90 mmol) in MeOH (1.3 mL) gave **3a** as a white solid (0.21 g, 62%); R_f = 0.10 (EtOAc); mp 133–136 °C; ^{1}H NMR (300 MHz, DMSO–d_6) δ 7.26–7.58 (m, 8Ar**H,** C(O)N**H**H'), 7.01 (br s, C(O)NH**H'**), 3.59 and 3.74 (AB_q, J = 13.7 Hz, C$\mathbf{H}_2$), 3.03 (q, J = 6.8 Hz, C**H**), 2.43 (br s, N**H**), 1.15 (d, J = 6.8 Hz, C$\mathbf{H}_3$); ^{13}C NMR (75 MHz, $CDCl_3$) δ 178.1 (**C**(O)), 159.8 (d, $J_{C–F}$ = 246.1 Hz), 139.0, 134.9, 130.7 (d, $J_{C–F}$ = 3.5 Hz), 129.2 (d, $J_{C–F}$ = 2.8 Hz), 128.8 (d, $J_{C–F}$ = 8.2 Hz), 128.1, 124.4 (d, $J_{C–F}$ = 3.7 Hz), 116.1 (d, $J_{C–F}$ = 22.6 Hz) (Ar**C**), 57.8 (**C**H), 52.2 (**C**H_2), 19.7 (**C**H_3).

(*S*)-2-(((3'-Fluoro-[1,1'-biphenyl]-4-yl)methyl)amino)propanamide (3b)

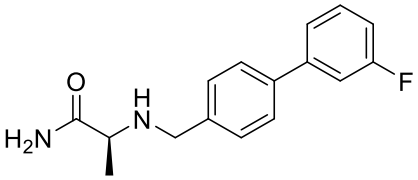

Using method B, L-alaninamide hydrochloride (0.58 g, 4.63 mmol), triethylamine (0.81 mL, 5.78 mmol), **2b** (0.77 g, 3.85 mmol) in MeOH (4.19 mL), and sodium cyanoborohydride (0.38 g, 5.78 mmol) in MeOH (3.85 mL) gave **3b** as a white solid (0.48 g, 45%); R_f = 0.20 (EtOAc); mp 128–130 °C; ^{1}H NMR (300 MHz, DMSO–d_6) δ 7.65 (d, J = 8.12 Hz, 2Ar**H**), 7.48–7.52 (m, 3Ar**H**), 7.43 (d, J = 8.2 Hz, 2Ar**H**), 7.34 (br s, C(O)N**H**H'), 7.14–7.21(m, 1Ar**H**), 6.99 (br s, C(O)NH**H'**), 3.59 and 3.73 (AB_q, J = 13.7 Hz, C$\mathbf{H}_2$), 3.03 (q, J = 6.9 Hz, C**H**), 2.43 (br s, N**H**), 1.15 (d, J = 6.87 Hz, C$\mathbf{H}_3$); ^{13}C NMR (75 MHz, $CDCl_3$) δ 178.1 (**C**(O)), 163.2 (d, $J_{C–F}$ = 244.0 Hz), 143.1 (d, $J_{C–F}$ = 7.6 Hz), 139.3, 139.0 (d, $J_{C–F}$ = 2.2 Hz), 130.3 (d, $J_{C–F}$ = 8.3 Hz), 128.6, 127.3, 122.7 (d, $J_{C–F}$ = 2.7 Hz), 114.1 (d, $J_{C–F}$ = 21.0 Hz), 113.9 (d, $J_{C–F}$ = 21.9 Hz) (Ar**C**), 57.7 (**C**H), 52.2 (**C**H_2), 19.7 (**C**H_3).

(*S*)-2-(((4'-Fluoro-[1,1'-biphenyl]-4-yl)methyl)amino)propanamide (3c)

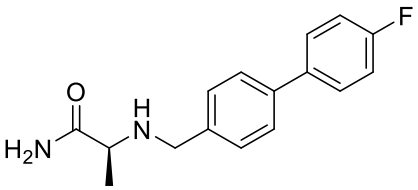

Using method B, L-alaninamide hydrochloride (0.37 g, 3.0 mmol), triethylamine (1.04 mL, 7.49 mmol), **2c** (0.50 g, 2.50 mmol) in MeOH (2.71 mL), and sodium cyanoborohydride (0.28 g, 3.75 mmol) in MeOH (2.50 mL) gave **3c** as a white solid (0.35 g, 51%); R_f = 0.20 (EtOAc); mp 129–133 °C; ^{1}H NMR (300 MHz, DMSO–d_6) δ 7.65–7.72 (m, 2Ar**H**), 7.58 (d, J = 8.2 Hz, 2Ar**H**), 7.35 (br s, C(O)N**H**H'), 7.24–7.31(m, 2Ar**H**), 6.99 (br s, C(O)NH**H'**), 3.58 and 3.72 (AB_q, J = 13.7 Hz, C**H**$_2$), 3.03 (q, J = 6.9 Hz, C**H** 1.15 (d, J = 6.9 Hz, C**H**$_3$), the remaining peak was not detected and is believed to overlap with H_2O signals; ^{13}C NMR (100 MHz, DMSO–d_6) δ 177.4 (**C**(O)), 162.2 (d, $J_{C–F}$ = 181.9 Hz), 140.4, 138.0, 137.0 (d, $J_{C–F}$ = 2.3 Hz), 129.0, 126.9 (d, $J_{C–F}$ = 5.2 Hz), 116.2 (Ar**C**), 56.9 (**C**H), 51.1 (**C**H$_2$), 19.8 (**C**H$_3$), the remaining aromatic peak was not detected.

(*S*)-2-(((2'-Chloro-[1,1'-biphenyl]-4-yl)methyl)amino)propanamide (3d)

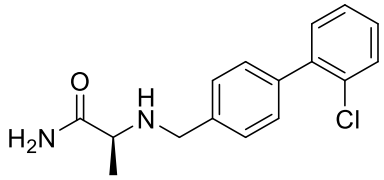

Using method B, L-alaninamide hydrochloride (0.16 g, 1.44 mmol), triethylamine (0.25 mL, 3.53 mmol), **2d** (0.26 g, 1.20 mmol) in MeOH (1.30 mL), and sodium cyanoborohydride (0.32 g, 4.80 mmol) in MeOH (1.20 mL) gave **3d** as a white solid 0.16 g, 47%); R_f = 0.15 (EtOAc); mp 91–94 °C; ^{1}H NMR (300 MHz, DMSO–d_6) δ 7.53–7.58 (m, 1Ar**H**), 7.30–7.48 (m, 7ArH, C(O)N**H**H'), 6.98 (br s, C(O)NH**H'**), 3.60 and 3.74 (AB_q, J = 13.6 Hz, C**H**$_2$), 3.06 (q, J = 6.8 Hz, C**H**), 2.44 (br s, N**H**), 1.17 (d, J = 6.8 Hz, C**H**$_3$); ^{13}C NMR (75 MHz, DMSO–d_6) δ 177.4 (**C**(O)), 140.7, 140.2, 137.5, 132.0, 131.8, 130.3, 129.5, 129.4, 128.2, 128.0 (Ar**C**), 57.1 (**C**H), 51.2 (**C**H$_2$), 19.9 (**C**H$_3$).

(*S*)-2-(((3'-Chloro-[1,1'-biphenyl]-4-yl)methyl)amino)propanamide (3e)

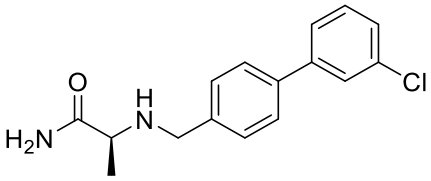

Using method B, L-alaninamide hydrochloride (0.21 g, 1.66 mmol), triethylamine (0.23 mL, 1.66 mmol), **2e** (0.30 g, 1.38 mmol), and sodium cyanoborohydride (0.13 g, 2.08 mmol) in MeOH (1.36 mL) gave **3e** as a white solid (0.22 mg, 54%); R_f = 0.10 (EtOAc); mp 121–123 °C; ^{1}H NMR (400 MHz, DMSO–d_6) δ 7.70 (s, 1Ar**H**), 7.62–7.65 (m, 3Ar**H**), 7.48 (t, J = 7.8 Hz, 1Ar**H**), 7.40–7.48 (m, 3Ar**H**), 7.34 (br s, C(O)N**H**H'), 6.99 (br s, C(O)NH**H'**), 3.59 and 3.74 (AB_q, J = 13.7 Hz, C**H**$_2$), 3.03 (q, J = 6.7 Hz, C**H**), 2.44 (br s, N**H**), 1.15 (d, J = 6.8 Hz, C**H**$_3$); ^{13}C NMR (75 MHz, DMSO–d$_6$) δ 177.4 (**C**(O)), 142.7, 141.1, 137.4, 134.2, 131.2, 129.0, 127.5, 127.0, 126.7, 125.7 (Ar**C**), 57.0(**C**H), 51.1(**C**H$_2$), 19.8 (**C**H$_3$).

(*S*)-2-(((4'-Chloro-[1,1'-biphenyl]-4-yl)methyl)amino)propanamide(3f)

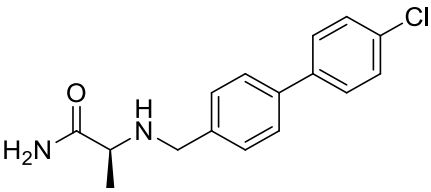

Using method B, L-alaninamide hydrochloride (0.35 g, 3.00 mmol), triethylamine (0.97 mL, 6.92 mmol), **2f** (0.50 g, 2.31 mmol) in MeOH (2.51 mL), and sodium cyanoborohydride (0.23 g, 3.46 mmol) in MeOH (2.31 mL) gave **3f** as a white solid (386 mg, 58%); R_f = 0.15 (EtOAc); mp 166–164 °C; ^{1}H NMR (300 MHz, DMSO–d_6) δ 7.66–7.70 (m, 2Ar**H**), 7.61 (d, J = 8.2 Hz, 2Ar**H**), 7.49–7.53 (m, 2Ar**H**), 7.42 (d, J = 8.2 Hz, 2Ar**H**), 7.33 (br s, C(O)N**H**H'), 6.99 (br s, C(O)NH**H'**), 3.58 and 3.73 (AB_q, J = 13.7 Hz, C**H**$_2$), 3.03 (q, J = 6.8 Hz, C**H**), 2.43 (br s, N**H**), 1.08 (d, J = 6.7 Hz, C**H**$_3$); ^{13}C NMR (75 MHz, DMSO–d$_6$) δ 177.4 (**C**(O)), 140.8, 139.3, 137.6, 132.6, 129.3, 129.0, 128.7, 126.9 (Ar**C**), 56.9 (**C**H), 51.1 (**C**H$_2$), 19.8 (**C**H$_3$).

(*S*)-2-(((2'-(Trifluoromethyl)-[1,1'-biphenyl]-4-yl)methyl)amino)propanamide (3g)

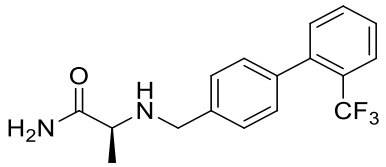

Using method D, L-alaninamide hydrochloride (**13**) (0.15 g, 1.34 mmol), triethylamine (0.23 mL, 1.68 mmol) **2g** (0.28 g, 1.11 mmol) in MeOH (1.22 mL) and sodium cyanoborohydride (0.30 g, 4.48 mmol) in MeOH (1.12 mL) gave **3g** as a white solid (0.17 g, 48%); R_f = 0.15 (EtOAc); mp 109–111 °C; ^{1}H NMR (400 MHz, DMSO–d_6) δ 7.82 (d, J = 7.6 Hz, 1Ar**H**), 7.70 (t, J = 7.6 Hz, 1Ar**H**), 7.59 (t, J = 7.6 Hz, 1Ar**H**), 7.32–7.45 (m, 3Ar**H,** C(O)N**H**H'), 7.24 (d, J = 7.8 Hz, 2Ar**H**), 7.00 (br s, C(O)NH**H'**), 3.60 and 3.73 (AB_q, J = 13.7 Hz, C$\mathbf{H}_2$), 3.05 (q, J = 6.8 Hz, C**H**), 2.48 (br s, N**H**), 1.16 (d, J = 6.8 Hz, C$\mathbf{H}_3$); ^{13}C NMR (75 MHz, DMSO–d_6) δ 177.4 (**C**(O)), 141.2, 140.7, 138.1, 132.7, 128.9, 128.4, 127.8, 127.3 (q, $J_{C–F}$ = 29.0 Hz), 126.4, 124.7 (q, $J_{C–F}$ = 273.6 Hz) (Ar**C**), 57.2 (**C**H), 51.2 (**C**H_2), 19.8 (**C**H_3).

(*S*)-2-(((3'-(Trifluoromethyl)-[1,1'-biphenyl]-4-yl)methyl)amino)propanamide (3h)

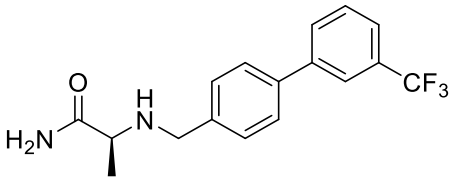

Using method B, L-alinamide hydrochloride (2.11 g, 16.91 mmol), triethylamine (2.34mL, 16.91 mmol), **2h** (3.30 g, 14.10 mmol), and sodium cyanoborohydride (1.40 g, 21.14 mmol) in MeOH (14.09 mL) gave **3h** as a white solid (1.15 g, 26%); R_f = 0.15 (EtOAc); mp 106–108 °C; ^{1}H NMR (400 MHz, DMSO–d_6) δ 7.94–7.99 (m, 2Ar**H**), 7.69–7.71 (m, 4Ar**H**), 7.45–7.47 (m, 2Ar**H**), 7.36 (br s, C(O)N**H**H'), 7.02 (br s, C(O)NH**H'**), 3.60 and 3.75 (AB_q, J = 13.8 Hz, NHC$\mathbf{H}_2$Ar), 3.04 (q, J = 6.8 Hz, C**H**), 1.16 (d, J = 6.8 Hz, C$\mathbf{H}_3$); ^{13}C NMR (75 MHz, DMSO–d_6) δ 177.5 (**C**(O)), 141.6, 141.3, 137.4, 131.0, 130.4, 130.3 (q, $J_{C–F}$ = 31.2 Hz), 129.1, 127.1, 124.7 (q, $J_{C–F}$ = 270.8 Hz), 124.2 (q, $J_{C–F}$ = 3.6 Hz) 123.3 (q, $J_{C–F}$ = 3.7 Hz) (Ar**C**), 57.0 (**C**H), 51.1 (**C**H_2), 19.8 (**C**H_3).

(*S*)-2-(((4'-(Trifluoromethyl)-[1,1'-biphenyl]-4-yl)methyl)amino)propanamide (3i)

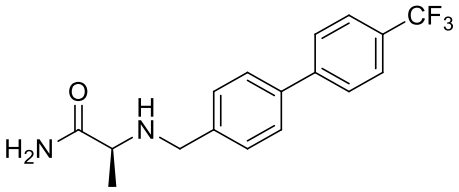

Using method B, L-alaninamide hydrochloride (0.30 g, 2.4 mmol), triethylamine (0.42 mL, 4.12 mmol), **2i** (0.50 g, 2.0 mmol) in MeOH (2.17 mL), and sodium cyanoborohydride (0.30 g, 3.0 mmol) in MeOH (2.0 mL) gave **3i** as a white solid (0.33 g, 53%); R_f = 0.10 (EtOAc); mp 144–147 °C; ^{1}H NMR (300 MHz, DMSO–d_6) δ 7.89 (d, J = 8.1 Hz, 2Ar**H**), 7.80 (d, J = 8.3 Hz, 2Ar**H**), 7.69 (d, J = 7.9 Hz, 2Ar**H**), 7.47 (d, J = 8.0 Hz, 2Ar**H**), 7.34 (br s, C(O)N**H**H'), 6.99 (br s, C(O)NH**H**'), 3.60 and 3.75 (AB_q, J = 13.8 Hz, C$\mathbf{H_2}$), 3.04 (q, J = 6.8 Hz, C**H**), 1.15 (d, J = 6.8 Hz, C$\mathbf{H_3}$), the remaining peak was not detected and is believed to overlap with H_2O signals; ^{13}C NMR (75 MHz, DMSO–d_6) δ 177.4 (**C**(O)), 144.5, 141.6, 137.4, 129.1, 128.1 (q, $J_{C–F}$ = 31.8 Hz), 127.7, 127.2, 126.2 (q, $J_{C–F}$ = 3.8 Hz), 124.8 (q, $J_{C–F}$ = 270.1 Hz) (Ar**C**), 57.0 (**C**H), 51.1 (**C**H_2), 19.8 (**C**H_3).

(*S*)-2-(((3'-(Trifluoromethoxy)-[1,1'-biphenyl]-4-yl)methyl)amino)propanamide (3j)

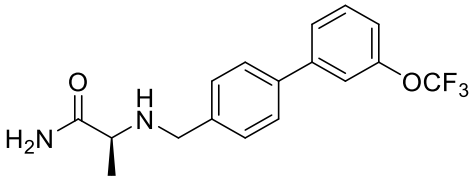

Using method B, L-alaninamide hydrochloride (0.28 g, 2.25 mmol), triethylamine (0.39 mL, 2.82 mmol), **2j** (0.50 g, 1.88 mmol) in MeOH (2.04 mL) and sodium cyanoborohydride (0.17 g, 2.57 mmol) in MeOH (1.71 mL) gave **3j** as a white solid (0.34 g, 54%); R_f = 0.10 (EtOAc); mp 95–97 °C; ^{1}H NMR (300 MHz, DMSO–d_6) δ 7.55–7.76 (m, 5Ar**H**), 7.44 (d, J = 7.8 Hz, 2Ar**H**), 7.30–7.38 (m, 1Ar**H**, C(O)N**H**H'), 6.99 (br s, C(O)NH**H'**), 3.59 and 3.74 (AB_q, J = 13.7 Hz, C$\mathbf{H_2}$), 3.03 (q, J = 6.8 Hz, C**H**), 2.43 (br s, N**H**), 1.15 (d, J = 6.8 Hz, C$\mathbf{H_3}$); ^{13}C NMR (75 MHz, $CDCl_3$) δ 178.0 (**C**(O)), 149.8(**C**OCF_3), 142.9, 139.4, 138.7, 130.1 128.6, 127.3, 125.4, 120.6 (q, $J_{C–F}$ = 255.7 Hz), 119.6 (Ar**C**), 57.7(**C**H), 52.2 (**C**H_2), 19.7 (**C**H_3).

(*S*)-2-(((4'-(Trifluoromethoxy)-[1,1'-biphenyl]-4-yl)methyl)amino)propanamide (3k)

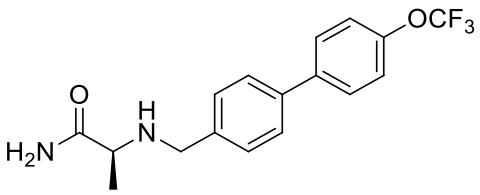

Using method B, L-alaninamide hydrochloride (0.23 g, 1.81 mmol), triethylamine (0.25 mL, 1.81 mmol), **2k** (0.40 g, 1.51 mmol) and sodium cyanoborohydride (0.15 g, 2.26 mmol) in MeOH (1.5 mL) gave compound **3k** as a white solid (0.32 g, 62%); R_f = 0.10 (EtOAc); mp 129–132 °C; ^{1}H NMR (400 MHz, DMSO–d_6) δ 7.78 (d, J = 8.6 Hz, 2Ar**H**), 7.63 (d, J = 8.0 Hz, 2Ar**H**), 7.41–7.53 (m, 4Ar**H**), 7.34 (br s, C(O)N**H**H'), 7.00 (br s, C(O)NH**H'**), 3.59 and 3.73 (AB_q, J = 13.7 Hz, C**H**$_2$), 2.98–3.11 (m, C**H**), 2.42 (br s, N**H**), 1.15 (d, J = 6.8 Hz, C**H**$_3$); ^{13}C NMR (75 MHz, $CDCl_3$) δ 178.1 (**C**(O)), 148.7 (**C**OCF_3), 139.6, 139.1, 128.9, 128.6, 128.4, 127.3, 121.3, 120.6 (q, $J_{C–F}$ = 255.4 Hz) (Ar**C**), 57.7 (**C**H), 52.2 (**C**H_2), 19.7 (**C**H_3).

(*S*)-2-(([1,1'-Biphenyl]-4-ylmethyl)amino)propanamide methanesulfonate (KDS2051)

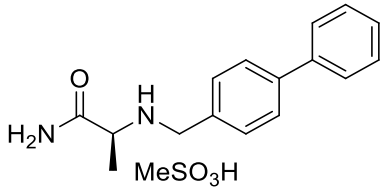

Using method E, to a solution of **24o** (0.15 g, 0.59 mmol), methanesulfonic acid (47.84 μL, 0.74 mmol) in EtOAc (1.18 mL) gave **35o** as a white solid (0.18 g, 86%); R_f = 0.00 (CH_2Cl_2/MeOH 10/1); mp 252–256 ˚C; HPLC purity: 6.2 min, >99.9%; ^{1}H NMR (300 MHz, DMSO–d_6) δ 9.19 (br s, $^+$N**H**$_2$), 7.98 (br s, C(O)N**H**H'), 7.75 (d, J = 8.0 Hz, 2Ar**H**), 7.70 (d, J = 7.8 Hz, 2Ar**H**), 7.65 (br s, C(O)NH**H'**), 7.60 (d, J = 8.0 Hz, 2Ar**H**), 7.48 (t, J = 7.5 Hz, 2Ar**H**), 7.34–7.43 (m, 1Ar**H**), 4.10–4.20 (m, C**H**$_2$), 3.78–3.94 (m, C**H**), 2.37 (s, SC**H**$_3$), 1.47 (d, J = 6.8 Hz, C**H**$_3$); ^{13}C NMR (75 MHz, DMSO–d_6) δ 170.9 (**C**(O)), 141.2, 139.8, 131.3, 131.2, 129.5, 128.3, 127.3, 127.2 (Ar**C**), 55.0 (**C**H), 48.6 (**C**H_2), 40.2 (S**C**H_3), 16.4 (**C**H_3); HRMS (M + H)$^+$(ESI$^+$) 255.1500 [M + H]$^+$ (calcd for $C_{16}H_{18}N_2OH^+$ 255.1497)

(*S*)-2-(((2'-Fluorobiphenyl-4-yl)methyl)amino)propanamide methanesulfonate (KDS0011)

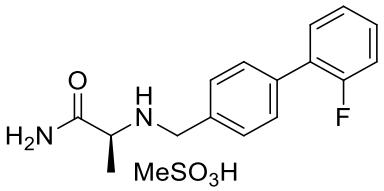

Using method C, **3a** (0.10 g, 0.37 mmol) and methanesulfonic acid (28.10 μL, 0.43 mmol) in EtOAc (1.50 mL) gave **KDS0011** as a white solid (0.12 g, 90%); R_f = 0.00 (CH_2Cl_2/MeOH 10/1); mp 131–135 °C; HPLC purity: 6.4 min, >99.9%; ^{1}H NMR (300 MHz, DMSO–d_6) δ 9.17 (br s, $^+$N**H**$_2$), 7.94 (br s, C(O)N**H**H'), 7.30–7.94 (m, 8Ar**H**, C(O)NH**H'**), 4.08–4.25 (m, C**H**$_2$), 3.80 (q, J = 6.7 Hz, C**H**), 2.30 (s, SC**H**$_3$), 1.45 (d, J = 6.7 Hz, C**H**$_3$); ^{13}C NMR (75 MHz, DMSO–d_6) δ 170.9 (**C**(O)), 159.5 (d, $J_{C–F}$ = 244.6 Hz), 136.2, 131.7, 131.2 (d, $J_{C–F}$ = 3.1 Hz), 130.8, 130.4 (d, $J_{C–F}$ = 5.4 Hz), 129.5 (d, $J_{C–F}$ = 2.7 Hz), 128.0 (d, $J_{C–F}$ = 13.0 Hz), 125.5 (d, $J_{C–F}$ = 3.4 Hz), 116.6 (d, $J_{C–F}$ = 22.3 Hz) (Ar**C**), 55.1 (**C**H), 48.7 (**C**H$_2$), 16.4 (**C**H$_3$), the S**C**H$_3$ peak was overlapped with the DMSO signals; HRMS (M + H)$^+$(ESI$^+$) 237.1399 [M + H]$^+$ (calcd for $C_{16}H_{17}FN_2OH^+$ 237.1403)

(*S*)-2-(((3'-Fluorobiphenyl-4-yl)methyl)amino)propanamide methanesulfonate (KDS0015)

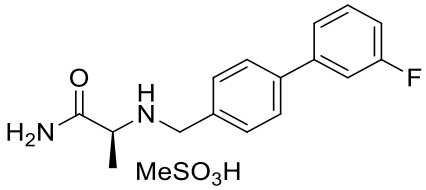

Using method C, **3b** (0.30 g, 1.10 mmol) and methanesulfonic acid (89.36 μL, 1.38 mmol) in EtOAc (2.50 mL) gave **KDS0015** as a white solid (0.39 g, 97%); R_f = 0.00 (CH_2Cl_2/MeOH 10/1); mp 235–238 °C; HPLC purity: 6.4 min, >99.9%; ^{1}H NMR (300 MHz, DMSO–d_6) δ 9.15 (br s, $^+$N**H**$_2$), 7.92 (br s, C(O)N**H**H'), 7.81 (d, J = 8.3 Hz, 2Ar**H**), 7.68 (br s, C(O)NH**H'**), 7.49–7.60 (m, 5Ar**H**), 7.21–7.27 (m, 1Ar**H**), 7.24 (m, 1Ar**H**), 4.11–4.20 (m, C**H**$_2$), 3.76 (q, J = 9.3 Hz, C**H**), 2.30 (s, SC**H**$_3$), 1.44 (d, J = 9.3 Hz, C**H**$_3$); ^{13}C NMR (75 MHz, DMSO–d_6) δ 171.0 (**C**(O)), 163.2 (d, $J_{C–F}$ = 241.9 Hz), 142.3, 139.8, 132.0, 131.5 (d, $J_{C–F}$ = 8.7 Hz), 131.2, 127.5, 123.3, 115.0 (d, $J_{C–F}$ = 21.1 Hz), 113.9 (d, $J_{C–F}$ = 21.9 Hz) (Ar**C**), 55.0 (**C**H), 48.6 (**C**H$_2$), 16.4 (**C**H$_3$), the S**C**H$_3$ peak was overlapped with the DMSO signals; HRMS (M + H)$^+$(ESI$^+$) 273.1401 [M + H]$^+$ (calcd for $C_{16}H_{17}FN_2OH^+$ 273.1403)

(*S*)-2-(((4'-Fluorobiphenyl-4-yl)methyl)amino)propanamide methanesulfonate (KDS2006)

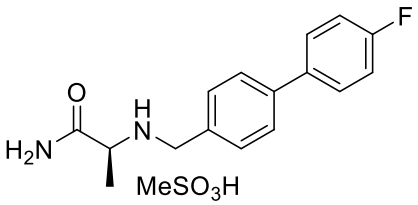

Using method C, **3c** (0.20 g, 0.73 mmol) and methanesulfonic acid (59.58 μL, 0.92 mmol) in EtOAc (1.46 mL) gave **KDS2006** as a white solid (0.24 g, 88%); R_f = 0.00 (CH_2Cl_2/MeOH 10/1); mp 162–164 °C; HPLC purity: 6.4 min, 97.6%; ^{1}H NMR (300 MHz, DMSO–d_6) δ 9.18 (br s, $^+$N**H**$_2$), 7.95 (br s, C(O)N**H**H'), 7.72–7.77 (m, 4Ar**H**), 7.65 (br s, C(O)NH**H'**), 7.58 (d, J = 8.2 Hz, 2Ar**H**), 7.28–7.34 (m, 2Ar**H**), 4.12–4.15 (m, C**H**$_2$), 3.78–3.84 (m, C**H**), 2.37 (s, SC**H**$_3$), 1.45 (d, J = 6.9 Hz, C**H**$_3$); ^{13}C NMR (75 MHz, DMSO–d_6) δ 171.0 (**C**(O)), 140.2, 136.3 (d, $J_{C–F}$ = 3.1 Hz), 131.2, 131.1, 129.2 (d, $J_{C–F}$ = 8.2 Hz), 127.3, 116.3 (d, $J_{C–F}$ = 21.2 Hz) (Ar**C**), 54.9 (**C**H), 48.5 (**C**H$_2$), 16.3 (**C**H$_3$), the S**C**H$_3$ peak was overlapped with the DMSO signals; HRMS (M + H)$^+$(ESI$^+$) 273.1399 [M + H]$^+$ (calcd for $C_{16}H_{17}FN_2OH^+$ 273.1403)

(*S*)-2-(((2'-Chlorobiphenyl-4-yl)methyl)amino)propanamide methanesulfonate (KDS2042)

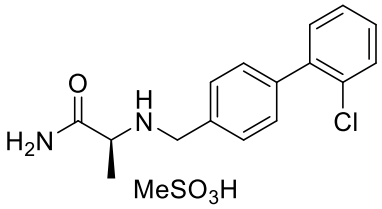

Using method C, **3d** (0.10 g, 0.35 mmol) and methanesulfonic acid (28.10 μL, 0.43 mmol) in EtOAc (3.46 mL) gave **KDS2042** as a white solid (0.08 g, 63%); R_f = 0.00 (CH_2Cl_2/MeOH 10/1); mp 216–220 °C; HPLC purity: 6.7 min, 97.8%; ^{1}H NMR (300 MHz, DMSO–d_6) δ 9.18 (br s, $^+$N**H**$_2$), 7.96 (br s, C(O)N**H**H'), 7.67 (br s, C(O)NH**H'**), 7.59 (d, J = 8.1 Hz, 3Ar**H**), 7.52 (d, J = 8.2 Hz, 2Ar**H**), 7.39–7.47 (m, 3Ar**H**), 4.09–4.28 (m, C**H**$_2$), 3.86–3.90 (m, C**H**), 2.30 (s, SC**H**$_3$), 1.47 (d, J = 6.9 Hz, C**H**$_3$); ^{13}C NMR (75 MHz, DMSO–d_6) δ 170.9 (**C**(O)), 139.8, 139.6, 131.9, 131.8, 131.7, 130.4, 130.0, 128.1, 55.2 (**C**H), 48.7 (**C**H$_2$), 16.4 (**C**H$_3$), the S**C**H$_3$ peak was overlapped with the DMSO signals. The remaining peak was not detected and is believed to overlap with the observed signals; HRMS (M + H)$^+$(ESI$^+$) 289.1105 [M + H]$^+$ (calcd for $C_{16}H_{17}ClN_2OH^+$ 289.1108)

(*S*)-2-(((3'-Chlorobiphenyl-4-yl)methyl)amino)propanamide methanesulfonate (KDS0014)

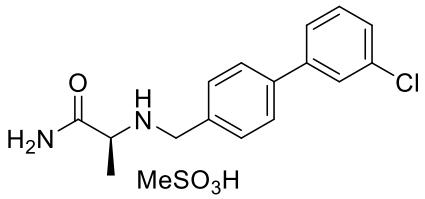

Using method C, **3e** (0.15 g, 0.52 mmol) and methanesulfonic acid (48.90 μL, 0.75 mmol) in EtOAc (0.52 mL) gave **KDS0014** as a white solid (0.18 g, 90%); R_f = 0.00 (CH_2Cl_2/MeOH 10/1); mp 220–223 °C; HPLC purity: 6.9 min, 97.3%; ^{1}H NMR (400 MHz, DMSO–d_6) δ 9.16 (br s, $^+$N**H₂**), 7.92 (br s, C(O)N**H**H'), 7.81 (d, J = 8.14 Hz, 2Ar**H**), 7.77 (br s, C(O)NH**H'**), 7.67–7.70 (m, 2Ar**H**), 7.59 (d, J = 8.1 Hz, 1Ar**H**), 7.52 (t, J = 7.9 Hz, 1Ar**H**), 7.46 (d, J = 8.1 Hz, 1Ar**H**), 4.12–4.20 (m, C**H₂**), 3.78 (q, J = 6.7 Hz, C**H**), 2.30 (s, SC**H₃**), 1.45 (d, J = 6.7 Hz, C**H₃**); ^{13}C NMR (75 MHz, DMSO–d_6) δ 170.9 (**C**(O)), 141.9, 139.5, 134.3, 132.0, 131.3, 131.2, 128.1, 127.5, 126.9, 125.9 (Ar**C**), 55.1 (**C**H), 48.6 (**C**H_2), 16.4 (**C**H_3), the S**C**H_3 peak was overlapped with the DMSO signals; HRMS (M + H)$^+$(ESI$^+$) 289.1106 [M + H]$^+$ (calcd for $C_{16}H_{17}ClN_2OH^+$ 289.1108)

(*S*)-2-(((4'-Chlorobiphenyl-4-yl)methyl)amino)propanamide methanesulfonate (KDS2005)

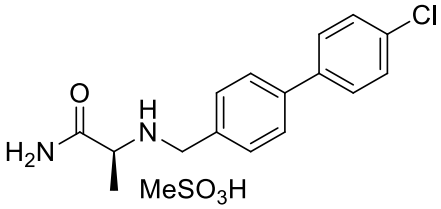

Using method C, **3f** (0.15 g, 0.52 mmol) and methanesulfonic acid (42.14 μL, 0.65 mmol) in EtOAc (1.04 mL) gave **KDS2005** as a white solid (0.17 g, 84%); R_f = 0.00 (CH_2Cl_2/MeOH 10/1); mp 220–223 °C; HPLC purity: 7.0 min, 98.2%; ^{1}H NMR (300 MHz, DMSO–d_6) δ 9.17 (br s, $^+$N**H₂**), 7.94 (br s, C(O)N**H**H'), 7.73–7.78 (m, 4Ar**H**), 7.66 (br s, C(O)NH**H'**), 7.53–7.60 (m, 4Ar**H**), 4.10–4.20 (m, C**H₂**), 3.76–3.82 (m, C**H**), 2.32 (s, SC**H₃**), 1.45 (d, J = 6.9 Hz, C**H₃**); ^{13}C NMR (100 MHz, DMSO–d_6) δ 170.9 (**C**(O)), 139.9, 138.6, 133.2, 131.7, 131.2, 129.4, 129.0, 127.3 (Ar**C**), 54.9, (**C**H), 48.5 (**C**H_2), 16.3 (**C**H_3), the S**C**H_3 peak was overlapped with the DMSO signals; HRMS (M + H)$^+$(ESI$^+$) 289.1109 [M + H]$^+$ (calcd for $C_{16}H_{17}ClN_2OH^+$ 289.1108)

(*S*)-2-(((2'-Trifluoromethylbiphenyl-4-yl)methyl)amino)propanamide methanesulfonate (KDS2041)

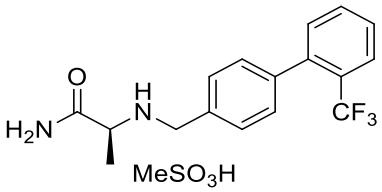

Using method C, **3g** (0.12 g, 0.37 mmol) and methanesulfonic acid (30.20 μL, 0.47 mmol) in EtOAc (3.72 mL) gave **KDS2041** as a white solid (0.14 g, 87%); R_f = 0.00 (CH_2Cl_2/MeOH 10/1); mp 224–227 °C; HPLC purity: 7.0 min, 95.8%; ^{1}H NMR (300 MHz, DMSO–d_6) δ 9.20 (br s, $^+$N**H**$_2$), 7.94 (br s, C(O)N**H**H'), 7.85 (d, J = 7.8 Hz, 1Ar**H**), 7.75 (t, J = 7.4 Hz, 1Ar**H**), 7.61–7.67 (m, 2Ar**H**), 7.57 (d, J = 7.2 Hz, 1Ar**H**), 7.39–7.41 (m, 2Ar**H**, C(O)NH**H'**), 4.11–4.22 (m, C**H**$_2$), 3.86–3.88 (m, C**H**), 2.32 (s, SC**H**$_3$), 1.47 (d, J = 6.7 Hz, C**H**$_3$); ^{13}C NMR (75 MHz, DMSO–d_6) δ 170.9 (**C**(O)), 140.5, 140.4, 132.8, 132.5, 131.9, 130.1, 129.4, 128.7, 127.3 (q, $J_{C–F}$ = 29.2 Hz), 126.5 (q, $J_{C–F}$ = 5.2 Hz), 124.6 (q, $J_{C–F}$ = 270.5 Hz), 55.4, (**C**H), 48.8 (**C**H$_2$), 40.2 (S**C**H$_3$), 16.4 (**C**H$_3$); HRMS (M + H)$^+$(ESI$^+$) 323.1368 [M + H]$^+$ (calcd for $C_{17}H_{17}F_3N_2OH^+$ 323.1371)

(*S*)-2-(((3'-Trifluoromethylbiphenyl-4-yl)methyl)amino)propanamide methanesulfonate (KDS0012)

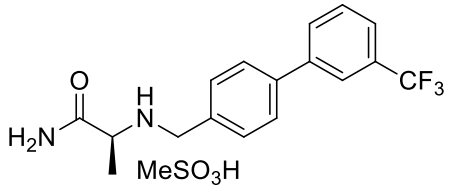

Using method C, **3h** (0.09 g, 0.28 mmol) and methanesulfonic acid (25.94 μL, 0.40 mmol) in EtOAc (1.10 mL) gave **KDS0012** as a white solid (0.10 g, 92%); R_f = 0.00 (CH_2Cl_2/MeOH 10/1); mp 215–217 °C; HPLC purity: 7.3 min, >99.9%; ^{1}H NMR (400 MHz, DMSO–d_6) δ 9.16 (br s, $^+$N**H**$_2$), 7.98–8.02 (m, 2Ar**H**), 7.90 (br s, C(O)N**H**H'), 7.84 (d, J = 8.1 Hz, 2Ar**H**), 7.69–7.76 (m, 2Ar**H**), 7.65 (br s, C(O)NH**H'**), 7.59 (d, J = 8.1 Hz, 2Ar**H**), 4.14 (m, C**H**$_2$), 3.69–3.84 (m, C**H**), 2.27 (S, SC**H**$_3$), 1.43 (d, J = 6.9 Hz, C**H**$_3$); ^{13}C NMR (75 MHz, DMSO–d_6) δ 171.0 (**C**(O)), 140.9, 139.5, 132.2, 131.3, 130.6, 130.3 (q, $J_{C–F}$ = 31.4 Hz), 127.6, 124.8, 124.6 (q, $J_{C–F}$ = 270.7 Hz), 123.5 (q, $J_{C–F}$ = 3.6 Hz) (Ar**C**), 55.2 (**C**H), 48.6 (**C**H$_2$), 16.4 (**C**H$_3$). The S**C**H$_3$ peak was overlapped with the DMSO signals. The remaining peak was not detected and is believed to

overlap with the observed signals; HRMS $(M + H)^+(ESI^+)$ 323.1373 $[M + H]^+$ (calcd for $C_{17}H_{17}F_3N_2OH^+$ 323.1371)

(*S*)-2-(((4'-Trifluoromethylbiphenyl-4-yl)methyl)amino)propanamide methanesulfonate (KDS2010)

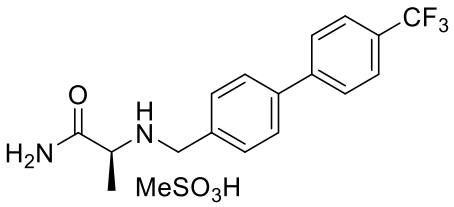

Using method C, **3i** (1.12 g, 3.63 mmol) and methanesulfonic acid (295.00 μL, 1.25 mmol) in EtOAc (7.26 mL) gave **KDS2010** as a white solid (1.26 g, 83%, 9:1 enantiomeric mixture); R_f = 0.00 (CH_2Cl_2/MeOH 10/1); mp 241–243 °C; HPLC purity: 7.4 min, 99.7%; ^{1}H NMR (300 MHz, DMSO–d_6) δ 9.20 (br s, $^+$N**H**$_2$), 7.94 (d, J = 7.7 Hz, 2Ar**H**, C(O)N**H**H'), 7.83–7.86 (m, 4Ar**H**), 7.63–7.66 (m, 2Ar**H**, C(O)NH**H'**), 4.12–4.23 (m, C**H**$_2$), 3.82 (q, J = 6.4 Hz, C**H**), 2.33 (s, SC**H**$_3$), 1.46 (d, J = 6.4 Hz, C**H**$_3$); ^{13}C NMR (75 MHz, DMSO–d_6) δ 170.9 (**C**(O)), 143.8, 139.6, 132.4, 131.3, 128.6 (q, $J_{C–F}$ = 31.9 Hz), 128.0, 127.8, 126.3 (q, $J_{C–F}$ = 3.8 Hz), 124.8 (q, $J_{C–F}$ = 270.3 Hz) (Ar**C**), 55.0 (C(O)**C**H$^+$NH$_2$), 48.5 (**C**H$_2$), 40.2 (S**C**H$_3$), 16.4 (**C**H$_3$); HRMS $(M + H)^+(ESI^+)$ 323.1374 $[M + H]^+$ (calcd for $C_{17}H_{17}F_3N_2OH^+$ 323.1371)

(*S*)-2-(((3'-Trifluoromethoxybiphenyl-4-yl)methyl)amino)propanamide methanesulfonate (KDS2002)

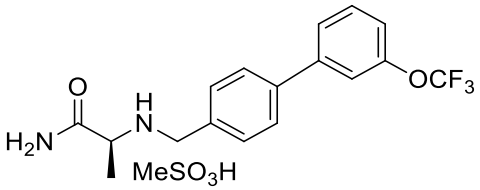

Using method C, **3j** (0.25 g, 0.74 mmol) and methanesulfonic acid (59.94 μL, 0.92 mmol) in EtOAc (1.48 mL) gave **KDS2002** as a white solid (0.29 g, 90%); R_f = 0.00 (CH_2Cl_2/MeOH 10/1); mp 209–212 °C; HPLC purity: 7.5 min, 98.8%; ^{1}H NMR (300 MHz, DMSO–d_6) δ 9.16 (br s, $^+$N**H**$_2$), 7.92 (br s, C(O)N**H**H'), 7.83 (d, J = 8.2 Hz, 2Ar**H**), 7.77 (d, J = 8.2 Hz, 1Ar**H**), 7.59–7.69 (m, 4Ar**H**, C(O)NH**H'**), 7.39–7.42 (m, 1Ar**H**), 4.08–4.23 (m, C**H**$_2$), 3.77 (q, J = 7.0 Hz, C**H**), 2.30 (s, SC**H**$_3$), 1.44 (d, J = 7.0 Hz, C**H**$_3$); ^{13}C NMR (100 MHz, DMSO–d_6) δ 170.9

(**C**(O)), 149.5, 142.2, 139.4, 132.2, 131.5, 131.2, 127.6, 126.3, 120.6 (q, $J_{C–F}$ = 254.7 Hz), 120.5, 119.7 (Ar**C**), 55.0, (**C**H), 48.5 (**C**H_2), 16.4 (**C**H_3), the S**C**H_3 peak was overlapped with the DMSO signals; HRMS (M + H)$^+$(ESI$^+$) 339.1322 [M + H]$^+$ (calcd for $C_{17}H_{17}F_3N_2O_2H^+$ 339.1320)

(*S*)-2-(((4'-Trifluoromethoxybiphenyl-4-yl)methyl)amino)propanamide methanesulfonate (KDS2001)

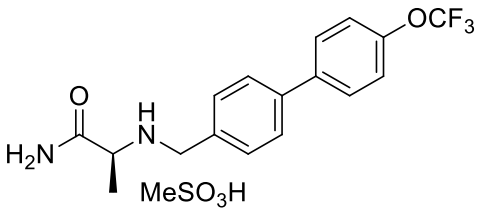

Using method C, **3k** (0.10 g, 0.30 mmol) and methanesulfonic acid (23.98 μL, 0.37 mmol) in EtOAc (0.59 mL) gave **KDS2001** as a white solid (0.12 g, 92%); R_f = 0.00 (CH_2Cl_2/MeOH 10/10); mp 256–259 °C; HPLC purity: 7.6 min, 99.8%; ^{1}H NMR (400 MHz, DMSO–d_6) δ 9.17 (br s, $^+$N**H**$_2$), 7.92 (br s, C(O)N**H**H'), 7.83 (d, J = 8.7 Hz, 2Ar**H**), 7.78 (d, J = 8.2 Hz, 2Ar**H**), 7.67 (br s, C(O)NH**H'**), 7.59 (d, J = 8.1 Hz, 2Ar**H**), 7.48 (d, J = 8.2 Hz, 2Ar**H**), 4.08–4.23 (m, C**H**$_2$), 3.71–3.88 (m, C**H**), 2.30 (s, SC**H**$_3$), 1.44 (d, J = 7.0 Hz, C**H**$_3$); ^{13}C NMR (100 MHz, DMSO–d_6) δ 170.9 (**C**(O)), 148.5, 139.7, 139.1, 131.8, 129.1, 127.5, 122.0, 120.6 (q, $J_{C–F}$ = 254.7 Hz) (Ar**C**), 55.0 (**C**H), 48.6 (**C**H_2), 16.4 (**C**H_3), the S**C**H_3 peak was overlapped with the DMSO signals; HRMS (M + H)$^+$(ESI$^+$) 339.1316 [M + H]$^+$ (calcd for $C_{17}H_{17}F_3N_2O_2H^+$ 339.1320)

(*R*)-2-(((4'-(Trifluoromethyl)-[1,1'-biphenyl]-4-yl)methyl)amino)propanamide (25b)

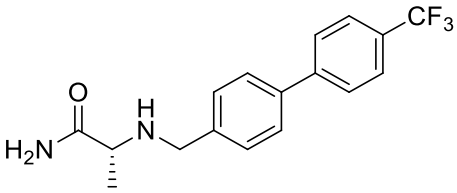

Using method D, D-alaninamide hydrochloride (**14**) (0.15 g, 1.20 mmol), triethylamine (0.21 mL, 1.50 mmol) **2b** (0.25 g, 1.00 mmol) in MeOH (1.09 mL) and sodium cyanoborohydride (0.26 g, 4.00 mmol) in MeOH (1.00 mL) gave **25b** as a white solid (0.21 g, 64%); R_f = 0.10 (EtOAc); mp 143–145 °C; ^{1}H NMR (300 MHz, DMSO–d_6) δ 7.89 (d, J = 8.3 Hz, 2Ar**H**), 7.80 (t, J = 8.3 Hz,

2Ar**H**), 7.69 (d, *J* = 8.1 Hz, 2Ar**H**), 7.47 (d, *J* = 8.1 Hz, 2Ar**H**), 7.35 (br s, C(O)N**H**H'), 7.00 (br s, C(O)NH**H'**), 3.60 and 3.75 (AB_q, *J* = 13.8 Hz, NHC**H₂**Ar), 3.03 (q, *J* = 6.8 Hz, C**H**), 2.44 (br s, N**H**), 1.15 (d, *J* = 6.8 Hz, C**H**$_3$); ^{13}C NMR (75 MHz, $CDCl_3$) δ 177.9 (**C**(O)), 144.3, 139.7, 138.8, 129.4 (q, $J_{C–F}$ = 32.3 Hz), 128.6, 127.5, 127.3, 125.8 (q, $J_{C–F}$ = 3.7 Hz), 124.3 (q, $J_{C–F}$ = 270.1 Hz) (Ar**C**), 57.7 (**C**H), 52.2 (**C**H_2), 19.7 (**C**H_3).

(*R*)-2-(((4'-(Trifluoromethylbiphenyl-4-yl)methyl)amino)propanamide methanesulfonate (KDS2029)(R-isomer of KDS2010)

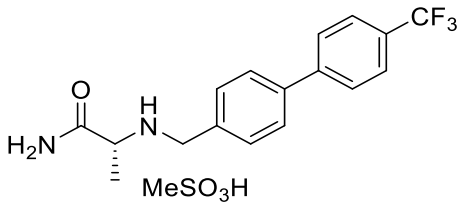

Using method B, D-alaninamide hydrochloride (0.15 g, 1.20 mmol, > 95% optical purity), triethylamine (0.21 mL, 1.50 mmol) **2i** (0.25 g, 1.00 mmol) in MeOH (1.09 mL) and sodium cyanoborohydride (0.26 g, 4.00 mmol) in MeOH (1.00 mL) gave free form of KDS2029 as a white solid (0.21 g, 64%, 9:1 enantiomeric mixture); R_f = 0.10 (EtOAc); mp 143–145 °C; ^{1}H NMR (300 MHz, DMSO–d_6) δ 7.89 (d, *J* = 8.3 Hz, 2Ar**H**), 7.80 (t, *J* = 8.3 Hz, 2Ar**H**), 7.69 (d, *J* = 8.1 Hz, 2Ar**H**), 7.47 (d, *J* = 8.1 Hz, 2Ar**H**), 7.35 (br s, C(O)N**H**H'), 7.00 (br s, C(O)NH**H'**), 3.60 and 3.75 (AB_q, *J* = 13.8 Hz, NHC**H₂**Ar), 3.03 (q, *J* = 6.8 Hz, C**H**), 2.44 (br s, N**H**), 1.15 (d, *J* = 6.8 Hz, C**H**$_3$); ^{13}C NMR (75 MHz, $CDCl_3$) δ 177.9 (**C**(O)), 144.3, 139.7, 138.8, 129.4 (q, $J_{C–F}$ = 32.3 Hz), 128.6, 127.5, 127.3, 125.8 (q, $J_{C–F}$ = 3.7 Hz), 124.3 (q, $J_{C–F}$ = 270.1 Hz) (Ar**C**), 57.7 (**C**H), 52.2 (**C**H_2), 19.7 (**C**H_3).

Using method C, the resulting solid (0.17 g, 0.53 mmol), methanesulfonic acid (42.80 μL, 0.66 mmol) in EtOAc (1.05 mL) gave KDS2029 as a white solid (0.19 g, 87%); R_f = 0.00 (CH_2Cl_2/MeOH 10/1); mp 241–244 °C; HPLC purity: 7.4 min, 99.8%; ^{1}H NMR (300 MHz, DMSO–d_6) δ 9.18 (br s, $^+$N**H₂**), 7.93–7.95 (m, 2Ar**H**, C(O)N**H**H'), 7.84 (d, *J* = 7.9 Hz, 4Ar**H**), 7.62–7.66 (m, 2Ar**H**, C(O)NH**H'**), 4.12–4.22 (m, C**H₂**), 3.80 (q, *J* = 6.5 Hz, C**H**), 2.31 (s, SC**H₃**), 1.45 (d, *J* = 6.5 Hz, C**H₃**); ^{13}C NMR (75 MHz, DMSO–d_6) δ 170.9 (**C**(O)), 143.8, 139.5, 132.4, 131.3, 128.6 (q, $J_{C–F}$ = 31.7 Hz) (Ar**C**), 55.1 (**C**H), 48.6 (**C**H_2), 40.2 (S**C**H_3), 16.4 (**C**H_3); HRMS $(M + H)^+$(ESI$^+$) 323.1373 $[M + H]^+$ (calcd for $C_{17}H_{17}F_3N_2OH^+$ 323.1371)

Chiral resolution of KDS2010

Analytical resolution was carried out using a SHIMADZU NEXERA supercritical fluid chromatography (SFC) system with LC-30AD SF CO_2 and LC-20AD LC pump, a SPD-M20A diode array detector connected to a SFC-30A back pressure regulator. 1 µL of the desired racemate (5 mg/1 mL MeOH) were injected on a DAICEL chiralpak AD-H 5 µm column 150 × 4.6 mm. The sample was eluted with CO_2:MeOH:DEA (80:20:1) with a flowrate of 3 mL/min at 25 °C. Retention time (RT) of the separated enantiomers of **KDS2010**: *S*) 2.59 min *R*) 2.84 min.

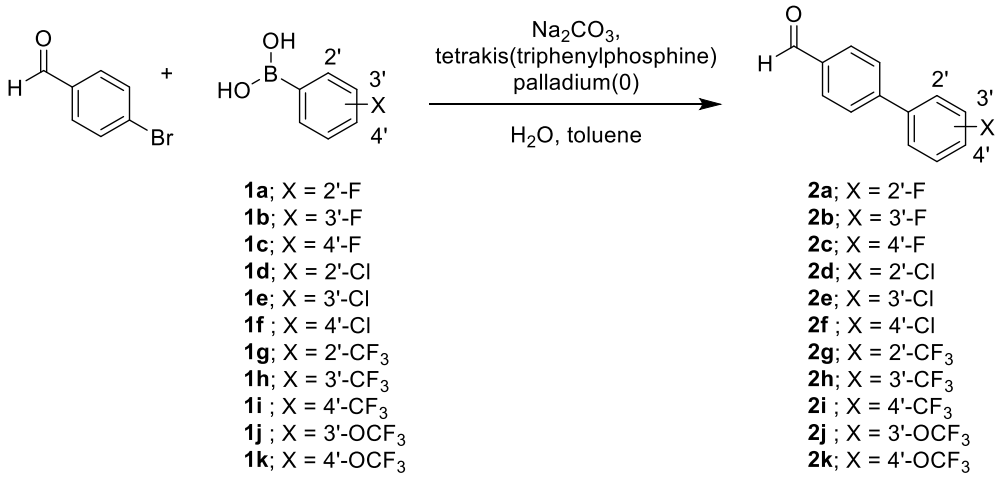

1a; X = 2'-F
1b; X = 3'-F
1c; X = 4'-F
1d; X = 2'-Cl
1e; X = 3'-Cl
1f ; X = 4'-Cl
1g; X = 2'-CF_3
1h; X = 3'-CF_3
1i ; X = 4'-CF_3
1j ; X = 3'-OCF_3
1k; X = 4'-OCF_3

2a; X = 2'-F
2b; X = 3'-F
2c; X = 4'-F
2d; X = 2'-Cl
2e; X = 3'-Cl
2f ; X = 4'-Cl
2g; X = 2'-CF_3
2h; X = 3'-CF_3
2i ; X = 4'-CF_3
2j ; X = 3'-OCF_3
2k; X = 4'-OCF_3

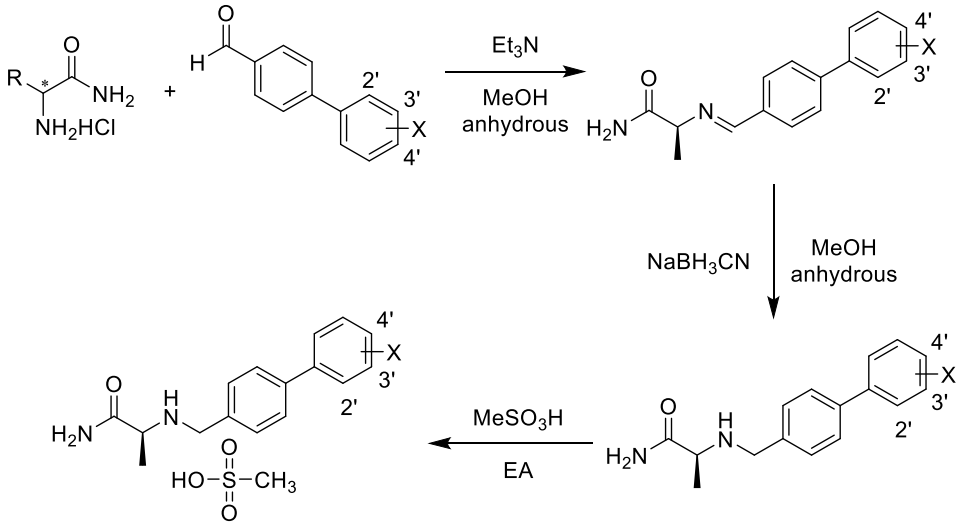

KDS0011; X = 2'-F
KDS0015; X = 3'-F
KDS2006; X = 4'-F
KDS2042; X = 2'-Cl
KDS0014; X = 3'-Cl
KDS2005; X = 4'-Cl
KDS2041; X = 2'-CF_3
KDS0012; X = 3'-CF_3
KDS2010; X = 4'-CF_3
KDS2002; X = 3'-OCF_3
KDS2001; X = 4'-OCF_3

3a; X = 2'-F
3b; X = 3'-F
3c; X = 4'-F
3d; X = 2'-Cl
3e; X = 3'-Cl
3f ; X = 4'-Cl
3g; X = 2'-CF_3
3h; X = 3'-CF_3
3i ; X = 4'-CF_3
3j ; X = 3'-OCF_3
3k; X = 4'-OCF_3

Fig. S1. General procedure for the preparation of KDS compounds.

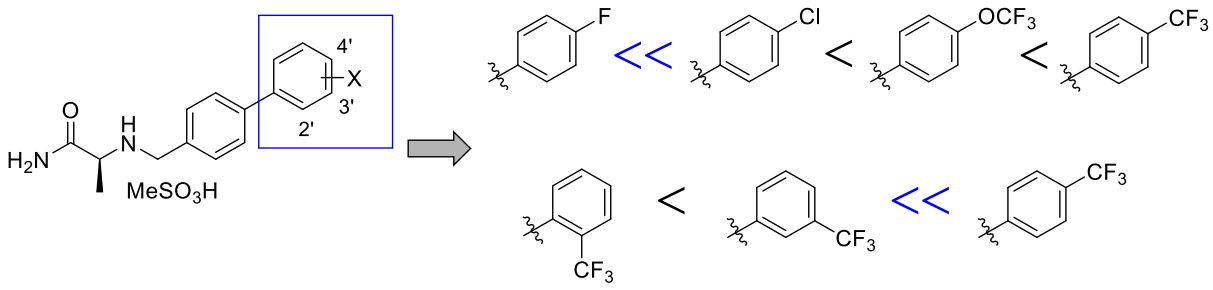

Fig. S2. Structure-activity relationship of the synthesized compounds.

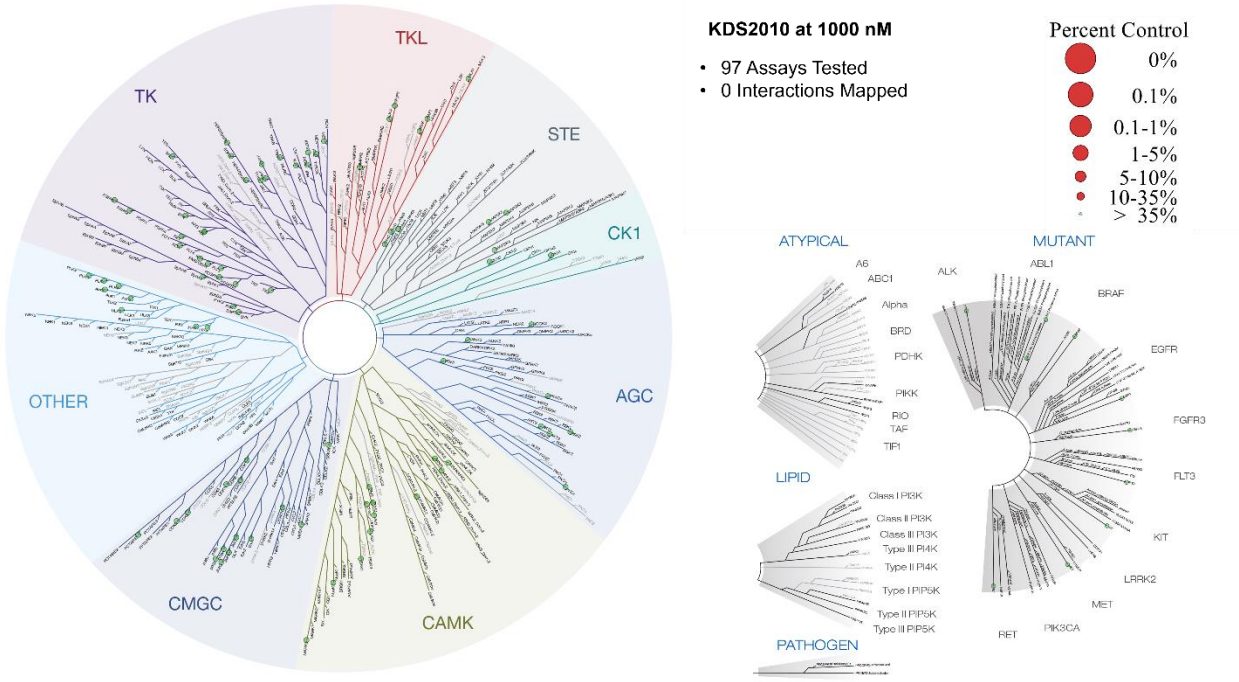

Fig. S3. The KINOMEscan screening results with 1000 nM of KDS2010 for off-target selectivity. Schematic diagram of the KINOME*scan*™ screening results categorizing human kinases and disease-associated mutant variants. Competitive binding assays for 97 human kinases were performed at 1000 nM KDS2010 and the amount of inhibition through the control ligand reaction was expressed as the size of the red circle and the green circle. Zero interaction mapped means there is no meaningful responses (≥ 50% inhibition). TK, Tyrosine Kinase; TKL, Tyrosine Kinase Like; STE, Yeast STE-MAPK family; CK1, Casein Kinase 1; AGC, PKA, PKG, PKC family; CAMK, Calmodulin/Calcium regulated kinases; CMGC, CDK, MAPK, GSK3 and CLK; see table S4 for the detailed results.

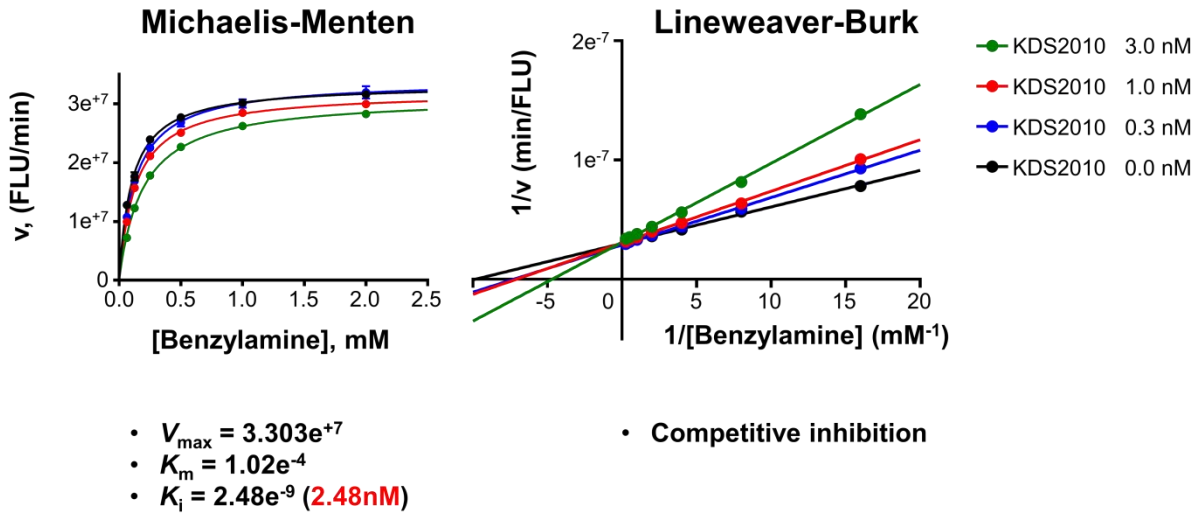

Fig. S4. Mode of KDS2010 binding with MAO-B. The catalytic rates were measured at different concentrations of benzylamine (0.065, 0.125, 0.25, 0.5, 1 and 2 mM) in the absence and in the presence of different concentrations (0.3, 1 and 3 nM) of KDS2010. The maximal velocity (V_{max}), Michaelis constant (K_m) and inhibition constant (K_i) were calculated using Sigma plot®.

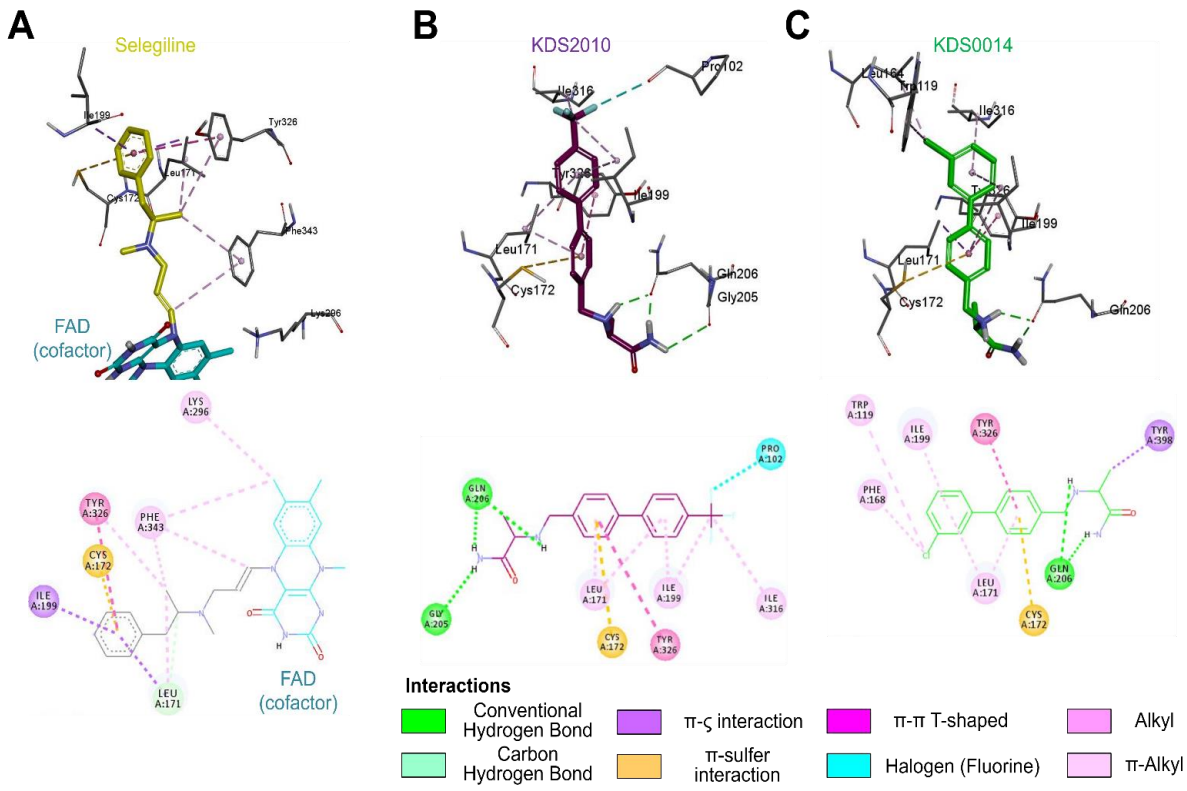

Fig. S5. Three-day and 2-day interactions of selegiline, KDS2010, and KDS0014 inside MAO-B. Selegiline, FAD, KDS2010, and KDS0014 shown in yellow, cyan, purple, and green color respectively. Amino acid residues surrounding 4Å of ligand shown in stick format. Color indication for a particular type of interactions explained below the 2D image of protein-ligand interactions.

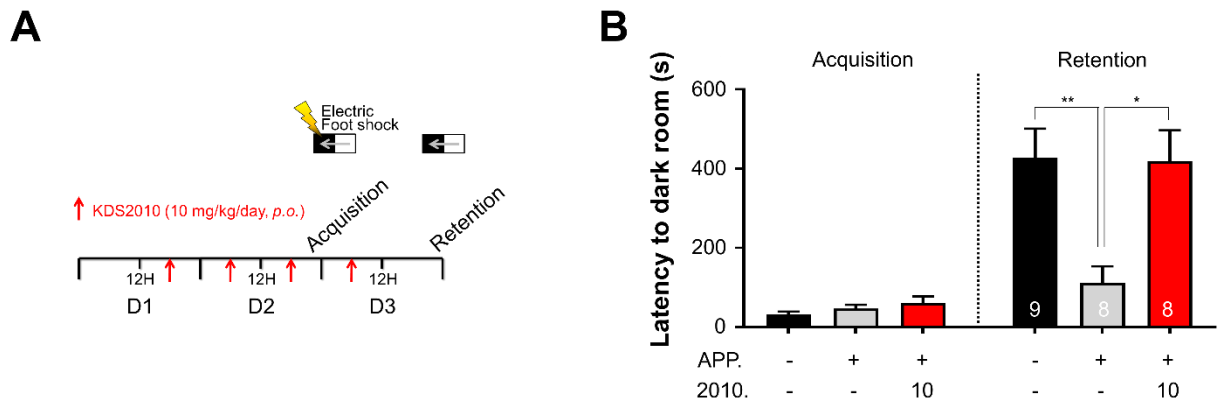

Fig. S6. Acute treatment of KDS2010 (3 days) restored memory impairment in APP/PS1 mice. (**A**) Schematic diagram of the passive avoidance test for wild-type (WT) and APP/PS1 mice with or without oral administration of KDS2010 (10 mg/kg for 3 days; *n*=9 for WT + water; *n*=8 for APP/PS1 + water; *n*=8 for APP/PS1 + KDS2010; both sexes at 10- to 11-month of age). (**B**) Latency to enter the dark chamber during the passive avoidance test. **p* < 0.05, ***p* < 0.01 (One-way ANOVA with *Tukey's* multiple comparisons test). Data are means ± s.e.m. Data distribution of bar graphs was presented in the Fig. S10.

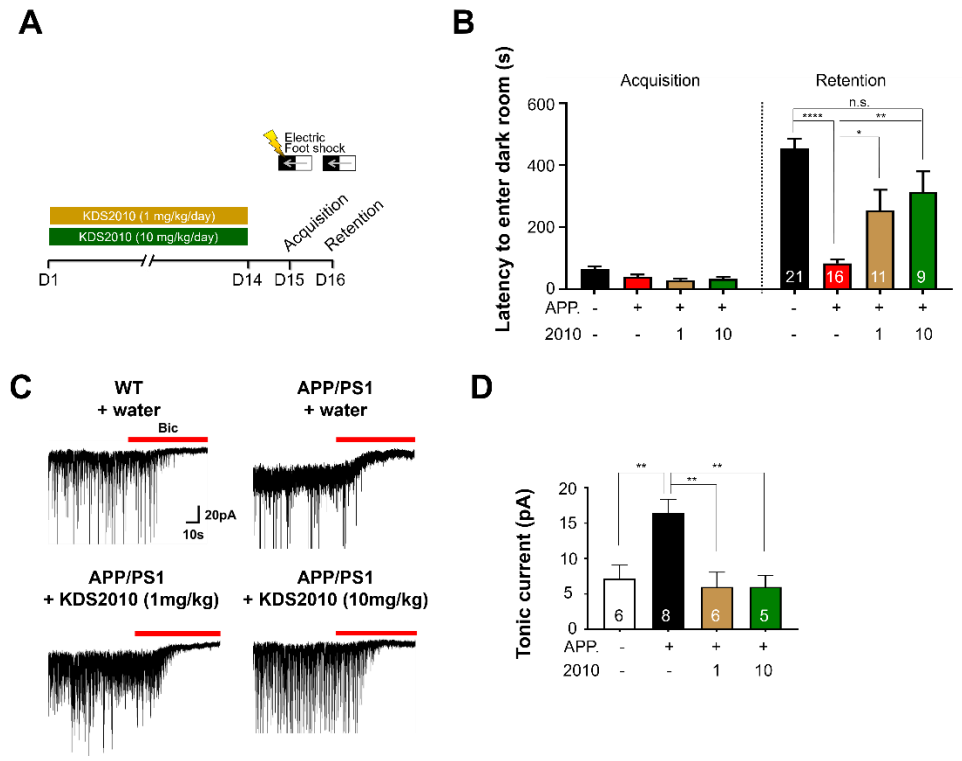

Fig. S7. Passive avoidance test for learning and memory in APP/PS1 mice with 2-week KDS2010 treatment. (**A**) Experimental protocol for the passive avoidance test for wild-type and APP/PS1 mice with oral administration of KDS2010 (1mg/kg or 10 mg/kg for 2-week). (**B**) Latency to enter the dark chamber during the passive avoidance test (*n*=21 for WT + water; *n*=16 for APP/PS1 + water; *n*=11 for APP/PS1 + KDS2010 1 mg/kg, *n*=9 for APP/PS1 + KDS2010 10 mg/kg; both sexes at 10- to 12-month of age). *$p < 0.05$, **$p < 0.01$, ****$p < 0.0001$, and (One-way ANOVA with *Tukey's* test). (**C**) Representative trace of $GABA_A$ receptor-mediated current recorded from granule cells of the dentate gyrus (*n*=6 for WT + water; *n*=8 for APP/PS1 + water; *n*=6 for APP/PS1 + KDS2010 1 mg/kg; *n*=5 for APP/PS1 + KDS2010 10 mg/kg; both sexes at 10- to 11-month of age). Red bars represent the application of $GABA_A$ receptor antagonist bicuculline (BIC; 20 μM). (**D**) Tonic GABA current by 20 μM BIC. **$p < 0.01$ (One-way ANOVA with *Tukey's* test). n.s., not significant Data are means ± s.e.m. Data distribution of bar graphs was presented in the Fig. S10.

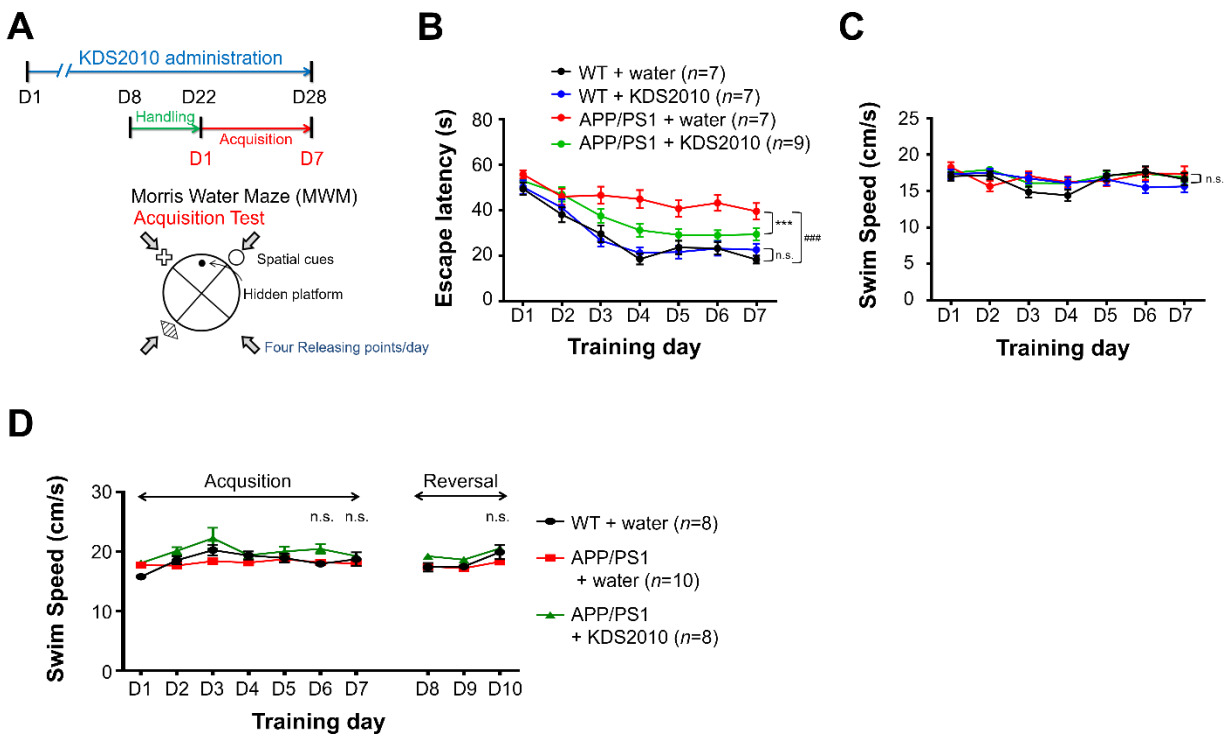

Fig. S8. KDS2010 significantly recovers spatial learning and memory in Morris water maze. (**A**) Experimental protocol for Morris water maze test for WT and APP/PS1 mice with or without oral administration of KDS2010 (10 mg/kg/day for 28 days; both sexes at 10- to 12-month of age). (**B**) Escape latency during acquisition test. ***p < 0.001, compared with APP/PS1, $^{###}p$ < 0.001, compared with WT (Two-way repeated measures ANOVA) (**C**) Swimming speed during acquisition test. n.s., not significant. (Two-way repeated measures ANOVA followed by Fisher's LSD analysis). (**D**) Swimming speed during acquisition and reversal test (37 day-treatment). Compared with APP/PS1 + water., n.s., not significant, Acquisition (One-way ANOVA with *Tukey's* test), Reversal (One-way ANOVA with *Dunnett's* test). Also see table S6.

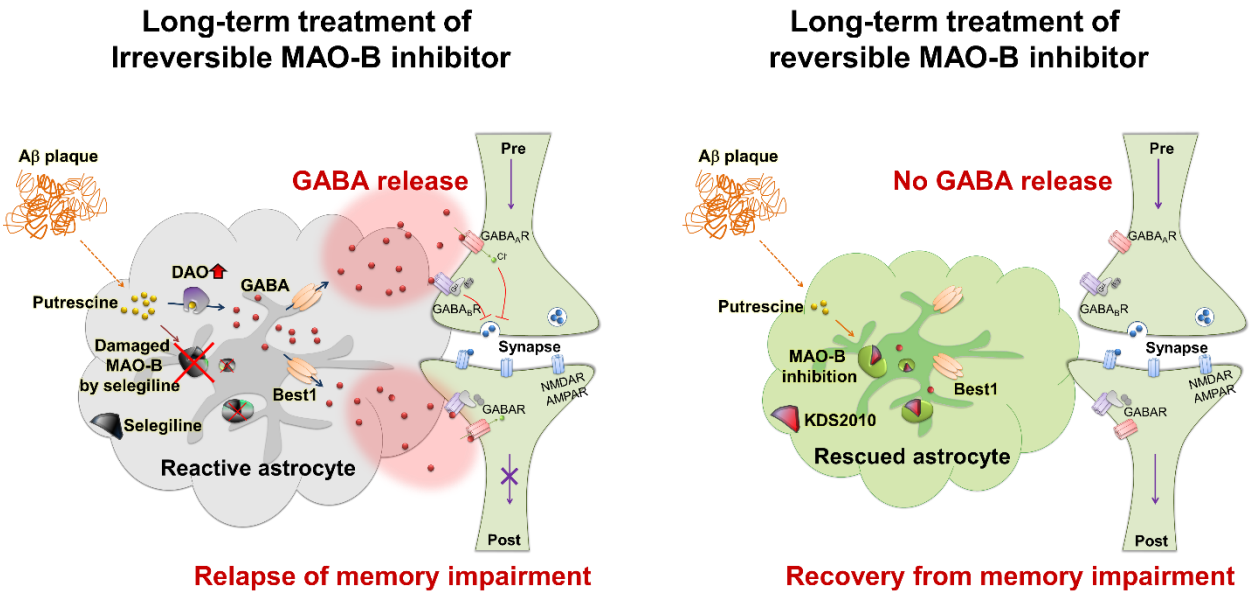

Fig. S9. Model diagrams of long-term treatment of AD with either irreversible or reversible MAO-B inhibitors. Aβ: amyloid-beta, MAO-B: monoamine oxidase-B, DAO: diamine oxidase, Best1: bestrophin 1, Pre: presynaptic terminal, Post: postsynapse, NMDAR: *N*-methy-*D*-aspartate receptor, AMPAR: α-amino-3-hydroxy-5-methyl-4-isoxazole propionate receptor

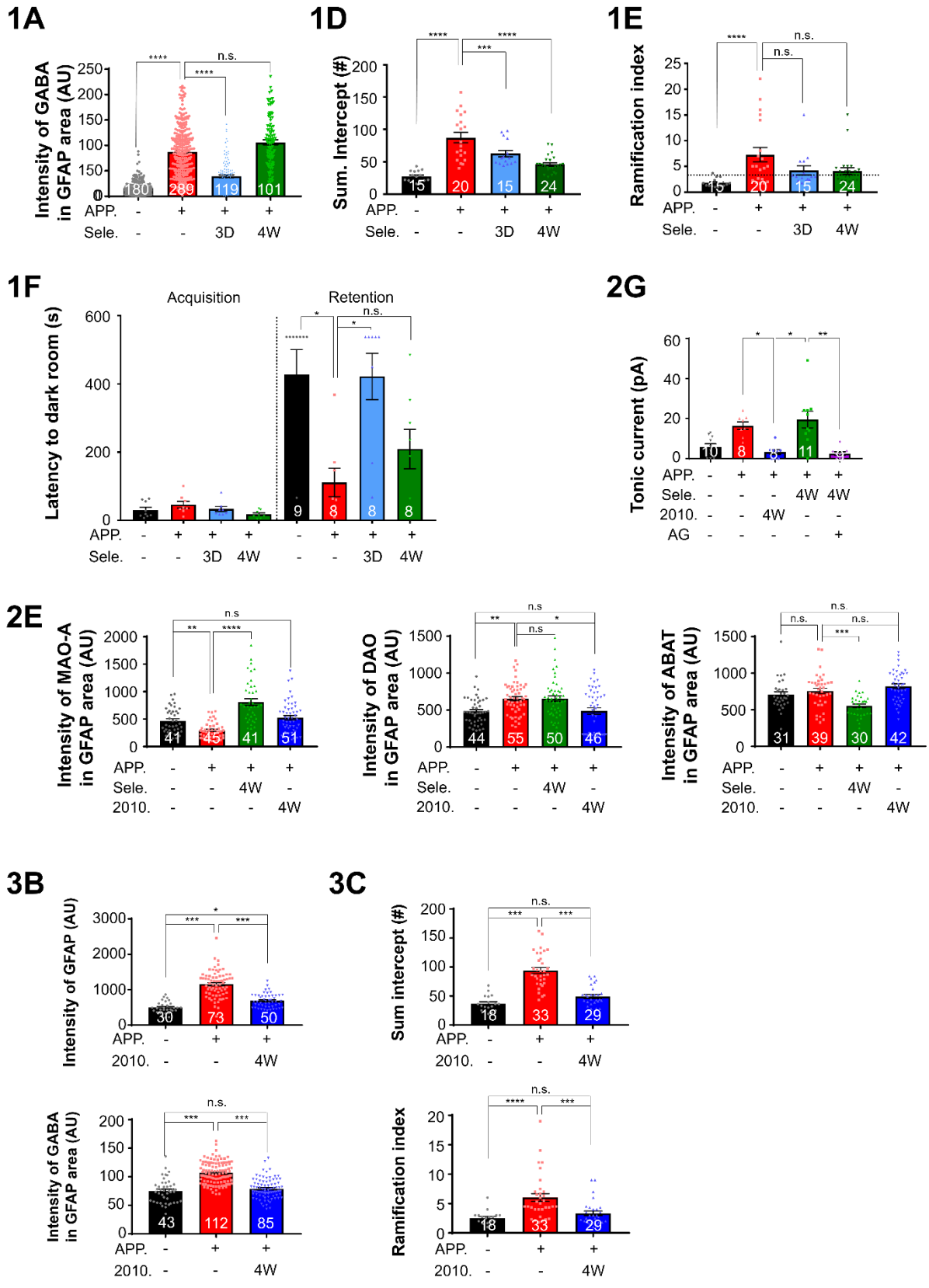

Fig. S10. Data distribution of bar graphs.

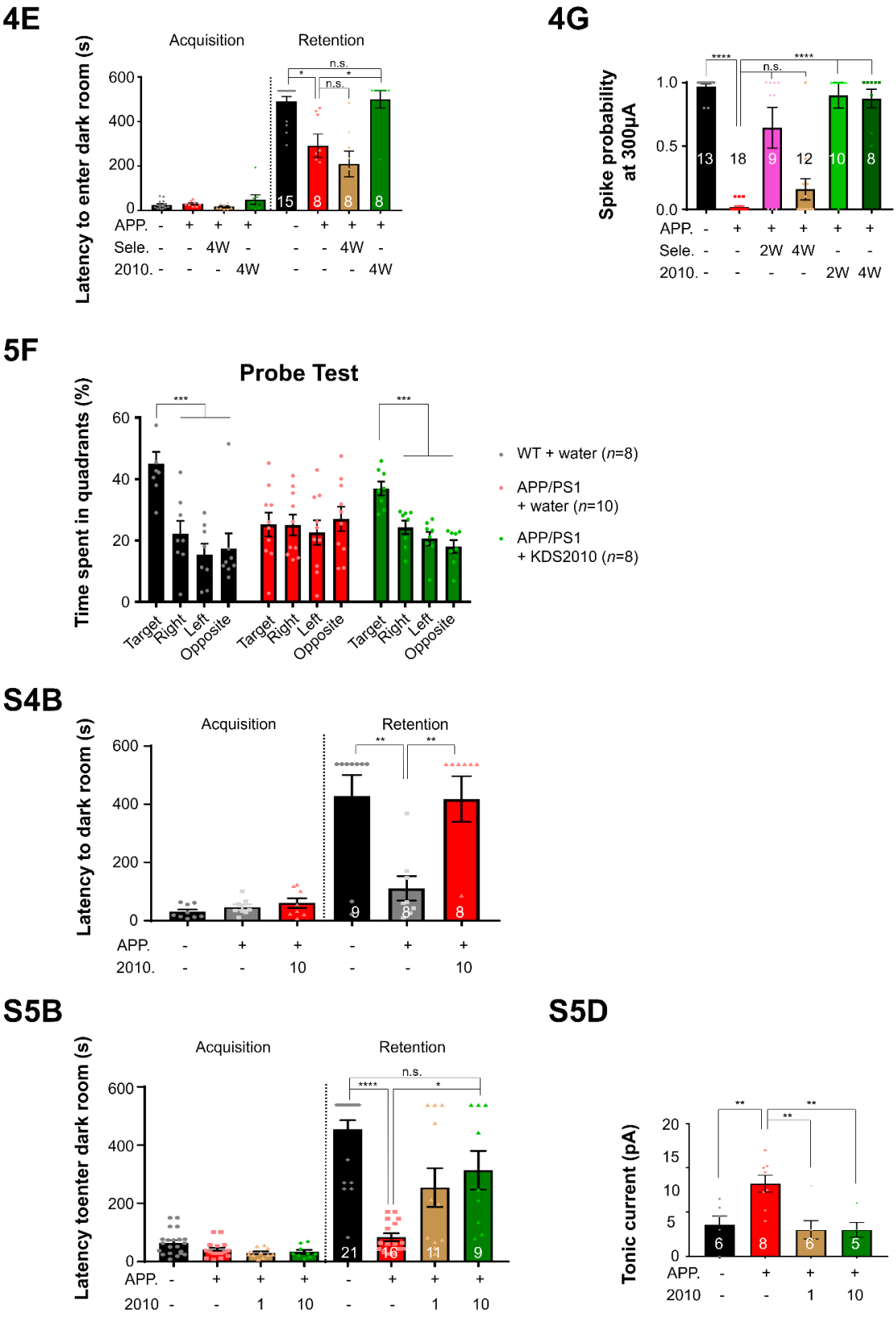

Fig. S10. Data distribution of bar graphs (continued).

Table S1. Inhibitory effects of the synthesized compounds against hMAO enzymes.

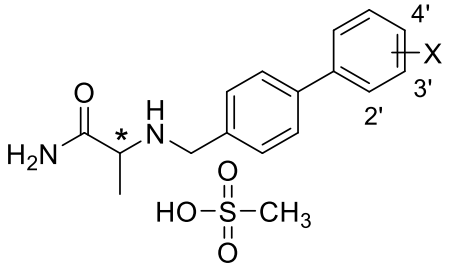

Compound Code	Stereo	X	Inhibition (IC_{50}, μM) [a]		SI [b]
			hMAO-B	hMAO-A	
KDS2051 [a]	*S*	H	>10	> 100	nd [e]
KDS0011	*S*	2'-F	8.24 ± 0.16	> 100	>12.1
KDS0015	*S*	3'-F	3.69 ± 0.08	> 100	>27.1
KDS2006	*S*	4'-F	4.29 ± 0.08	> 100	>23.3
KDS2042	*S*	2'-Cl	> 10	> 100	nd [e]
KDS0014	*S*	3'-Cl	0.242 ± 0.008	> 100	>413
KDS2005	*S*	4'-Cl	0.182 ± 0.007	> 100	>549
KDS2041	*S*	2'-CF_3	> 10	> 100	nd [e]
KDS0012	*S*	3'-CF_3	0.316 ± 0.006	> 100	>316
KDS2010	*S* [c]	4'-CF_3	0.008 ± 0.001	> 100	>10,000
KDS2002	*S*	3'-OCF_3	0.216 ± 0.005	> 100	>463
KDS2001	*S*	4'-OCF_3	0.098 ± 0.003	> 100	>1,020
KDS2029 (*R*-isomer of KDS2010)	*R* [c]	4'-CF_3	0.058 ± 0.003	> 100	>1,724
Selegiline [d]			0.010 ± 0.001	1.5 ± 0.02	150
Sembragiline [d]			0.015 ± 0.005 0.006 ± 0.001 [f]	3.85 [f]	653 [f]

[a] Inhibition data are reported as IC_{50} (μM) ; the SEM was always less than ±5%.
[b] SI; selectivity index, the selectivity for the MAO-B isoform and is given as the ratio of IC_{50}(MAO-A)/IC_{50}(MAO-B).
[c] Enantiomeric purity of KDS2010 & KDS2029; both ~9:1 enantiomeric mixture
[d] Positive controls; selegiine: irreversible inhibitor, sembragiline: reversible inhibitor.
[e] nd: not determined.
[f]: Borroni, E. et al. Sembragiline: a novel, selective monoamine oxidase type B inhibitor for the treatment of Alzheimer's disease. *J. Pharmacol. Exp. Ther*. 362, 413-423 (2017)

Table S2. In vitro and in vivo ADME/Tox profile of KDS2010.

Stability (% remaining)[a]			CYP inhibition		*In vivo* Toxicity (Rat)		hERG inhibition, IC_{50} (μM)[d]
Species	Microsomes	Plasma	Subtype	% Inhibition at 10 μM	Dosing (*p.o.*)	NOAEL[b] (mg/kg)	
Human	92.2±7.2	98.3±5.2	1A2	62.5±2.8	Single	>1000	>50
Dog	60.7±5.2	nd[c]	2C9	99.1±4.3	Repeated (2weeks)	>200	
Rat	59.5±6.5	95.2±6.7	2C19	84.0±3.8			
Mouse	66.0±3.1	nd[c]	2D6	89.3±6.1			
			3A4	98.8±5.7			

[a]% Parent compound remaining was determined after 30 min (microsomes) or 120 min (plasma) incubation.
[b]NOAEL; No observed adverse effect level, the highest tested dose at which no such adverse effect is found in exposed test organisms. %.
[c]nd; Not determined. %.
[d]hERG channel binding assay was performed using predictor hERG fluorescence polarization assay. IC_{50} value was calculated with nonlinear regression fit with four parameters.

Table S3. In vivo pharmacokinetic parameters of KDS2010.

Compd.	PK[a]						
	i.v.				*p.o.*		*F* (%)
	AUC_{all} (ng*h/mL)	*CL* (mL/min/kg)	V_{ss} (L/kg)	$t_{1/2}$ (h)	C_{max} (ng/mL)	AUC_{all} (ng*h/mL)	
KDS2010	421.1±42.6	39.9±4.0	10.1±0.8	3.3±0.2	952.1±80.3	5201.5±458	123.5

Compd.	Plasma concentration (ng/mL)	Brain concentration[b] (ng/g)	Brain-to-plasma ratio[c] (B/P)
KDS2010	730.2±51.3	6,716.3±260.6	9.2

[a]Rats (n = 5) were dosed with 1 mg/kg for *i.v.* and 10 mg/kg for *p.o.*. Parameters were calculated from composite mean plasma concentration-time data. Data are expressed as the mean ± SD. %.

[b]Brain concentration was determined by the amount of KDS2010 in total brain homogenate from rats (n = 5, 2 h after oral administration with 10 mg/kg).

[c]B/P: brain concentration/plasma concentration (2 h after oral administration with 10 mg/kg) calculated using 1 g/mL brain density.

Abbreviations: *Compd*, compound; *AUC*, area under the plasma concentration–time curve; *CL*, time-averaged total body clearance; V_{ss}, apparent volume of distribution at steady state; $t_{1/2}$, elimination half-life; C_{max}, maximum concentration of the drug; *F*, bioavailability

Table S4. KDS2010 interactions with 87 primary molecular targets including GPCRs, kinases, non-kinase enzymes, nuclear receptors, transporters, and various ion channels.

Target	Abbreviation	Species	Substrate	% Binding response at 1μM
GPCR				
Adenosine A_1	A_1	Human	1.0 nM [^{3}H] DPCPX	3
Adenosine A_{2A}	A_{2A}	Human	0.050 μM [^{3}H] CGS-21680	-2
Adrenergic α_{1A}	α_{1A}	Rat	0.25 nM [^{3}H] Prazosin	5
Adrenergic α_{1B}	α_{1B}	Rat	0.25 nM [^{3}H] Prazosin	2
Adrenergic α_{1D}	α_{1D}	Human	0.60 nM [^{3}H] Prazosin	-3
Adrenergic α_{2A}	α_{2A}	Human	1.50 nM [^{3}H] Rauwolscine	8
Adrenergic α_{2B}	α_{2B}	Human	2.50 nM [^{3}H] Rauwolscine	-3
Adrenergic β_1	β_1	Human	0.030 nM [^{125}I] Cyanopindolol	-3
Adrenergic β_2	β_2	Human	0.20 nM [^{3}H] CGP-12177	0
Angiotensin AT_1	AT_1	Human	20.0 pM [^{125I}] (Sar^1, Ile^8)-Angiotensin II	-2
Bradykinin B_2	B_2	Human	0.50 nM [^{3}H] Bradykinin	-2
Cannabinoid CB_1	CB_1	Human	2.0 nM [^{3}H] SR141716A	-5
Cannabinoid CB_2	CB_2	Human	2.40 nM [^{3}H] WIN-55,212-2	11
Chemokine CCR1	CCR1	Human	0.10 nM [^{125}I] MIP-1α	-4
Chemokine CXCR2 (IL-8RB)	CXCR2	Human	15.0 pM [^{125}I] IL-8	10
Cholecystokinin CCK_1 (CCK_A)	CCK_1	Human	0.11 nM [^{125}I] CCK-8	-13
Cholecystokinin CCK_2 (CCK_B)	CCK_2	Human	0.050 nM [^{125}I] CCK-8	10
Dopamine D_1	D_1	Human	1.40 nM [^{3}H] SCH-23390	2
Dopamine D_{2L}	D_{2L}	Human	0.16 nM [^{3}H] Spiperone	5
Dopamine D_{2S}	D_{2S}	Human	0.16 nM [^{3}H] Spiperone	0
Endothelin ET_A	ET_A	Human	0.030 nM [^{125}I] Endothelin-1	11
$GABA_{B1A}$	$GABA_{B1A}$	Human	4.0 nM [^{3}H] CGP-54626	-4
Glutamate, Metabotropic,$mGlu_5$	$mGlu_5$	Human	0.030 μM [^{3}H] Quisqualic acid	14
Histamine H_1	H_1	Human	1.20 nM [^{3}H] Pyrilamine	11
Histamine H_2	H_2	Human	0.10 nM [^{125}I] Aminopotentidine	1
Leukotriene, Cysteinyl $CysLT_1$	$CysLT_1$	Human	0.30 nM [^{3}H] LTD4	2
Melanocortin MC_1	MC_1	Human	0.040 nM [^{125}I] NDP-α-MSH	-3
Melanocortin MC_4	MC_4	Human	20.0 pM [^{125}I] NDP-α-MSH	8
Muscarinic M_1	M_1	Human	0.80 nM [^{3}H] N-Methylscopolamine	-3
Muscarinic M_2	M_2	Human	0.80 nM [^{3}H] N-Methylscopolamine	-2
Muscarinic M_3	M_3	Human	0.80 nM [^{3}H] N-Methylscopolamine	1
Muscarinic M_4	M_4	Human	0.80 nM [^{3}H] N-Methylscopolamine	3
Tachykinin NK_1	NK_1	Human	0.80 nM [^{3}H] Substance P	-11
Opiate δ1 (OP1, DOP)	DOP	Human	1.30 nM [^{3}H] Naltrindole	7
Neuropeptide Y Y_1	NPY_1	Human	15.0 pM [^{125}I] Peptide YY	-4
Opiate κ(OP2, KOP)	KOP	Human	0.60 nM [^{3}H] Diprenorphine	-1
Opiate μ(OP3, MOP)	MOP	Human	0.60 nM [^{3}H] Diprenorphine	14
Platelet Activating Factor (PAF)	PAF	Human	0.12 nM [^{3}H] PAF	-10
Serotonin (5-Hydroxytryptamine) $5\text{-}HT_{1A}$	$5\text{-}HT_{1A}$	Human	1.50 nM [^{3}H] 8-OH-DPAT	2
Serotonin (5-Hydroxytryptamine) $5\text{-}HT_{1B}$	$5\text{-}HT_{1B}$	Human	1.0 nM [^{3}H] GR125743	-3
Serotonin (5-Hydroxytryptamine) $5\text{-}HT_{2A}$	$5\text{-}HT_{2A}$	Human	0.50 nM [^{3}H] Ketanserin	-3
Serotonin (5-Hydroxytryptamine) $5\text{-}HT_{2B}$	$5\text{-}HT_{2B}$	Human	1.20 nM [^{3}H] Lysergic acid diethylamide (LSD)	19
Serotonin (5-Hydroxytryptamine) $5\text{-}HT_{2C}$	$5\text{-}HT_{2C}$	Human	1.0 nM [^{3}H] Mesulergine	-5

Vasopressin V_{1A}	V_{1A}	Human	0.030 nM [^{125}I]PhenylacetylTyr(Me)PheGlnAsnArg ProArgTyr	-6
Kinase				
Protein Tyrosine Kinase, Insulin Receptor	IR	Human	200 µg/mL Poly(Glu:Tyr)	-15
Protein Tyrosine Kinase, LCK	LCK	Human	200 µg/mL Poly(Glu:Tyr)	0
Protein Serine/Threonine Kinase, PKC, Nonselective	PKC	Rat	370 µg/mL Histone	12
Non-Kinase Enzyme				
ATPase, Na^+/K^+, Heart	ATPase	Pig	100 µM ATP	-9
Phosphodiesterase PDE4	PDE4	Human	1.01 µM [^{3}H]cAMP + cAMP	-5
Peptidase, CTSG (Cathepsin G)	CTSG	Human	20.0 µM Suc-Ala-Ala-Pro-Phe-AMC	0
Peptidase, Angiotensin Converting Enzyme	ACE	Rabbit	500 µM (N-3-[2-furyl] acryloyl)-Phe-Gly-Gly (FAPGG)	0
Cholinesterase, Acetyl	ACES	Human	700 µM Acetylthiocholine	27
Cyclooxygenase COX-1	COX-1	Human	100 µM Arachidonic acid	15
Cyclooxygenase COX-2	COX-2	Human	0.30 µM Arachidonic acid	-11
Monoamine Oxidase MAO-A	Mao-a	Human	50.0 µM Kynuramine	5
Monoamine Oxidase MAO-B	Mao-b	Human	50.0 µM Kynuramine	99
Phosphodiesterase PDE3	PDE3	Human	1.01 µM [^{3}H]cAMP + cAMP	-7
PPARγ	PPARγ	Human	5.0 nM [^{3}H] Rosiglitazone	-3
Nuclear Receptor				
Androgen (Testosterone)	AR	Human	0.50 nM [^{3}H] Methyltrienolone	-3
Estrogen ERα	ERα	Human	0.50 nM [^{3}H] Estradiol	1
Glucocorticoid	GR	Human	5.0 nM [^{3}H] Dexamethasone	7
Progesterone PR-B	PR-B	Human	0.50 nM [^{3}H] Progesterone	-4
Transporter				
Transporter, Adenosine	AT	Guinea Pig	0.50 nM [^{3}H] Nitrobenzylthioinosine	5
Transporter, Dopamine (DAT)	DAT	Human	0.15 nM [^{125}I] RTI-55	8
Transporter, GABA	GAT	Rat	6.0 nM [^{3}H] GABA	4
Transporter, Norepinephrine (NET)	NET	Human	0.20 nM [^{125}I] RTI-55	12
Transporter, Serotonin (SERT)	SERT	Human	0.40 nM [^{3}H] Paroxetine	-3
Channel				
$GABA_A$, Chloride Channel, TBOB	$GABA_A$, C	Rat	3.0 nM [^{3}H] TBOB	0
$GABA_A$, Flunitrazepam, Central	$GABA_A$, F	Rat	1.0 nM [^{3}H] Flunitrazepam	9
Glutamate, NMDA, Agonism	NMDA, A	Rat	2.0 nM [^{3}H] CGP-39653	2
$GABA_A$, Ro-15-1788, Hippocamp`us	$GABA_A$, R	Rat	1.0 nM [^{3}H] Ro-15-1788	17
Glutamate, AMPA	AMPA	Rat	5.0 nM [^{3}H] AMPA	2
Glutamate, Kainate	Kainate	Rat	5.0 nM [^{3}H] Kainic acid	-1
Glutamate, NMDA, Glycine	NMDA, G	Rat	0.33 nM [^{3}H] MDL 105,519	1
Glutamate, NMDA, Phencyclidine	NMDA, Ph	Rat	4.0 nM [^{3}H] TCP	3
Glutamate, NMDA, Polyamine	NMDA, Poly	Rat	2.0 nM [^{3}H] Ifenprodil	2
Glycine, Strychnine-Sensitive	Glycine	Rat	10 nM [^{3}H] Strychnine	2
Nicotinic Acetylcholine	nAchR	Human	0.10 nM [^{125}I] Epibatidine	-10
Nicotinic Acetylcholine α1, Bungarotoxin	nAchR α1	Human	0.60 nM [^{125}I] α-Bungarotoxin	-5
Serotonin (5-Hydroxytryptamine) 5-HT_3	5-HT_3	Human	0.69 nM [^{3}H] GR-65630	11
Calcium Channel L-Type, Dihydropyridine	CAV (L-TYPE), D	Rat	0.10 nM [^{3}H] Nitrendipine	-1
Calcium Channel L-Type, Benzothiazepine	CAV (L-TYPE), B	Rat	2.0 nM [^{3}H] Diltiazem	-8
Calcium Channel L-Type,	CAV	Rat	0.40 nM [^{3}H] (-)-Desmethoxyverapamil	16

Phenylalkylamine	(L-TYPE), P		(D-888)	
Calcium Channel N-Type	CAV (N-TYPE)	Rat	10 pM [^{125}I] ω-Conotoxin GVIA	0
Potassium Channel [K_{ATP}]	K_{ATP}	Human	5.0 nM [^{3}H] Glyburide	-7
Potassium Channel hERG	hERG	Human	1.50 nM [^{3}H] Astemizole	3
Sodium Channel, Site 2	Na channel	Rat	5.0 nM [^{3}H] Batrachotoxinin	38

Table S5. KDS2010 interactions with 97 kinase including TK, TKL, STE, CK1, AGC, CAMK, CMGC, ATYPICAL, LIPID, and Mutant form.

Target	Abbreviation	%Ctrl comp. inhibition at 1 μM
TK		
c-abl oncogene 1, receptor tyrosine kinase	ABL1-nonphosphorylated	10
c-abl oncogene 1, receptor tyrosine kinase	ABL1-phosphorylated	8
anaplastic lymphoma receptor tyrosine kinase	ALK	41
AXL receptor tyrosine kinase	AXL	17
bone morphogenetic protein receptor, type II (serine/threonine kinase)	BMPR2	0
Bruton agammaglobulinemia tyrosine kinase	BTK	5
colony stimulating factor 1 receptor	CSF1R	1
epidermal growth factor receptor	EGFR	0
EPH receptor A2	EPHA2	15
erb-b2 receptor tyrosine kinase 2	ERBB2	8
erb-b2 receptor tyrosine kinase 4	ERBB4	6
PTK2 protein tyrosine kinase 2	PTK2	4
fibroblast growth factor receptor 2	FGFR2	10
fibroblast growth factor receptor 3	FGFR3	6
fms-related tyrosine kinase 3	FLT3	14
insulin-like growth factor 1 receptor	IGF1R	0
insulin receptor	INSR	28
Janus kinase 2	JAK2(JH1 domain-catalytic)	28
Janus kinase 3	JAK3 (JH1 domain-catalytic)	10
v-kit Hardy-Zuckerman 4 feline sarcoma viral oncogene homolog	KIT	0
met proto-oncogene (hepatocyte growth factor receptor)	MET	4
platelet-derived growth factor receptor, alpha polypeptide	PDGFRA	6
platelet-derived growth factor receptor, beta polypeptide	PDGFRB	0
ret proto-oncogene	RET	13
SRC proto-oncogene, non-receptor tyrosine kinase	SRC	10
TEK tyrosine kinase, endothelial	TEK	5
neurotrophic tyrosine kinase, receptor, type 1	NTRK1	0
tyrosine kinase 2	TYK2	44
kinase insert domain receptor (a type III receptor tyrosine kinase)	KDR	0
zeta-chain (TCR) associated protein kinase 70kDa	ZAP70	0
TKL		
activin A receptor, type IB	ACVR1B	5
v-raf murine sarcoma viral oncogene homolog B1	BRAF	6
mitogen-activated protein kinase kinase kinase 9	MAP3K9	9
v-raf-1 murine leukemia viral oncogene homolog 1	RAF1	3
transforming growth factor, beta receptor 1	TGFBR1	17
STE		
mitogen-activated protein kinase kinase kinase 4	MAP3K4	1
mitogen-activated protein kinase kinase 1	MAP2K1	9
mitogen-activated protein kinase kinase 2	MAP2K2	0
p21 protein (Cdc42/Rac)-activated kinase 1	PAK1	6
p21 protein (Cdc42/Rac)-activated kinase 2	PAK2	22
p21 protein (Cdc42/Rac)-activated kinase 3	PAK4	0
CK1		
casein kinase 1, delta	CSNK1D	0
casein kinase 1, gamma 2	CSNK1G2	2

AGC		
v-akt murine thymoma viral oncogene homolog 1	AKT1	7
v-akt murine thymoma viral oncogene homolog 2	AKT2	0
3-phosphoinositide dependent protein kinase-1	PDPK1	2
protein kinase, cAMP-dependent, catalytic, alpha	PRKACA	21
protein kinase C, epsilon	PRKCE	0
Rho-associated, coiled-coil containing protein kinase 2	ROCK2	0
ribosomal protein S6 kinase, 90kDa, polypeptide 3	RPS6KA3	0
serine/threonine kinase 32C	STK32C	0
CAMK		
checkpoint kinase 1	CHEK1	0
doublecortin-like kinase 1	DCLK1	33
serine/threonine kinase 11	STK11	0
mitogen-activated protein kinase-activated protein kinase 2	MAPKAPK2	21
MAP/microtubule affinity-regulating kinase 3	MARK3	2
MAP kinase interacting serine/threonine kinase 1	MKNK1	5
MAP kinase interacting serine/threonine kinase 2	MKNK2	15
pim-1 oncogene	PIM1	0
pim-2 oncogene	PIM2	6
pim-3 oncogene	PIM3	5
NUAK family, SNF1-like kinase, 2	NUAK2	0
testis-specific serine kinase 1B	TSSK1B	0
CMGC		
cyclin-dependent kinase 19	CDK19	2
cyclin-dependent kinase 2	CDK2	4
cyclin-dependent kinase 3	CDK3	3
cyclin-dependent kinase 7	CDK7	3
cyclin-dependent kinase 9	CDK9	0
dual-specificity tyrosine-(Y)-phosphorylation regulated kinase 1B	DYRK1B	3
MAP/microtubule affinity-regulating kinase 3	MAPK3	4
glycogen synthase kinase 3 beta	GSK3B	8
mitogen-activated protein kinase 8	MAPK8	14
mitogen-activated protein kinase 9	MAPK9	4
mitogen-activated protein kinase 10	MAPK10	14
mitogen-activated protein kinase 14	MAPK14	3
mitogen-activated protein kinase 11	MAPK11	0
cyclin-dependent kinase 16	CDK16	30
polo-like kinase 1	PLK1	11
polo-like kinase 3	PLK3	13
polo-like kinase 4	PLK4	28
SFRS protein kinase 3	SRPK3	21
OTHER		
aurora kinase A	AURKA	20
aurora kinase B	AURKB	8
conserved helix-loop-helix ubiquitous kinase	CHUK	3
inhibitor of kappa light polypeptide gene enhancer in B-cells, kinase beta	IKBKB	12
unc-51-like kinase 2	ULK2	0
ATYPICAL		
coenzyme Q8A	CABC1	11
RIO kinase 2	RIOK2	3
LIPID		
phosphoinositide-3-kinase, class 2, beta polypeptide	PIK3C2B	2
phosphoinositide-3-kinase, catalytic, alpha polypeptide	PIK3CA	0
phosphoinositide-3-kinase, catalytic, gamma polypeptide	PIK3CG	0
MUTANT		
c-abl oncogene 1, receptor tyrosine kinase	ABL1(E255K)-phosphorylated	0

c-abl oncogene 1, receptor tyrosine kinase	ABL1(T315I)-phosphorylated	10
v-raf murine sarcoma viral oncogene homolog B1	BRAF(V600E)	9
epidermal growth factor receptor	EGFR(L858R)	29
v-kit Hardy-Zuckerman 4 feline sarcoma viral oncogene homolog	KIT(D816V)	8
v-kit Hardy-Zuckerman 4 feline sarcoma viral oncogene homolog	KIT(V559D,T670I)	5

Table S6. Detailed information for statistical analysis.

Figure No.	Result from statistical analysis
1B	WT + water (16.0068 ± 1.077, *n*=180), APP/PS1 + water (87.4866 ± 2.946, *n*=289), APP/PS1 + Selegiline 3D (39.5503 ± 2.691, *n*=119), APP/PS1 + Selegiline 4W (105.996 ± 5.117, *n*=101) *Kruskal-Wallis* test with *Dunnett's* multiple comparisons test Kruskal-Wallis statistcs = 354.1 WT + water vs. APP/PS1 + Water, $p < 0.0001$; APP/PS1 + water vs. APP/PS1 + Selegiline 3D, $p < 0.0001$; APP/PS1 + water vs. APP/PS1 + Selegiline 4W, $p = 0.1111$
1D	WT + water (27.47 ± 2.178, *n*=15), APP/PS1 + water (87.15 ± 7.899, *n*=20), APP/PS1 + Selegiline 3D (62.53 ± 5.079, *n*=15), APP/PS1 + Selegiline 4W (45.92 ± 2.746, *n*=24) One-way ANOVA with *Tukey's* multiple comparisons test $F(3, 70) = 23.59$, $p < 0.0001$ WT + water vs. APP/PS1 + water, $p < 0.0001$; APP/PS1 + water vs. APP/PS1 + Selegiline 3D, $p = 0.0092$; APP/PS1 + water vs. APP/PS1 + Selegiline 4W, $p < 0.0001$
1E	WT + water (1.789 ± 0.2144, *n*=15), APP/PS1 + water (7.265 ± 1.388, *n*=20), APP/PS1 + Selegiline 3D (4.233 ± 0.8632, *n*=15), APP/PS1 + Selegiline 4W (4.072 ± 0.6429, *n*=24) *Kruskal-Wallis* test with *Dunnett's* multiple comparisons test Kruskal-Wallis statistcs = 22.3 WT + water vs. APP/PS1 + water, $p < 0.0001$; APP/PS1 + water vs. APP/PS1 + Selegiline 3D, $p > 0.9999$; APP/PS1 + water vs. APP/PS1 + Selegiline 4W, $p = 0.8297$
1F	Acquisition: WT + water (30.92 ± 7.659, *n*=9), APP/PS1 + water (46.31 ± 9.886, *n*=8), APP/PS1 + Selegiline 3D (33.46 ± 7.607, *n*=8), APP/PS1 + Selegiline 4W (17.76 ± 4.116, *n*=8) Retention: WT + water (428.3 ± 72.65, *n*=9), APP/PS1 + water (111.2 ± 41.86, *n*=8), APP/PS1 + Selegiline 3D (422.1 ± 67.81, *n*=8), APP/PS1 + Selegiline 4W (209.3 ± 57.79, *n*=8) *Kruskal-Wallis* test with *Dunnett's* multiple comparisons test Kruskal-Wallis statistcs = 13.59 WT + water vs. APP/PS1 + Water, $p = 0.0152$; APP/PS1 + water vs. APP/PS1 + Selegiline 3D, $p = 0.0205$; APP/PS1 + water vs. APP/PS1 + Selegiline 4W, $p > 0.9999$
3F	WT + water (483.8.3 ± 25.87, *n*=44), APP/PS1 + water (654 ± 29.49, *n*=55), APP/PS1 + Selegiline 4W (654.5 ± 39.16, *n*=50), APP/PS1 + KDS2010 4W (486.8 ± 43.39, *n*=46) *Kruskal-Wallis* test with *Dunnett's* multiple comparisons test Kruskal-Wallis statistcs = 19.68 WT + water vs. APP/PS1 + water, $p = 0.0020$; WT + water vs. APP/PS1 + KDS2010 4W, $p > 0.9999$; APP/PS1 + water vs. APP/PS1 + Selegiline 4W, $p > 0.9999$; APP/PS1 + water vs. APP/PS1 + KDS2010 4W, $p = 0.0126$
3H	WT + water (7.167 ± 1.956, *n*=10), APP/PS1 + water (16.41 ± 1.916, *n*=8), APP/PS1 + KDS2010 4W (3.3 ± 1.243, *n*=8), APP/PS1 + Selegiline 4W (17.71 ± 4.122, *n*=11), APP/PS1 + Selegiline 4W + AG (2.467 ± 0.8841, *n*=9) *Kruskal-Wallis* test with *Dunnett's* multiple comparisons test Kruskal-Wallis statistcs = 24.02 APP/PS1 + water vs. APP/PS1 + KDS2010 4W, $p = 0.0282$; APP/PS1 + KDS2010 4W vs. APP/PS1 + Selegiline 4W, $p = 0.0178$;

	APP/PS1 + Selegiline 4W vs. APP/PS1 + Selegiline 4W+AG, $p = 0.0023$
4B	WT + water (495.9 ± 30.33, n=30), APP/PS1 + water (1156 ± 42.93, n=73), APP/PS1 + KDS2010 4W (688.9 ± 27.55, n=50) One-way ANOVA with *Tukey's* multiple comparisons test F(2, 149) = 72.41, $p < 0.0001$ WT + water vs. APP/PS1 + water, $p < 0.0001$; WT + water vs. APP/PS1 + KDS2010 4W, $p = 0.0107$; APP/PS1 + water vs. APP/PS1 + KDS2010 4W, $p < 0.0001$
	WT + water (75.25 ± 3.18, n=43), APP/PS1 + water (106.6 ± 1.808, n=112), APP/PS1 + KDS2010 4W (78.87 ± 1.867, n=85) *Kruskal-Wallis* test with *Dunnett's* multiple comparisons test Kruskal-Wallis statistcs = 94.82 WT + water vs. APP/PS1 + water, $p < 0.0001$; WT + water vs. APP/PS1 + KDS2010 4W, $p > 0.9999$; APP/PS1 + water vs. APP/PS1 + KDS2010 4W, $p < 0.0001$
4C	WT + water (36.89± 3.195, n=18), APP/PS1 + water (93.88 ± 5.23, n=33), APP/PS1 + KDS2010 4W (49.03 ± 3.391, n=29) One-way ANOVA with *Tukey's* multiple comparisons test F(2, 77) = 45.75, $p < 0.0001$ WT + water vs. APP/PS1 + water, $p < 0.0001$; WT + water vs. APP/PS1 + KDS2010 4W, $p = 0.1947$; APP/PS1 + water vs. APP/PS1 + KDS2010 4W, $p < 0.0001$
	WT + water (2.533± 0.2713, n=18), APP/PS1 + water (6.017 ± 0.6702, n=33), APP/PS1+KDS2010 4W (3.344 ± 0.388, n=29) *Kruskal-Wallis* test with *Dunnett's* multiple comparisons test Kruskal-Wallis statistcs = 22.45 WT + water vs. APP/PS1 + water, $p < 0.0001$; WT + water vs. APP/PS1 + KDS2010 4W, $p = 0.8135$; APP/PS1 + water vs. APP/PS1 + KDS2010 4W, $p = 0.0009$
4E	Acquisition: WT + water (26.27 ± 4.744, n=15), APP/PS1 + water (17.76 ± 4.116, n=8), APP/PS1 + Selegiline 4W (17.76 ± 4.116, n=8), APP/PS1 + KDS2010 4W (49.93 ± 21.46, n=8) Retention: WT + water (489.6 ± 22.15, n=15), APP/PS1 + water (291.3 ± 52.68, n=8), APP/PS1 + Selegiline 4W (209.3 ± 57.79, n=8), APP/PS1+KDS2010 4W (499.3 ± 38.66, n=8) *Kruskal-Wallis* test with *Dunnett's* multiple comparisons test Kruskal-Wallis statistcs = 22.59 WT + water vs. APP/PS1 + water, $p = 0.0103$; WT + water vs. APP/PS1 + KDS2010 4W, $p > 0.9999$; APP/PS1 + water vs. APP/PS1 + Selegiline 4W, $p > 0.9999$; APP/PS1 + water vs. APP/PS1 + KDS2010 4W, $p = 0.0167$
4G	WT + water (0.9692± 0.02083, n=13), APP/PS1 + water (0.01667 ± 0.009039, n=18), APP/PS1 + Selegiline 2W (0.6444 ± 0.1617, n=9), APP/PS1 + Selegiline 4W (0.1583 ± 0.0848, n=12), APP/PS1 + KDS2010 2W (0.9 ± 0.1, n=10), APP/PS1 + KDS2010 4W (0.875 ± 0.07258, n=8) *Kruskal-Wallis* test with *Dunnett's* multiple comparisons test Kruskal-Wallis statistcs = 45.47 WT + water vs. APP/PS1 + water, $p < 0.0001$; APP/PS1 + water vs. APP/PS1 + Selegiline 2W, $p = 0.0726$; APP/PS1 + water vs. APP/PS1 + Selegiline 4W, $p > 0.9999$; APP/PS1 + water vs. APP/PS1 + KDS2010 2W, $p < 0.0001$; APP/PS1 + water vs. APP/PS1 + KDS2010 4W, $p = 0.0010$

5B	Latency-Acquisition Test; One-way repeated measures ANOVA with *Fisher's LSD* post-hoc analysis F(2,101) = 28.789, $p < 0.001$ WT + water vs. APP/PS1 + water, $p < 0.001$; WT + water vs. APP/PS1 + KDS2010, $p < 0.001$; APP/PS1 + water vs. APP/PS1 + KDS2010, $p = 0.067$ One-way ANOVA with *Fisher's LSD* post-hoc analysis (for each day) Day 1−5: not significant; Day 6: APP/PS1 + water vs. APP/PS1 + KDS2010, $p = 0.016$; Day 7: APP/PS1 + water vs. APP/PS1 + KDS2010, $p < 0.001$
5C	Probe Test; One-way ANOVA with *Fisher's LSD* post-hoc test WT + water, F(3,28) = 10.560, $p < 0.001$; APP/PS1 + water, F(3,36) = 0.232, $p = 0.874$; APP/PS1 + KDS2010, F(3,28) = 14.779, $p < 0.001$
5D	Latency-Reversal Test; One-way repeated measures ANOVA with *Fisher's LSD* post-hoc analysis F(2,101) = 12.963, $p < 0.001$ WT + water vs. APP/PS1 + water, $p < 0.001$; WT + water vs. APP/PS1 + KDS2010, $p = 0.019$; APP/PS1 + water vs. APP/PS1 + KDS2010, $p = 0.012$ One-way ANOVA with *Fisher's LSD* post-hoc analysis (for each day) Day 1−2: not significant; Day 3: APP/PS1 + water vs. APP/PS1 + KDS2010, $p = 0.002$
Supple 6B	Acquisition: WT + water (30.92 ± 7.659, n=9), APP/PS1 + water (46.31 ± 9.886, n=8), APP/PS1 + KDS2010 3D (60.58 ± 16.69, n=8) Retention: WT + water (428.3 ± 72.65, n=9), APP/PS1 + water (111.2 ± 41.86, n=8), APP/PS1+KDS2010 3D (418.3 ± 78.46, n=8) One-way ANOVA with *Tukey's* multiple comparisons test F(2, 22) = 7.106, $p = 0.0042$ WT + water vs. APP/PS1 + water, $p = 0.0074$; APP/PS1 + water vs. APP/PS1 + KDS2010 3D, $p = 0.0117$
Supple 7B	Acquisition: WT + water (64.26 ± 9.091, n=21), APP/PS1 + water (40.37 ± 7.054, n=16), APP/PS1+ KDS2010 1 mg/kg (29.88 ± 4.766, n=11), APP/PS1 + KDS2010 10 mg/kg (33.22 ± 6.943, n=9) Retention: WT + water (454.4 ± 31.06, n=21), APP/PS1 + water (83.76 ± 13.28, n=16), APP/PS1+KDS2010 1 mg/kg (254.2 ± 66.54, n=11), APP/PS1+KDS2010 10 mg/kg (313.7 ± 66.47, n=9) One-way ANOVA with *Tukey's* multiple comparisons test F(3, 53) = 17.88, $p < 0.0001$ WT + water vs. APP/PS1 + water, $p < 0.0001$; WT + water vs. APP/PS1 + KDS2010 10 mg/kg, $p = 0.1114$; APP/PS1 + water vs. APP/PS1 + KDS2010 1 mg/kg, $p = 0.0323$; APP/PS1 + water vs. APP/PS1 + KDS2010 10 mg/kg, $p = 0.0039$
Supple 7D	WT + water (7.167 ± 1.956, n=6), APP/PS1 + water (16.41 ± 1.916, n=8), APP/PS1 + KDS2010 1 mg/kg (6.000 ± 2.066, n=6), APP/PS1+KDS2010 10 mg/kg (6.000 ± 1.643, n=5) One-way ANOVA with *Dunnett's* multiple comparisons test F(3, 21) = 7.654, $p = 0.0012$ WT + water vs. APP/PS1 + water, $p = 0.0085$;

	APP/PS1 + water vs. APP/PS1 + KDS2010 1 mg/kg, $p = 0.0045$; APP/PS1 + water vs. APP/PS1 + KDS2010 10 mg/kg, $p = 0.0061$
Supple 8B	Latency-Acquisition Test; Two-way repeated measures ANOVA Genotype effect: $F(1,116) = 71.076$, $p < 0.001$ Drug effect: $F(1,116) = 7.844$, $p = 0.006$ Genotype * Drug interaction: $F(1,116) = 11.498$, $p = 0.001$ One-way ANOVA with *Fisher's LSD* post-hoc analysis WT + water vs. WT + KDS2010, $p = 0.686$; WT + water vs. APP/PS1 + water, $p < 0.001$; WT + KDS2010 vs. APP/PS1 + water, $p < 0.001$; WT + KDS2010 vs. APP/PS1 + KDS2010, $p < 0.001$; APP/PS1 + water vs. APP/PS1 + KDS2010, $p < 0.001$
Supple 8C	Swim speed-Acquisition Test Two-way repeated measures ANOVA Genotype effect: $F(1,116) = 1.328$, $p = 0.252$ Drug effect: $F(1,116) = 0.035$, $p = 0.851$ Genotype * Drug interaction: $F(1,116) = 0.001$, $p = 0.979$ One-way ANOVA with *Fisher's LSD* post-hoc analysis WT + water vs. WT + KDS2010, $p = 0.912$; WT + water vs. APP/PS1 + water, $p = 0.441$; WT + water vs. APP/PS1 + KDS2010, $p = 0.331$; WT + KDS2010 vs. APP/PS1 + water, $p = 0.509$; WT + KDS2010 vs. APP/PS1 + KDS2010, $p = 0.392$; APP/PS1 + water vs. APP/PS1 + KDS2010, $p = 0.876$
Supple 8D	Swim speed-Acquisition Test; Day 6; One-way ANOVA with *Tukey's* multiple comparisons test $F(2, 23) = 3.227$, $p = 0.0582$ APP/PS1 + water vs. APP/PS1 + KDS2010, $p = 0.067$ Day 7; One-way ANOVA with *Tukey's* multiple comparisons test $F(2, 23) = 3.227$, $p = 0.9492$ APP/PS1 + water vs. APP/PS1 + KDS2010, $p = 0.3706$
	Swim speed-Reversal Test; Day 10; *Kruskal-Wallis* test with *Dunnett's* multiple comparisons test Kruskal-Wallis statistcs = 4.762 APP/PS1 + water vs. APP/PS1 + KDS2010, $p = 0.0979$

Table S7. Primer sequences for each enzyme (F: forward primer and R: reverse primer).

Gene	Gene ID	Species	Primer sequence	
MAOB	109731	*Mus musculus*	F R	5'- AGTTGAGCGGCTGATACACT -3' 5'- TGGCCCATCTCATCCATTGT -3'
DAO	13142	*Mus musculus*	F R	5'- CACTCGCTTACAAACCCACC -3' 5'- TCAAGTGTGGGCTGGACTAG -3'
GAD65	14417	*Mus musculus*	F R	5'- GGGATGTCAACTACGCGTTT -3' 5'- CATTGGGGTAATGGAAATCG -3'
GAD67	14415	*Mus musculus*	F R	5'- CACAAACTCAGCGGCATAGA -3' 5'- CTGGAAGAGGTAGCCTGCAC -3'

Additional data in 2-week toxicity: body weight changes, hematology, coagulation value, urinalysis value and organ weight changes.

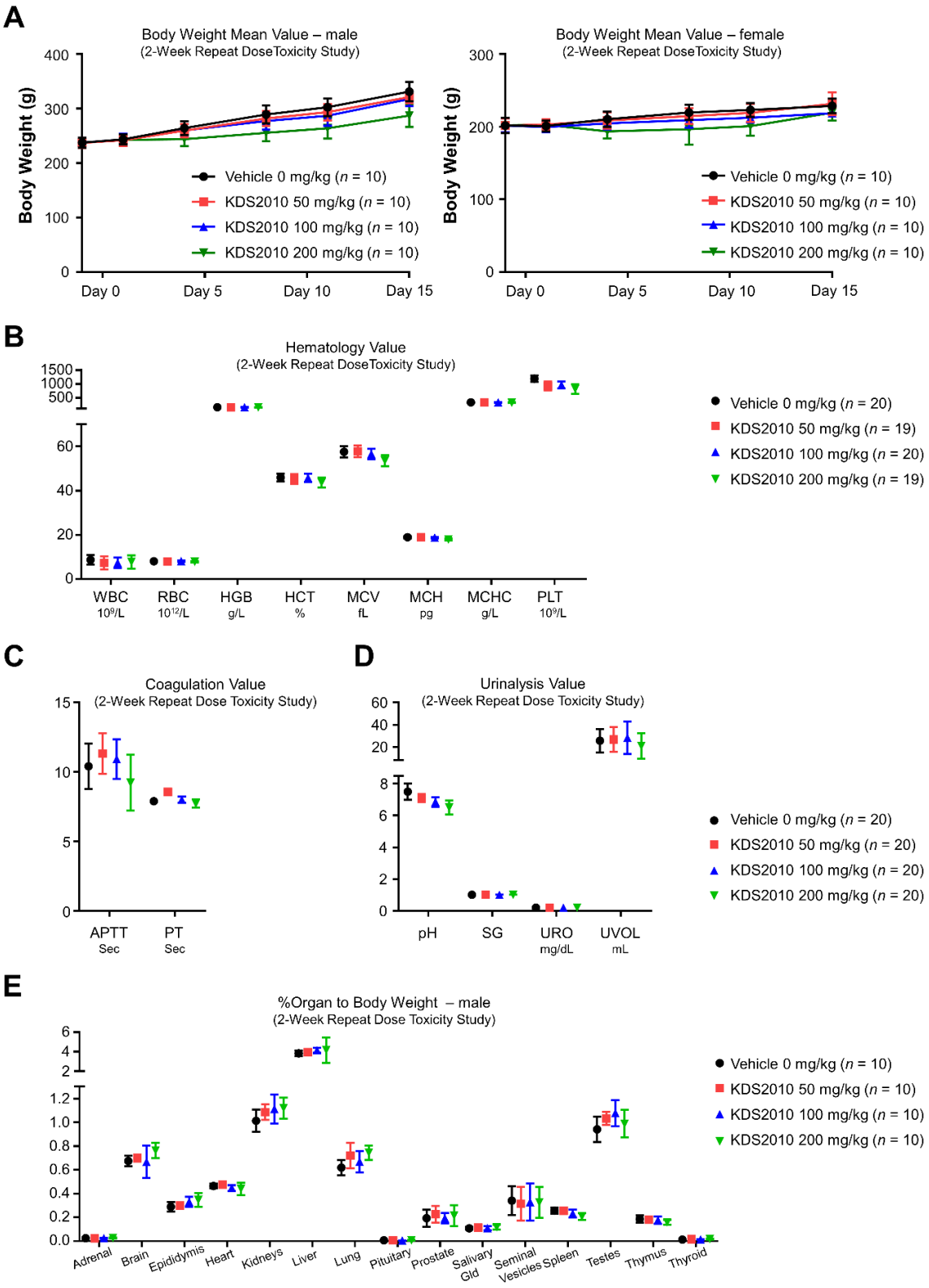

^{1}H and ^{13}C-NMR spectra

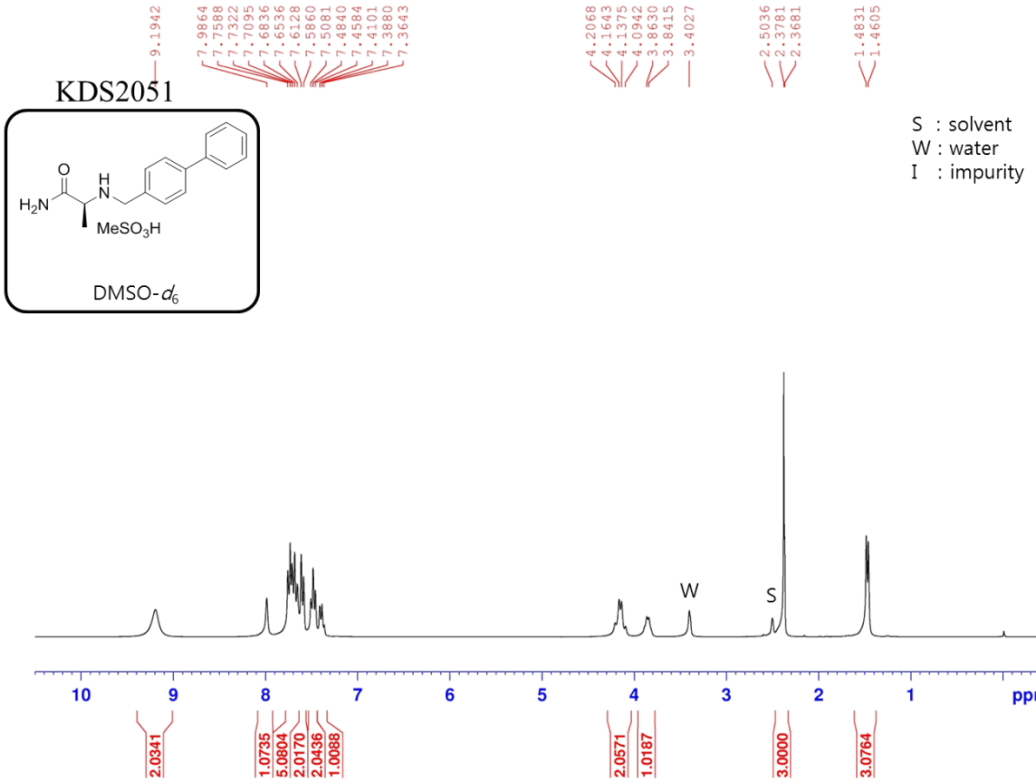

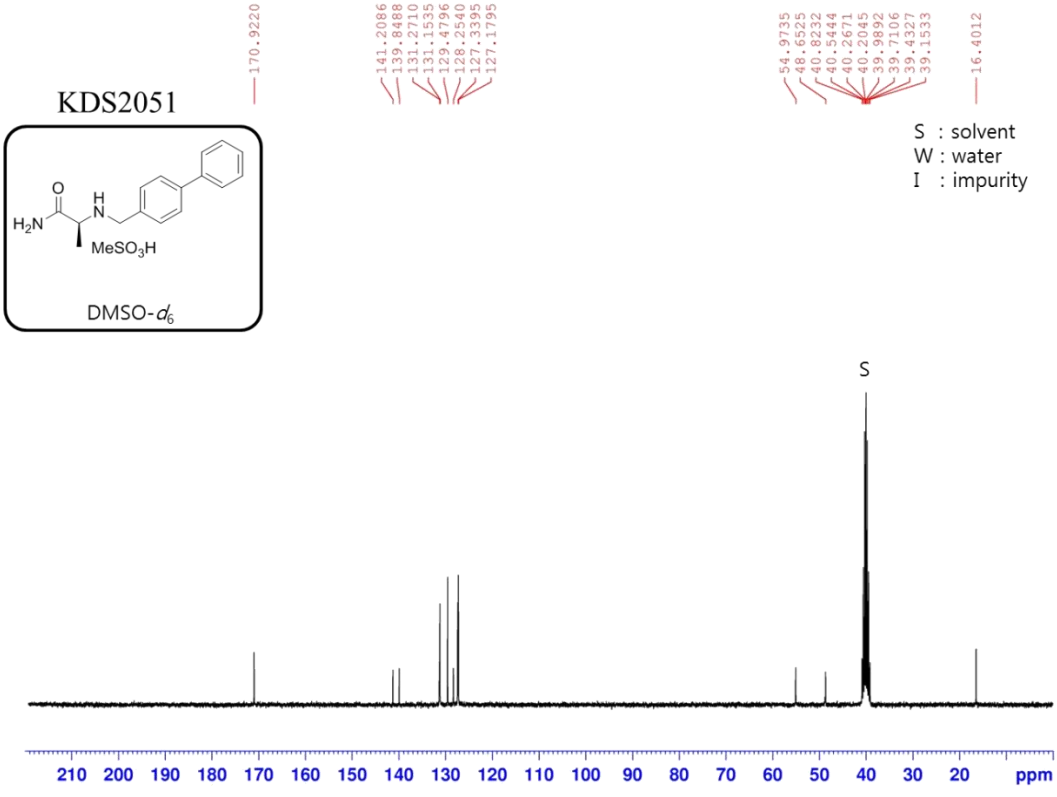

KDS0011

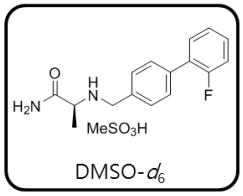

KDS0011

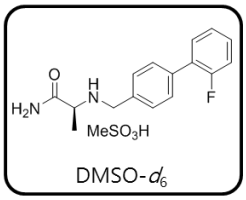

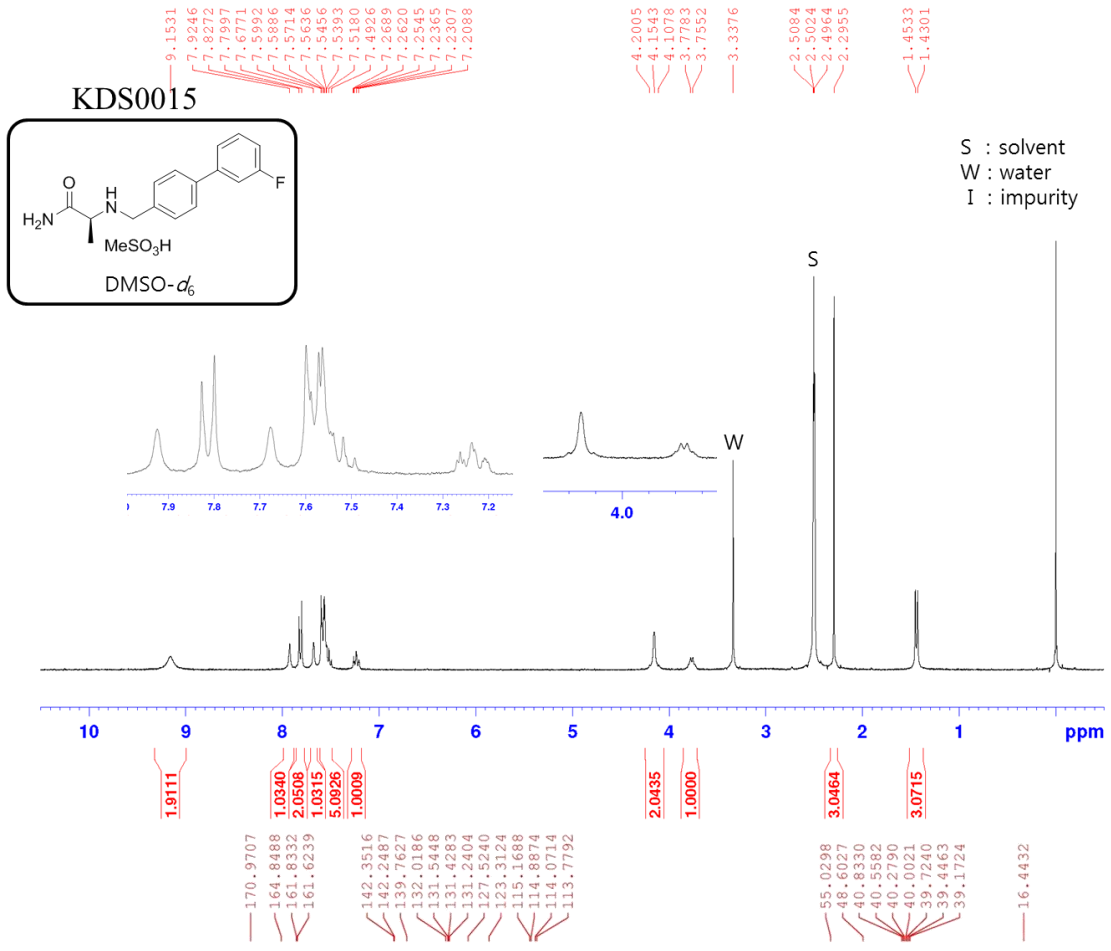
KDS0015
S : solvent
W : water
I : impurity
MeSO3H
DMSO-d6
S
W
ppm

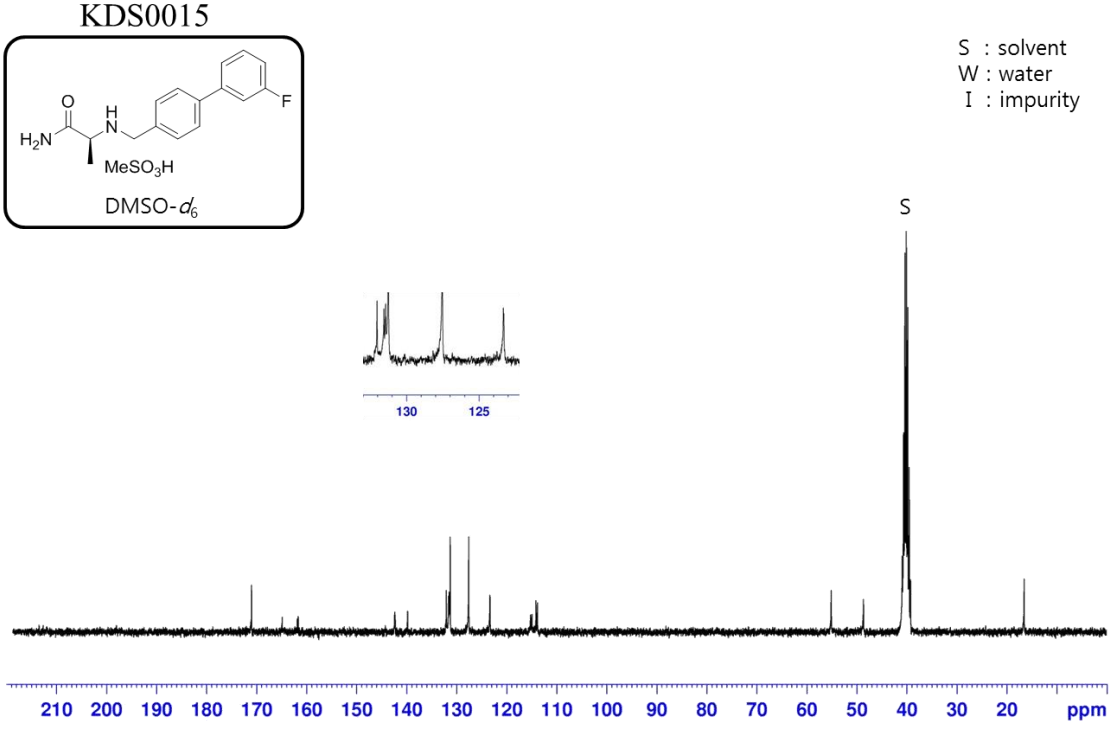
KDS0015
S : solvent
W : water
I : impurity
MeSO3H
DMSO-d6
S
ppm

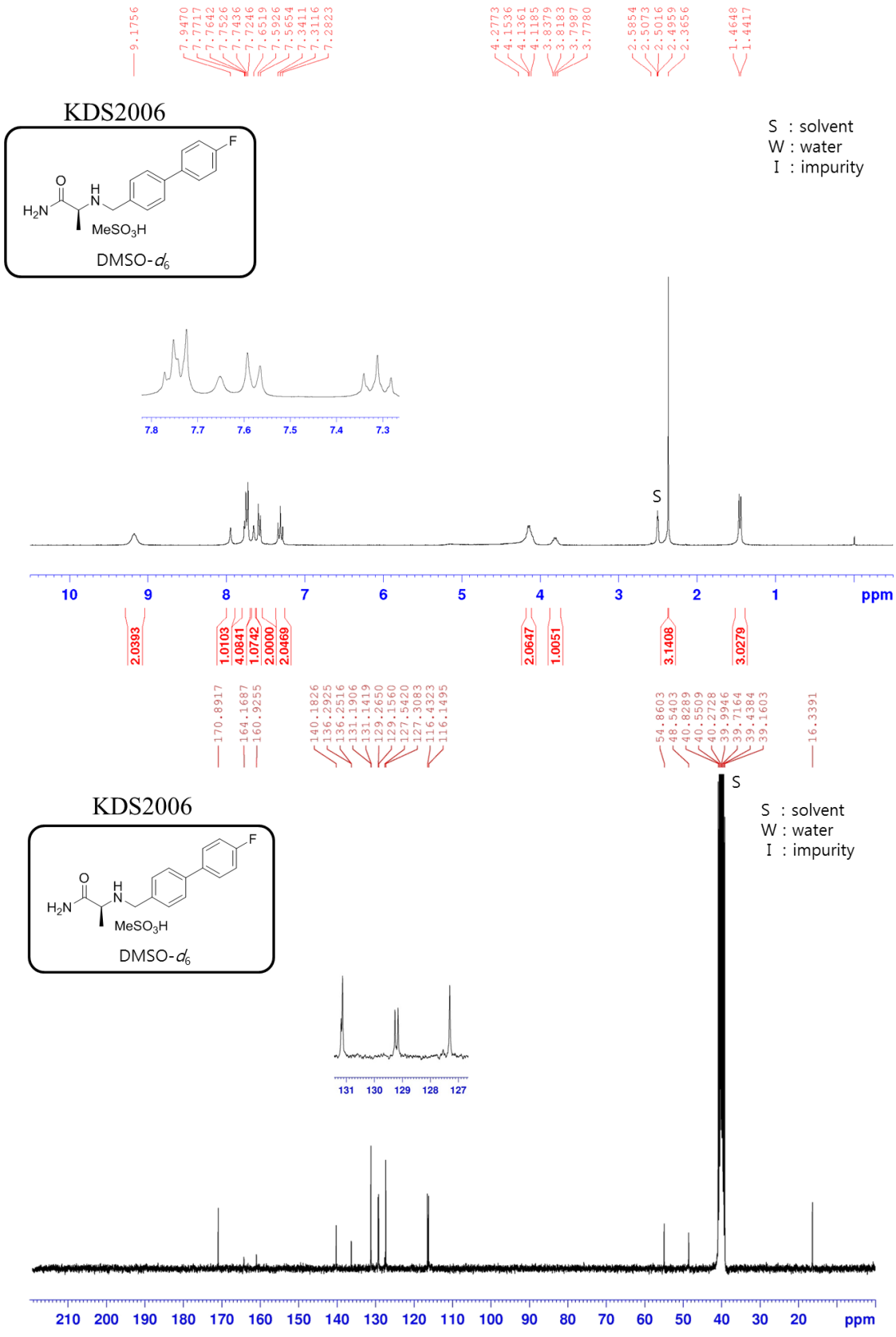
9.1756
7.9470
7.7717
7.7642
7.7526
7.7436
7.7246
7.6519
7.5926
7.5654
7.3411
7.3116
7.2823
4.2773
4.1536
4.1361
4.1185
3.8379
3.8183
3.7987
3.7780
2.5854
2.5073
2.5016
2.4959
2.3656
1.4648
1.4417
KDS2006
S : solvent
W : water
I : impurity
F
O
H
N
H2N
MeSO3H
DMSO-d6
7.8
7.7
7.6
7.5
7.4
7.3
S
10
9
8
7
6
5
4
3
2
1
ppm
2.0393
1.0103
4.0841
1.0742
2.0000
2.0469
2.0647
1.0051
3.1408
3.0279
170.8917
164.1687
160.9255
140.1826
136.2925
136.2516
131.1906
131.1419
129.2650
129.1560
127.5420
127.3083
116.4323
116.1495
54.8603
48.5403
40.8289
40.5509
40.2728
39.9946
39.7164
39.4384
39.1603
16.3391
KDS2006
S : solvent
W : water
I : impurity
131
130
129
128
127
210
200
190
180
170
160
150
140
130
120
110
100
90
80
70
60
50
40
30
20
ppm

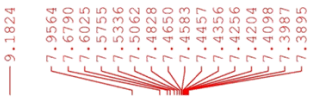

KDS2042

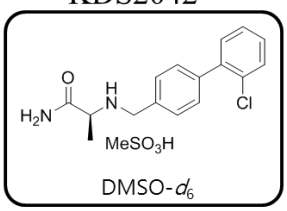

S : solvent
W : water
I : impurity

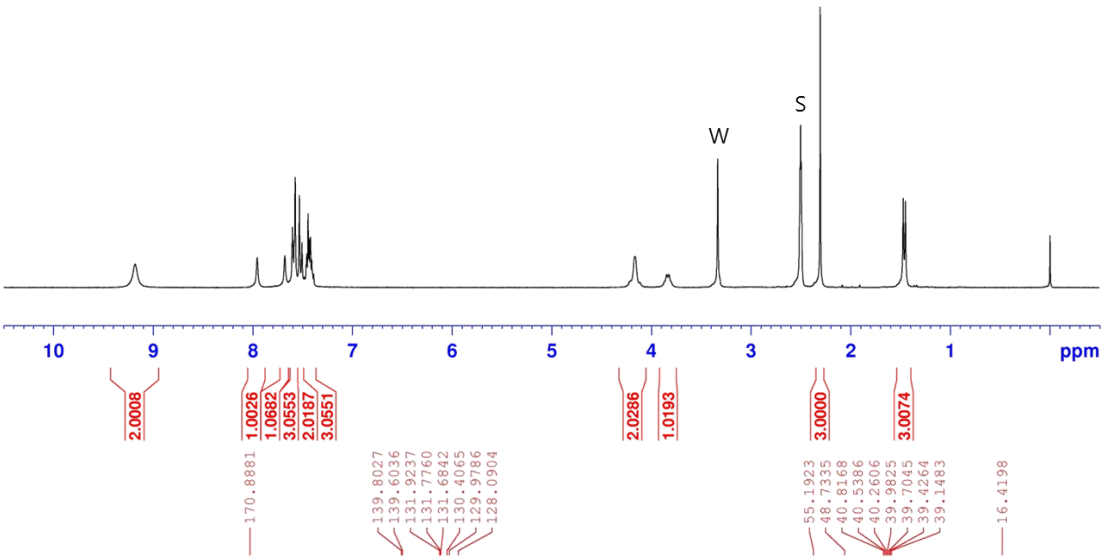

KDS2042

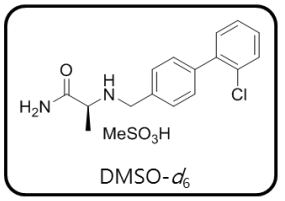

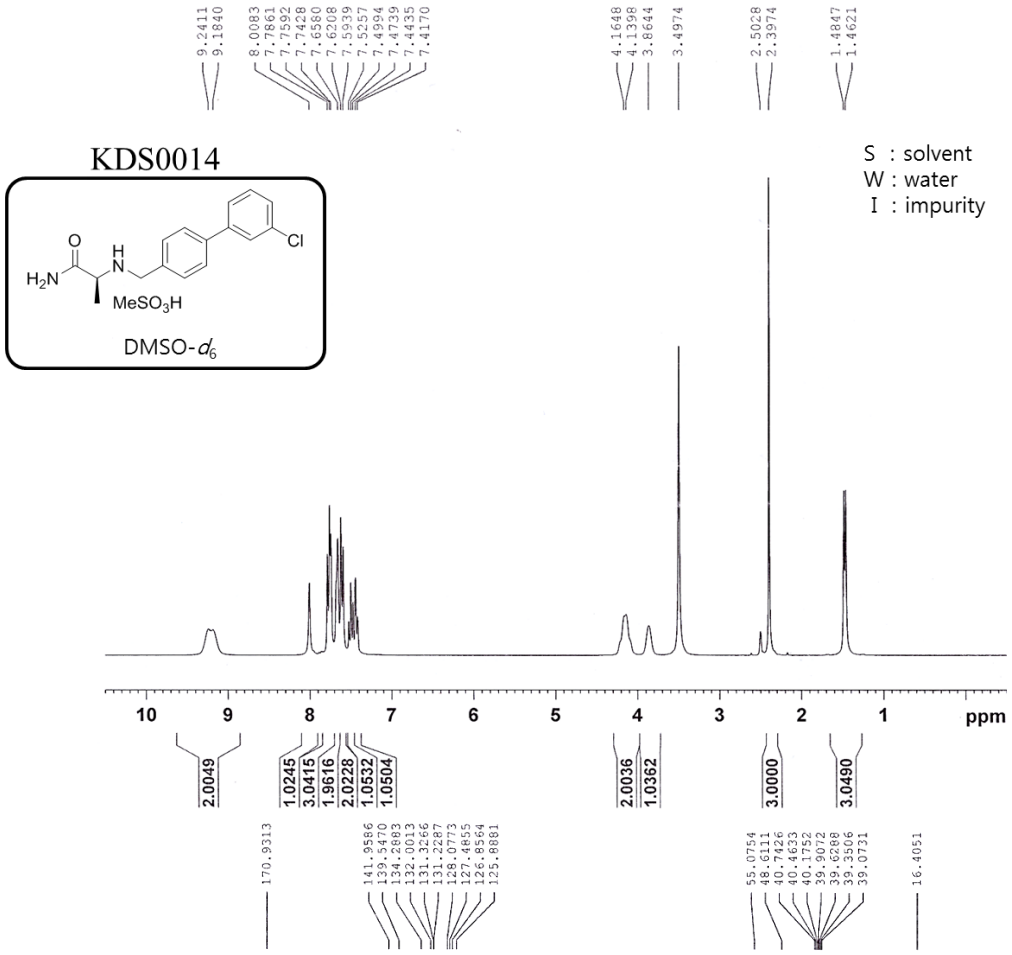
KDS0014
S : solvent
W : water
I : impurity
DMSO-d_6
ppm

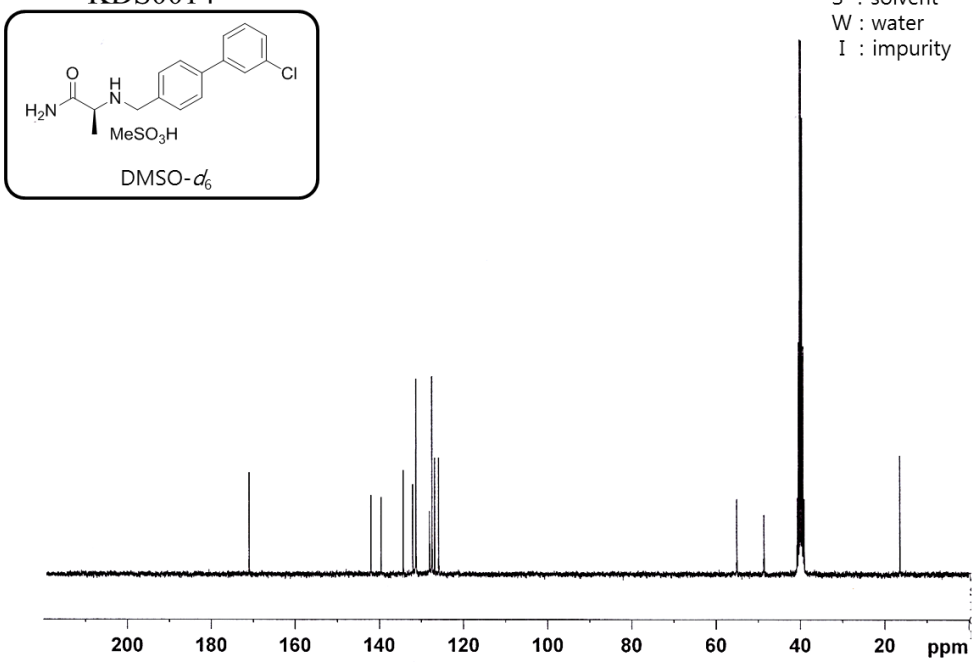
KDS0014
S : solvent
W : water
I : impurity
DMSO-d_6
ppm

KDS2005

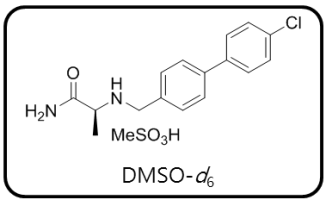

DMSO-d_6

S : solvent
W : water
I : impurity

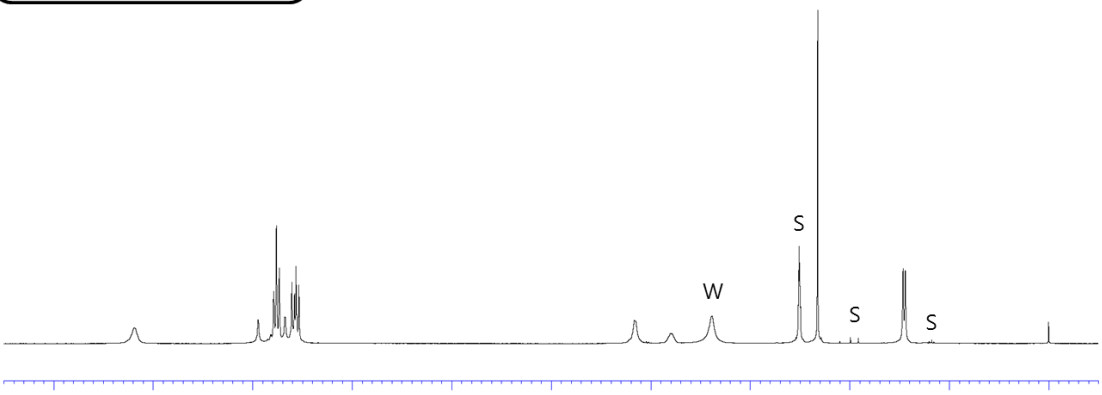

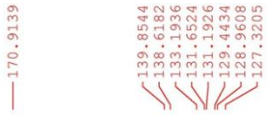

KDS2005

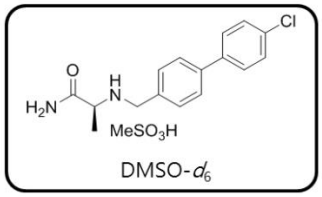

DMSO-d_6

S : solvent
W : water
I : impurity

KDS2041

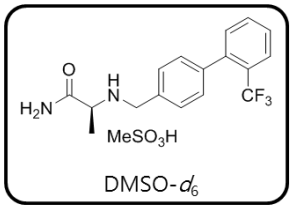

S : solvent
W : water
I : impurity

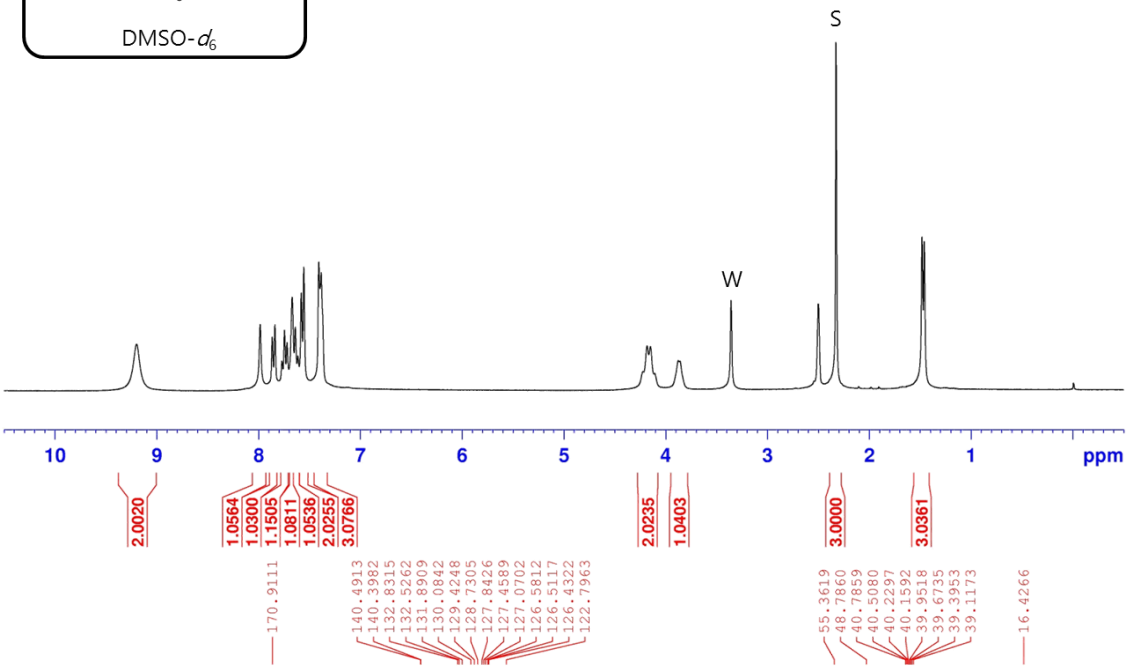

KDS2041

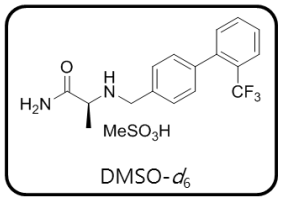

S : solvent
W : water
I : impurity

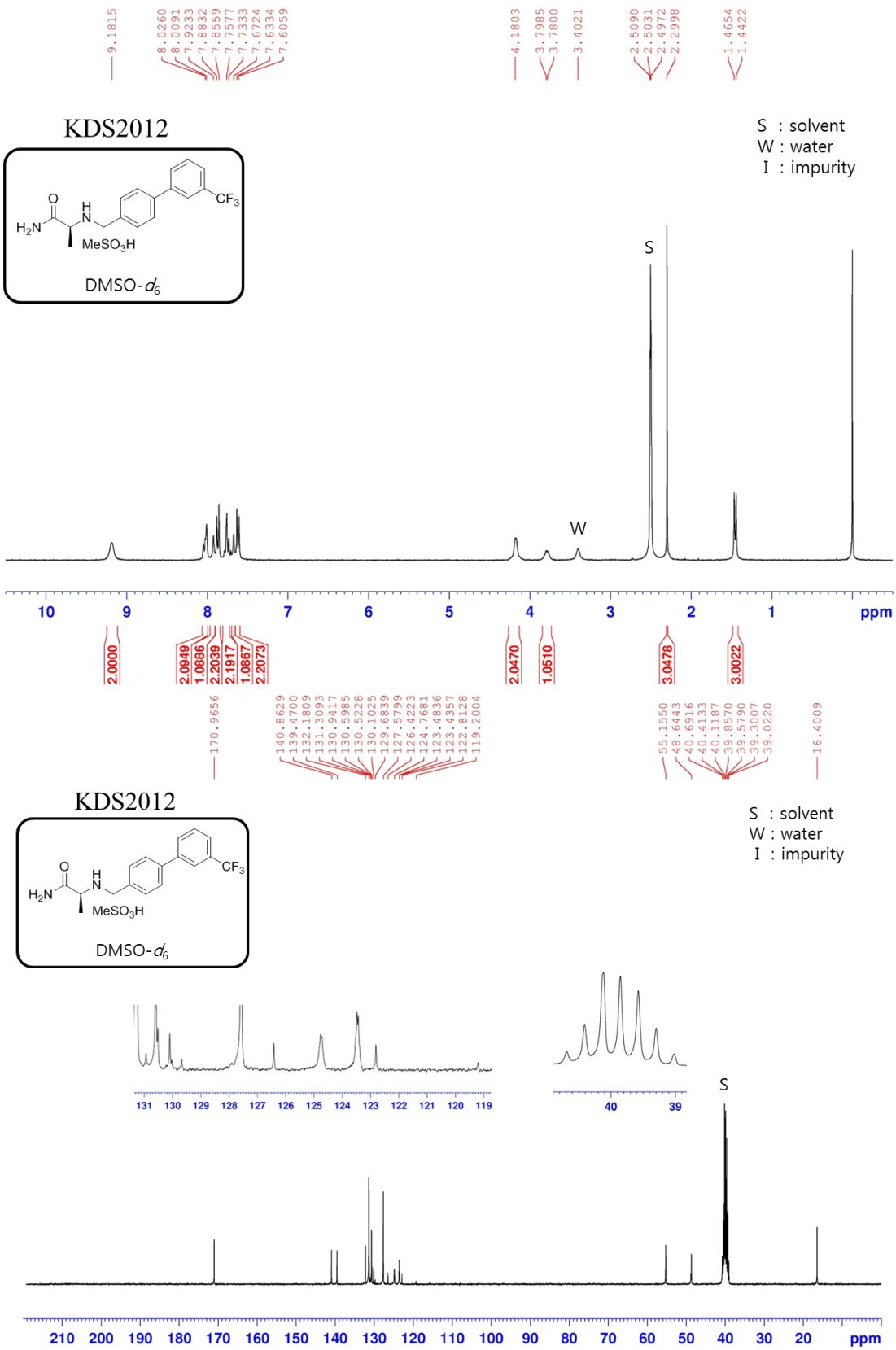
KDS2012
S : solvent
W : water
I : impurity
DMSO-d_6
S
W
ppm
KDS2012
S : solvent
W : water
I : impurity
DMSO-d_6
S
ppm

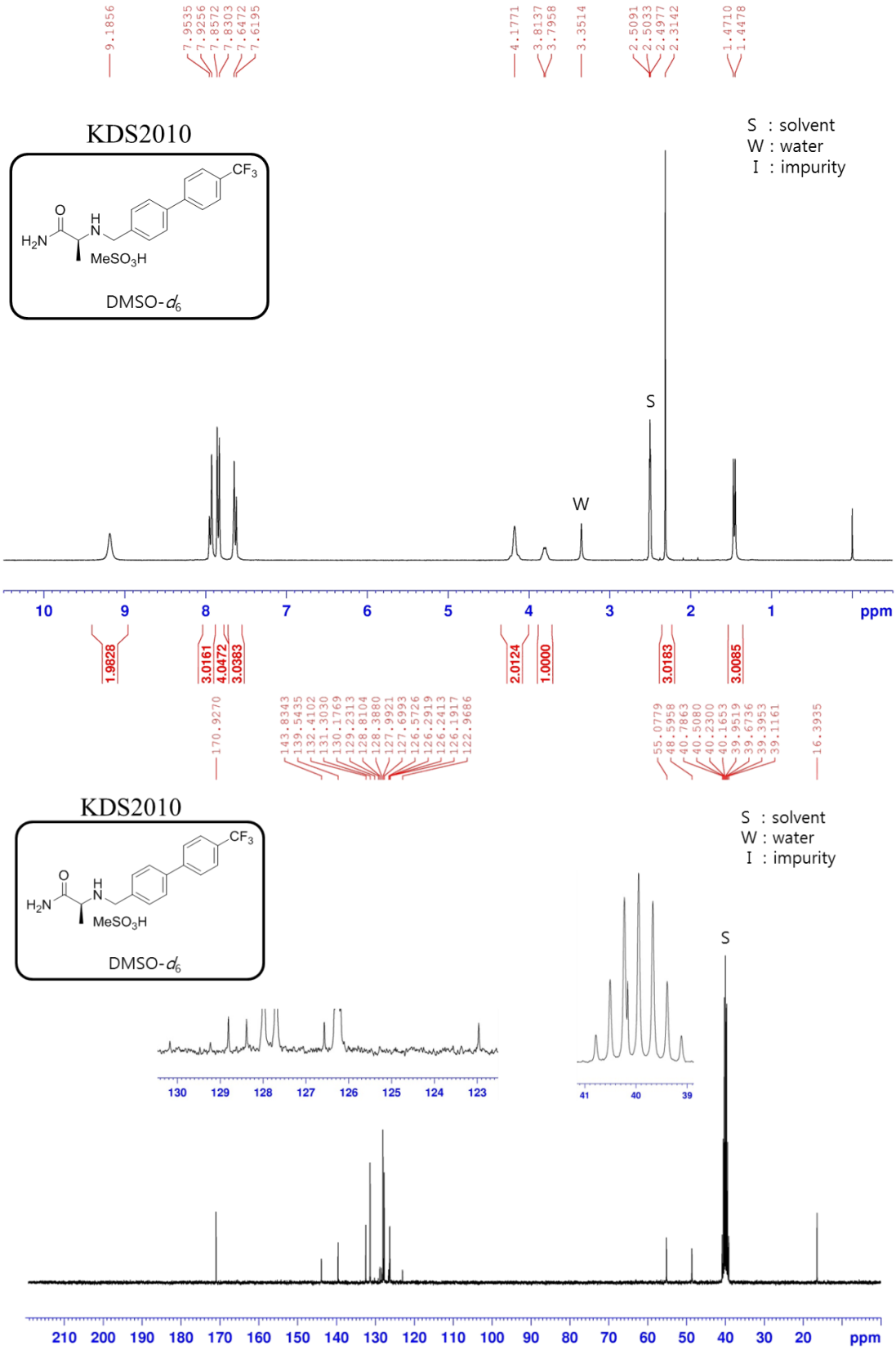
9.1856
7.9535
7.9256
7.8572
7.8303
7.6472
7.6195
4.1771
3.8137
3.7958
3.3514
2.5091
2.5033
2.4977
2.3142
1.4710
1.4478
KDS2010
S : solvent
W : water
I : impurity
CF3
H2N
O
H
N
MeSO3H
DMSO-d6
S
W
10
9
8
7
6
5
4
3
2
1
ppm
1.9828
3.0161
4.0472
3.0383
2.0124
1.0000
3.0183
3.0085
170.9270
143.8343
139.5435
132.4102
131.3030
130.1769
129.2313
128.8104
128.3880
127.9921
127.6993
126.5726
126.2919
126.2413
126.1917
122.9686
55.0779
48.5958
40.7863
40.5080
40.2300
40.1653
39.9519
39.6736
39.3953
39.1161
16.3935
KDS2010
S : solvent
W : water
I : impurity
CF3
H2N
O
H
N
MeSO3H
DMSO-d6
S
130
129
128
127
126
125
124
123
41
40
39
210
200
190
180
170
160
150
140
130
120
110
100
90
80
70
60
50
40
30
20
ppm

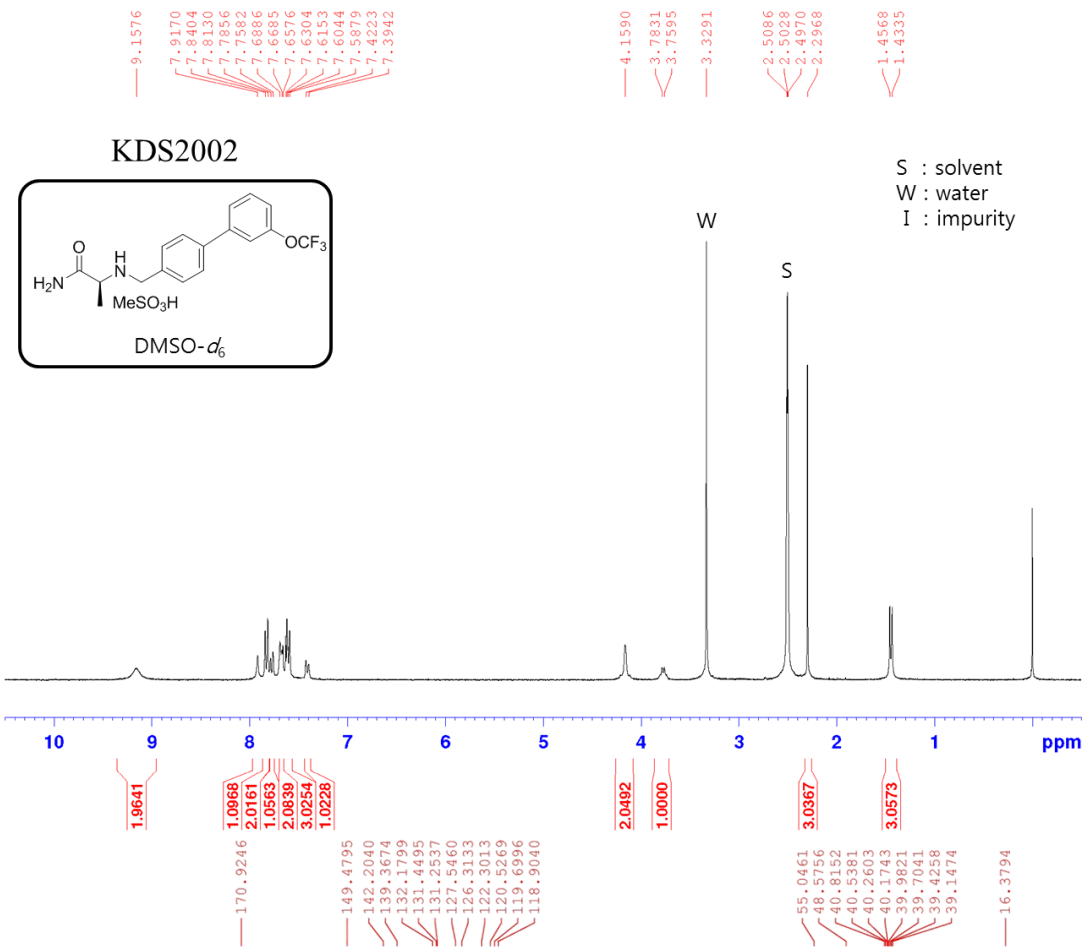
KDS2002
S : solvent
W : water
I : impurity
W
S
OCF3
H2N
O
H
N
MeSO3H
DMSO-d6
9.1576
7.9170
7.8404
7.8130
7.7856
7.7582
7.6886
7.6685
7.6576
7.6304
7.6153
7.6044
7.5879
7.4223
7.3942
4.1590
3.7831
3.7595
3.3291
2.5086
2.5028
2.4970
2.2968
1.4568
1.4335
1.9641
1.0968
2.0161
1.0563
2.0839
3.0254
1.0228
2.0492
1.0000
3.0367
3.0573
170.9246
149.4795
142.2040
139.3674
132.1799
131.4495
131.2537
127.5460
126.3133
122.3013
120.5269
119.6996
118.9040
55.0461
48.5756
40.8152
40.5381
40.2603
40.1743
39.9821
39.7041
39.4258
39.1474
16.3794
10
9
8
7
6
5
4
3
2
1
ppm

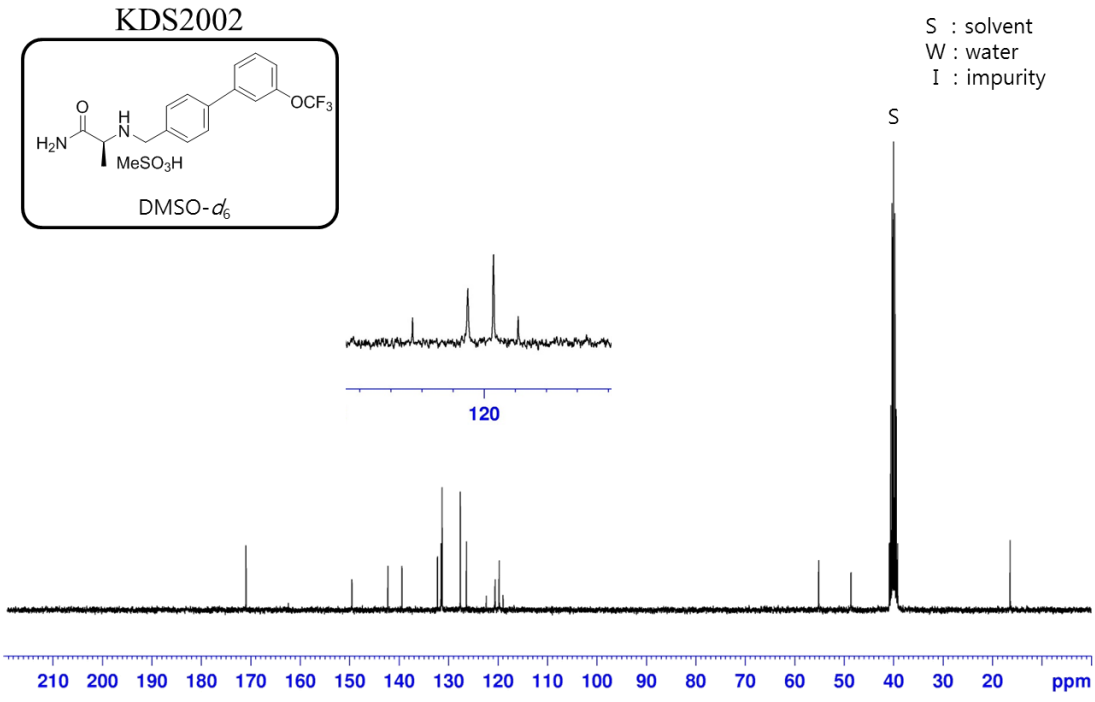
KDS2002
S : solvent
W : water
I : impurity
S
OCF3
H2N
O
H
N
MeSO3H
DMSO-d6
120
210
200
190
180
170
160
150
140
130
120
110
100
90
80
70
60
50
40
30
20
ppm

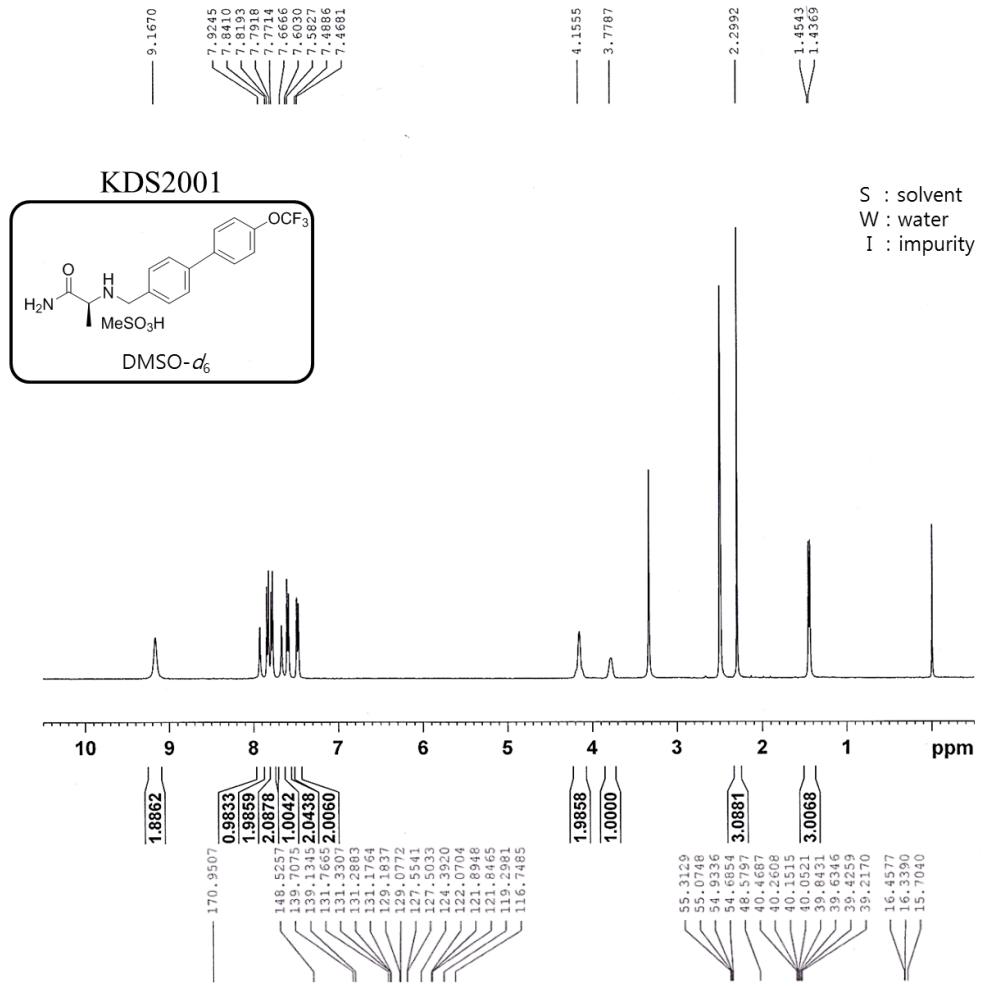
KDS2001
S : solvent
W : water
I : impurity
DMSO-d_6
ppm

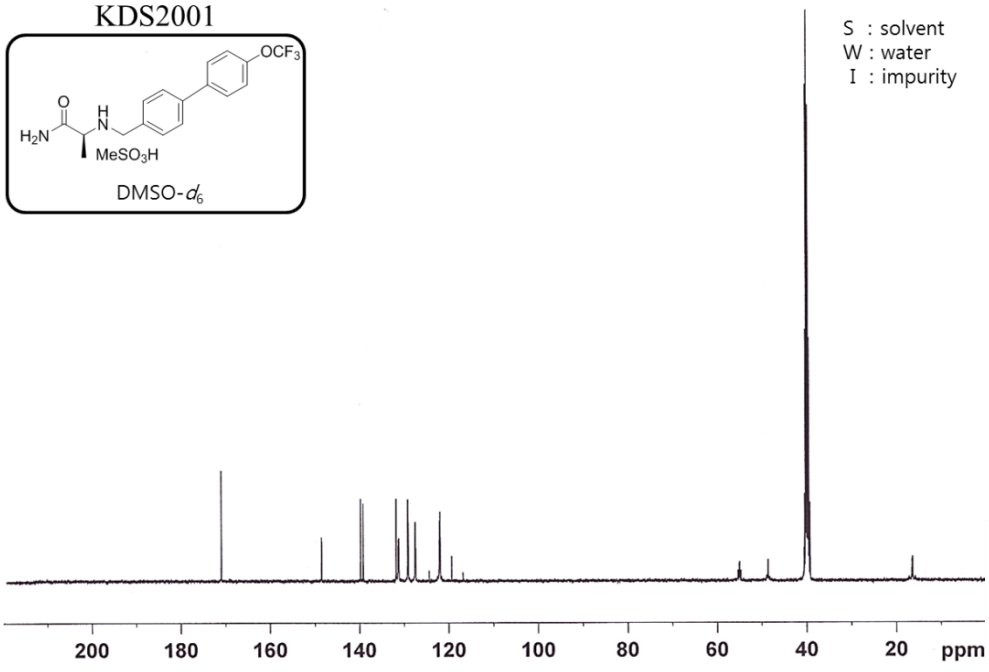
KDS2001
S : solvent
W : water
I : impurity
DMSO-d_6
ppm

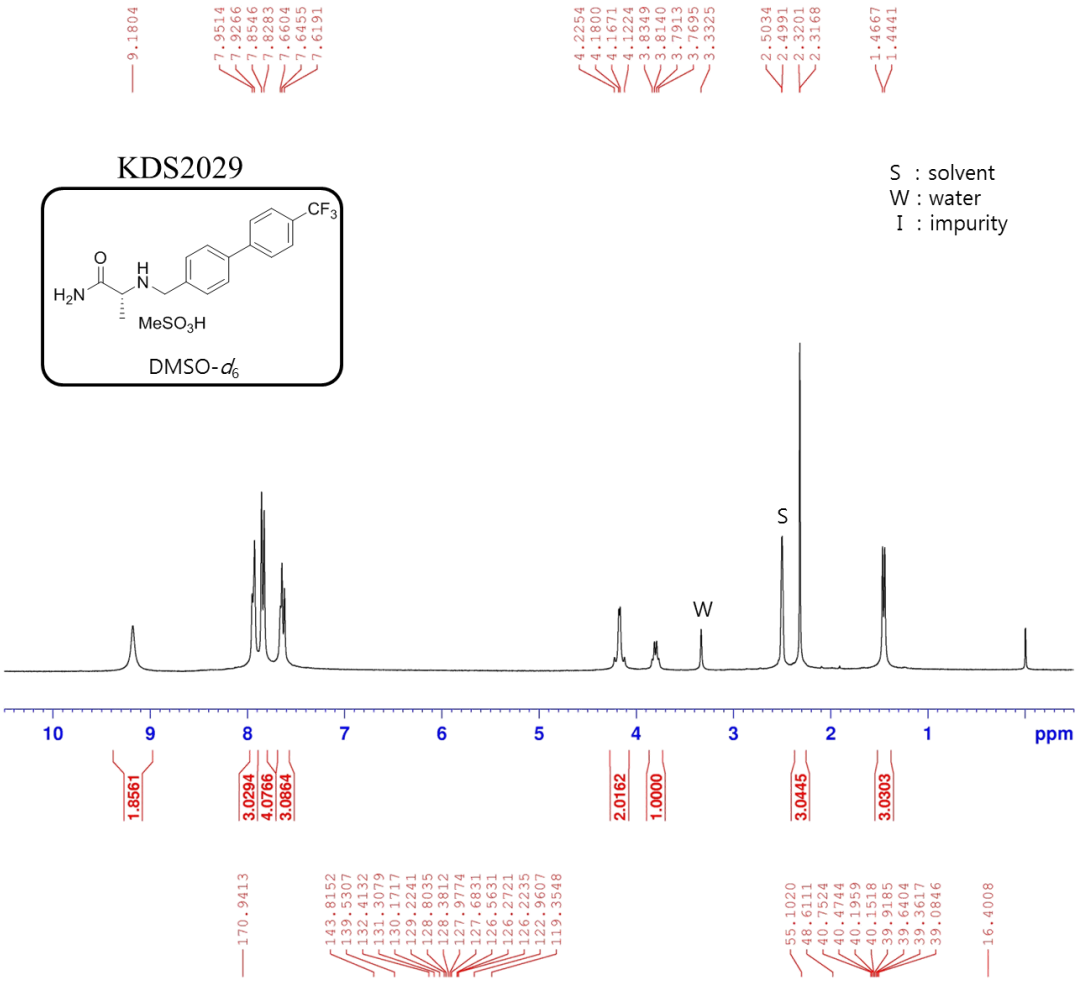
9.1804
7.9514
7.9266
7.8546
7.8283
7.6604
7.6455
7.6191
4.2254
4.1800
4.1671
4.1224
3.8349
3.8140
3.7913
3.7695
3.3325
2.5034
2.4991
2.3201
2.3168
1.4667
1.4441
KDS2029
S : solvent
W : water
I : impurity
CF3
H2N
O
H
N
MeSO3H
DMSO-d6
S
W
10
9
8
7
6
5
4
3
2
1
ppm
1.8561
3.0294
4.0766
3.0864
2.0162
1.0000
3.0445
3.0303

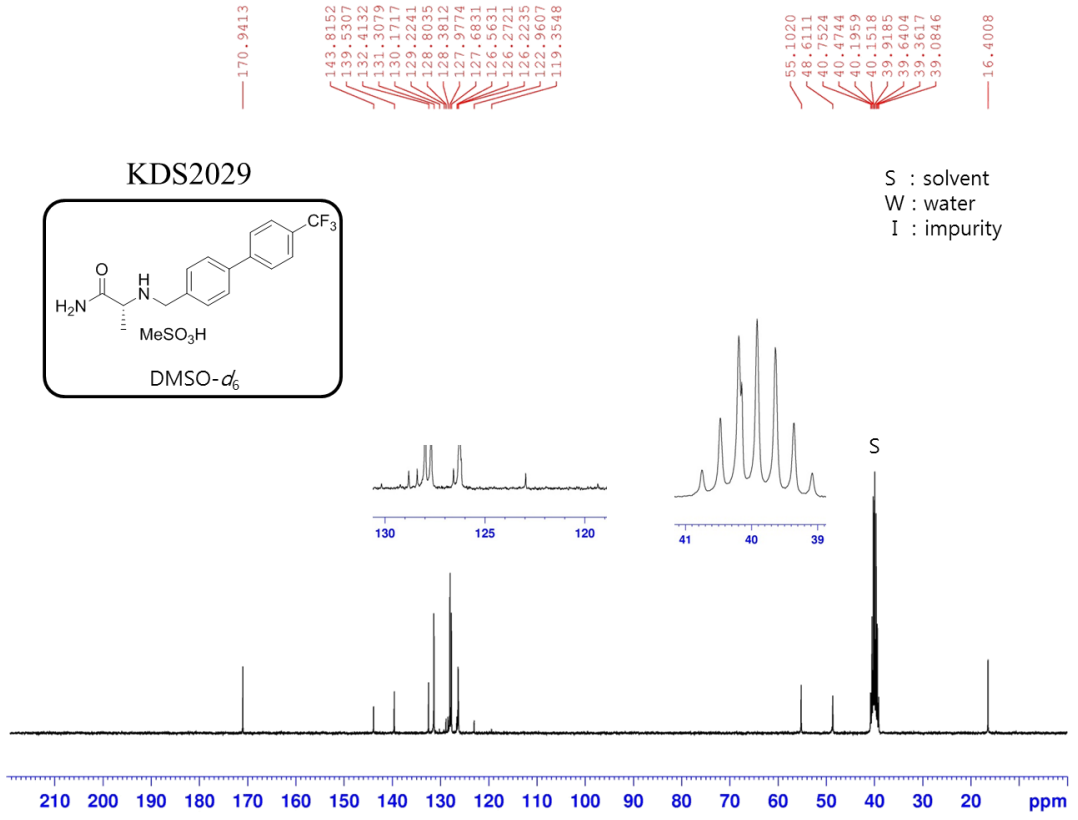
170.9413
143.8152
139.5307
132.4132
131.3079
130.1717
129.2241
128.8035
128.3812
127.9774
127.6831
126.5631
126.2721
126.2235
122.9607
119.3548
55.1020
48.6111
40.7524
40.4744
40.1959
40.1518
39.9185
39.6404
39.3617
39.0846
16.4008
KDS2029
S : solvent
W : water
I : impurity
CF3
H2N
O
H
N
MeSO3H
DMSO-d6
S
130
125
120
41
40
39
210
200
190
180
170
160
150
140
130
120
110
100
90
80
70
60
50
40
30
20
ppm

Chiral HPLC analysis of (*S*)/(*R*)-KDS2010

KDS2010

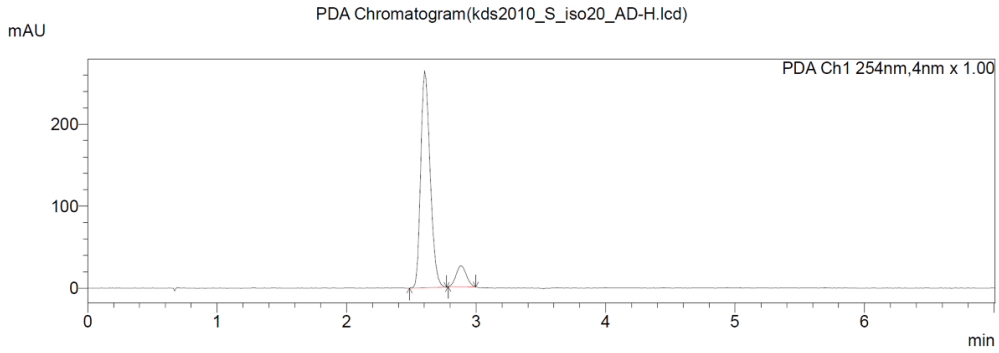

PDA Peak Table(kds2010_S_iso20_AD-H.lcd)

PDA Ch1 254nm

Peak#	Ret. Time	Area	Height	Mark	Conc.	Unit	ID#	Name	Area%
1	2.604	1335242	264015		0.000				90.372
2	2.883	142254	25786	M	0.000				9.628
Total		1477497	289801		0.000				100.000

KDS2029 (*R*-isomer of KDS2010)

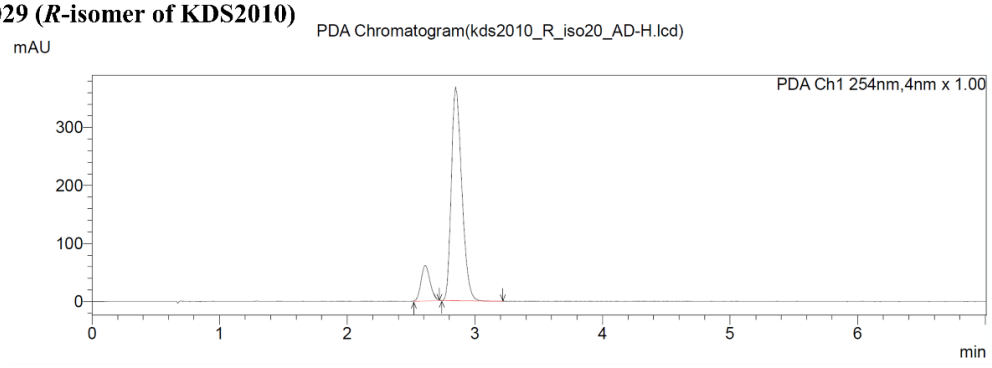

PDA Peak Table(kds2010_R_iso20_AD-H.lcd)

PDA Ch1 254nm

Peak#	Ret. Time	Area	Height	Mark	Conc.	Unit	ID#	Name	Area%
1	2.611	247381	56152	M	0.000				10.573
2	2.850	2092461	367978	M	0.000				89.427
Total		2339842	424130		0.000				100.000

KDS2010/KDS2029 = 1/1 mixture

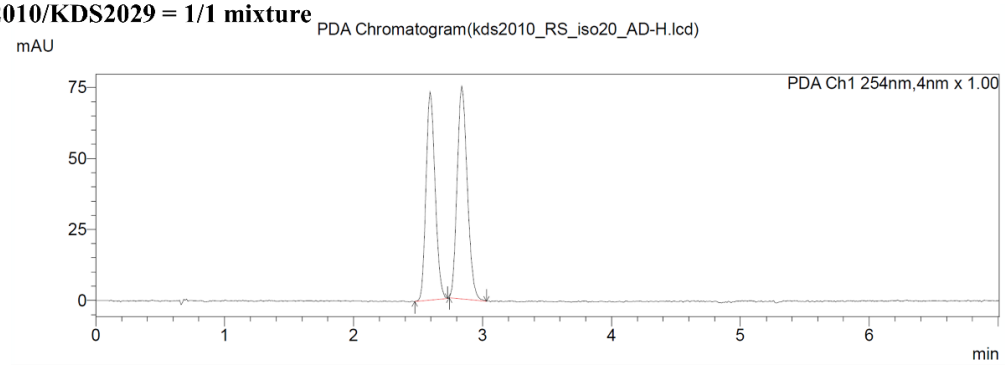

PDA Peak Table(kds2010_RS_iso20_AD-H.lcd)

PDA Ch1 254nm

Peak#	Ret. Time	Area	Height	Mark	Conc.	Unit	ID#	Name	Area%
1	2.594	359576	73351		0.000				46.905
2	2.839	407023	74891	M	0.000				53.095
Total		766599	148242		0.000				100.000

HPLC Traces of the synthesized compounds

KDS2051

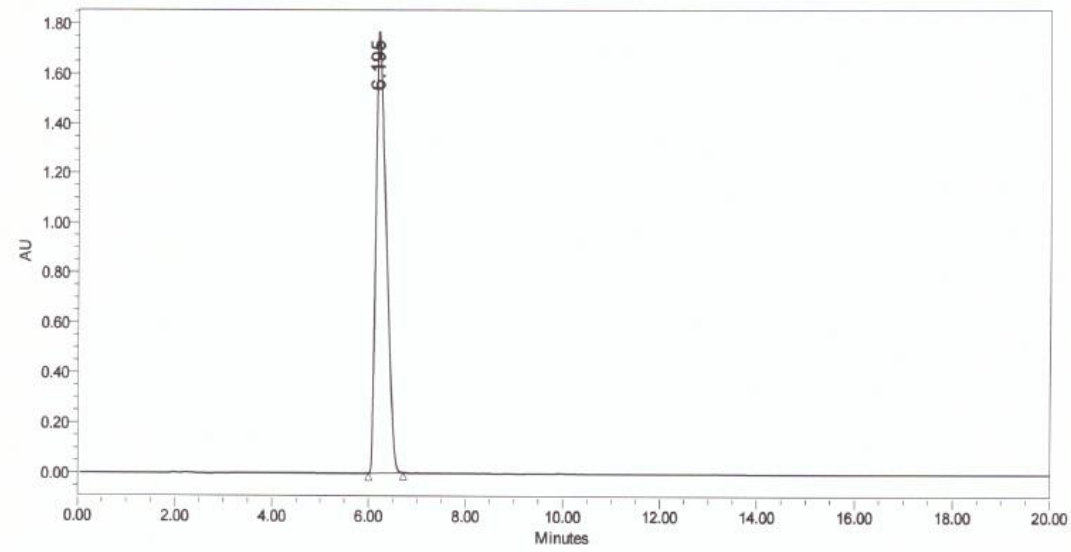

	RT	Area	% Area	Height
1	6.195	26611952	100.00	1767689

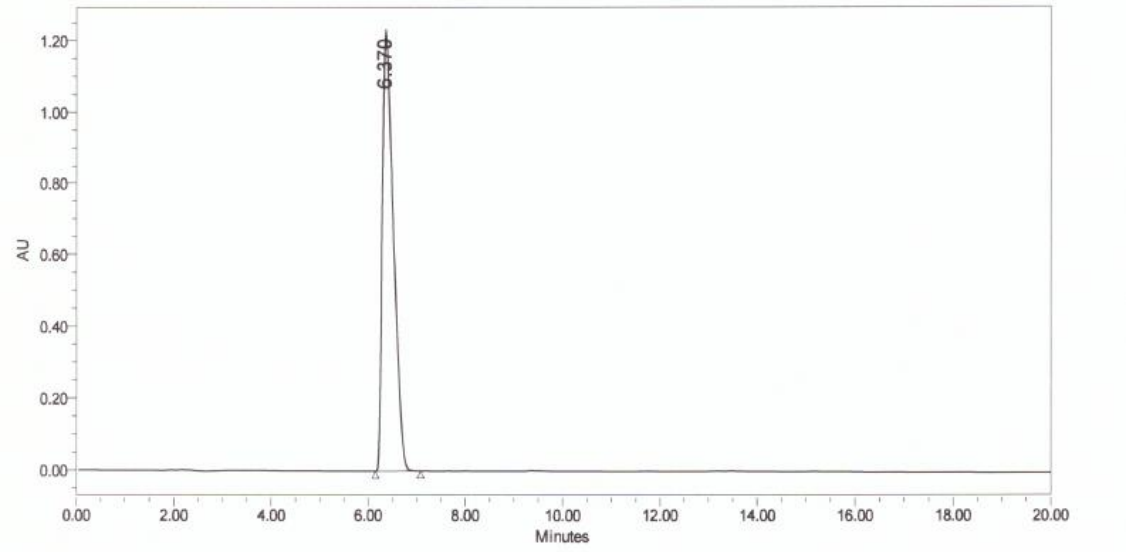

	RT	Area	% Area	Height
1	6.370	19771280	100.00	1234101

KDS0011

KDS0015

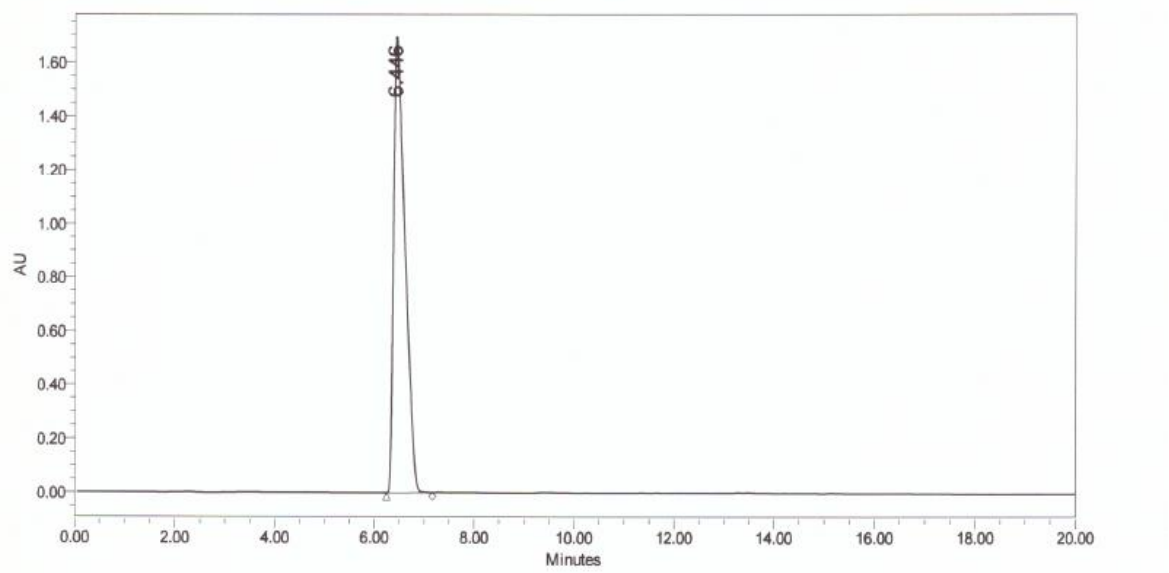

	RT	Area	% Area	Height
1	6.446	27159808	100.00	1696729

KDS2006

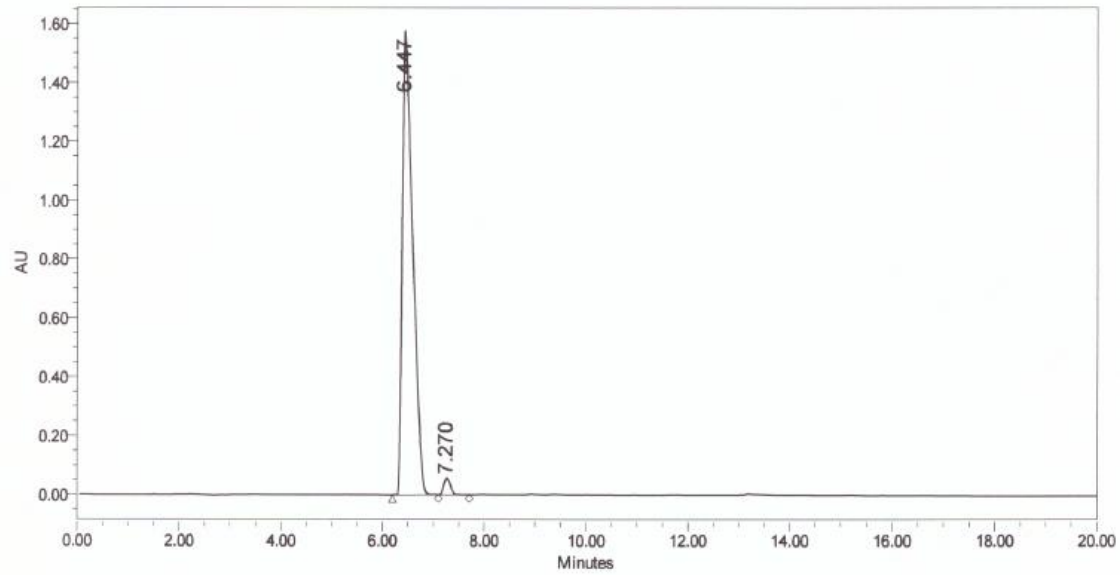

	RT	Area	% Area	Height
1	6.447	22794877	97.64	1579035
2	7.270	549803	2.36	57435

KDS2042

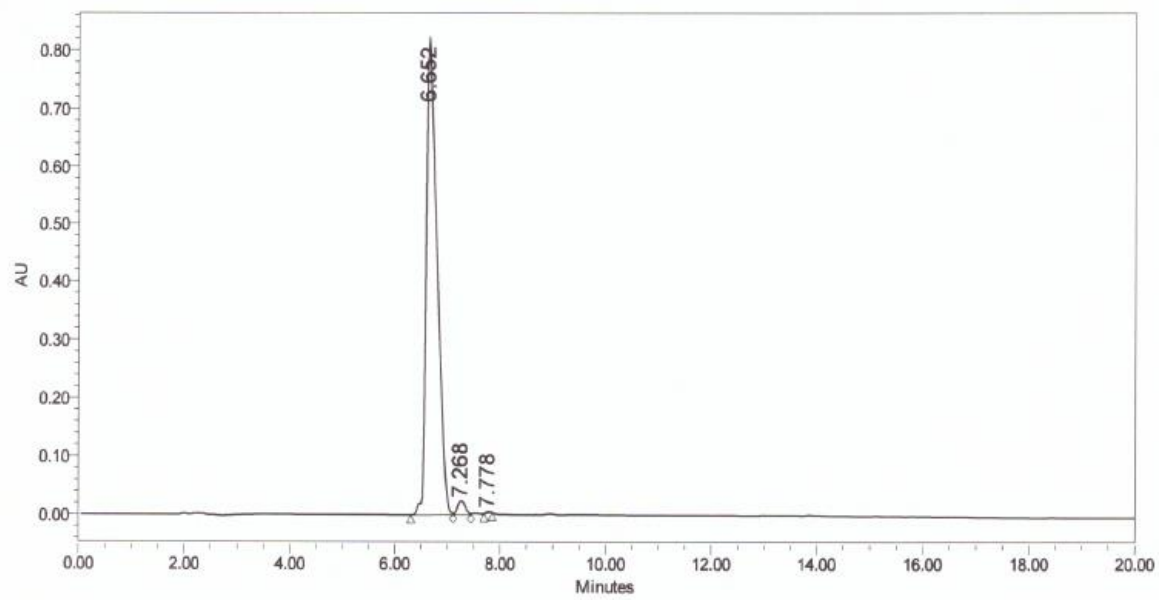

	RT	Area	% Area	Height
1	6.652	11925173	97.84	823295
2	7.268	249195	2.04	23315
3	7.778	14041	0.12	2524

KDS0014

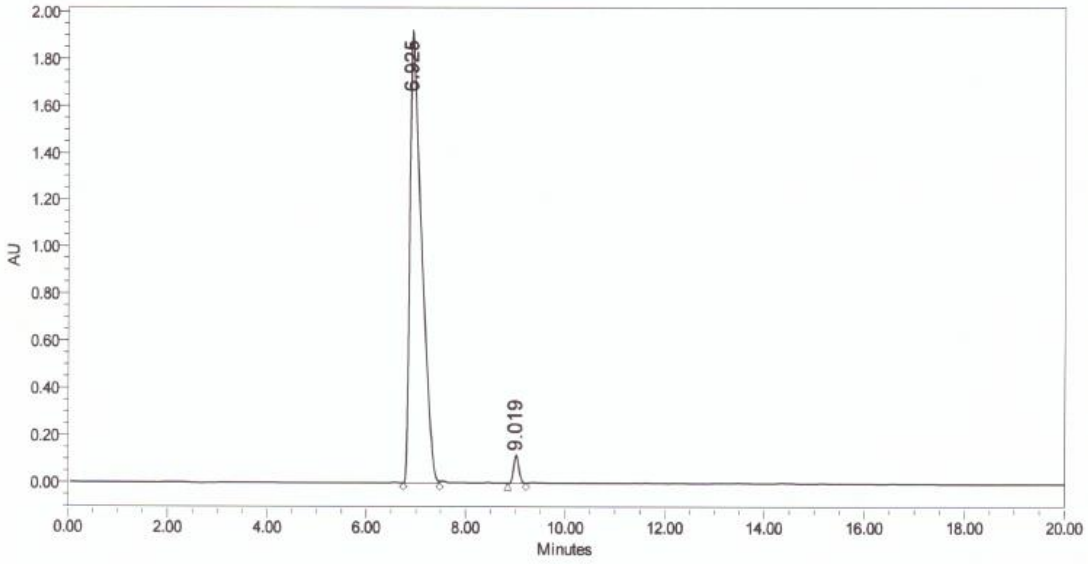

	RT	Area	% Area	Height
1	6.925	31881871	97.30	1936560
2	9.019	883771	2.70	120329

KDS2005

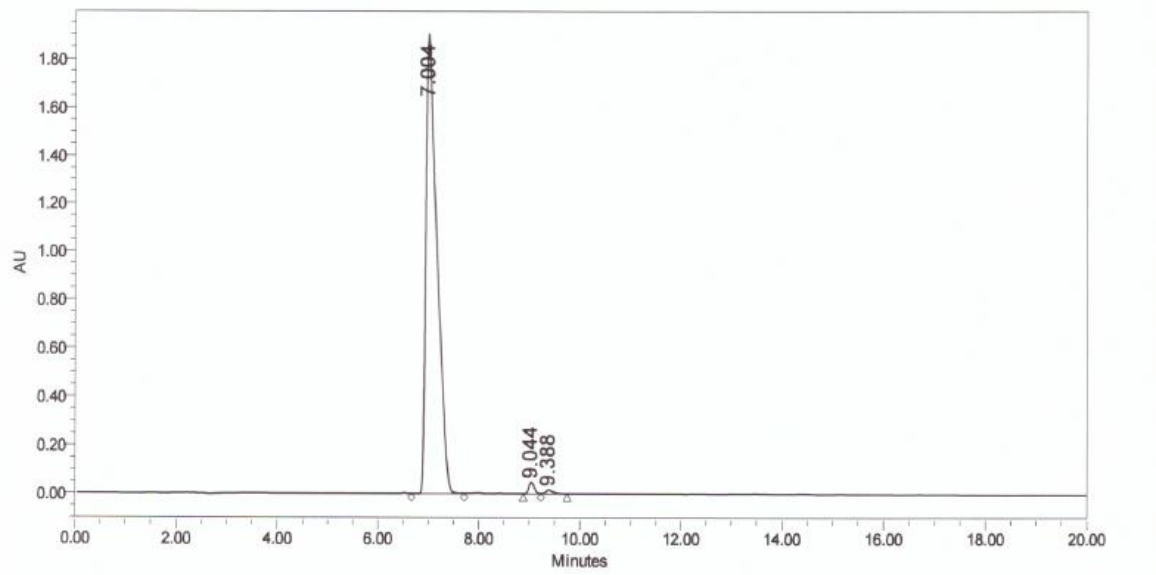

	RT	Area	% Area	Height
1	7.004	29361216	98.23	1904414
2	9.044	376171	1.26	48058
3	9.388	154312	0.52	15967

KDS2041

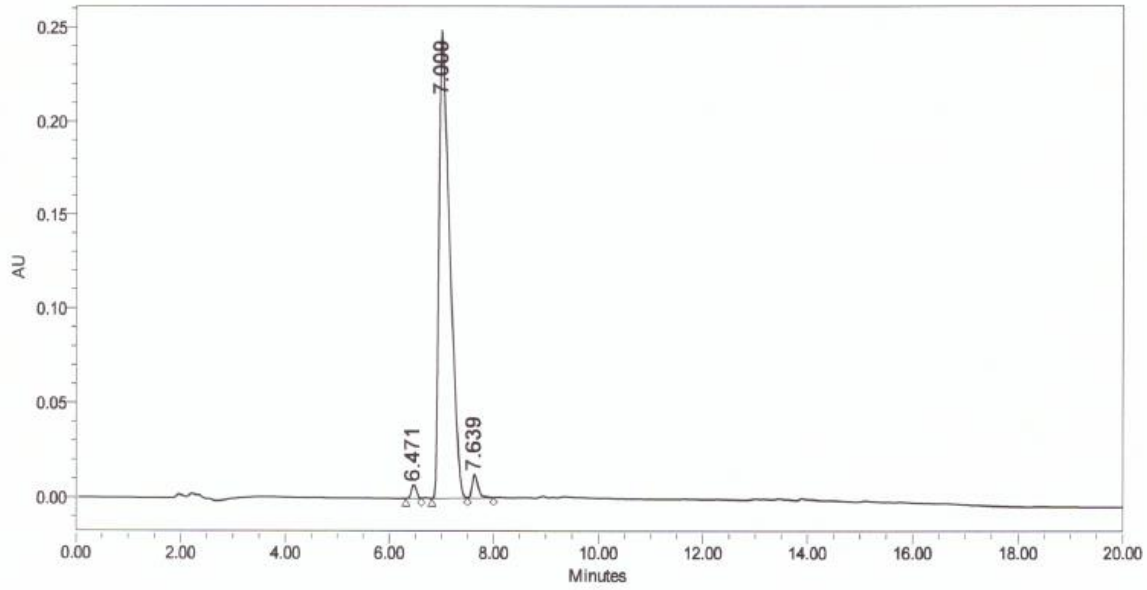

	RT	Area	% Area	Height
1	6.471	52462	1.37	7270
2	7.009	3673357	95.77	250417
3	7.639	109735	2.86	12586

KDS0012

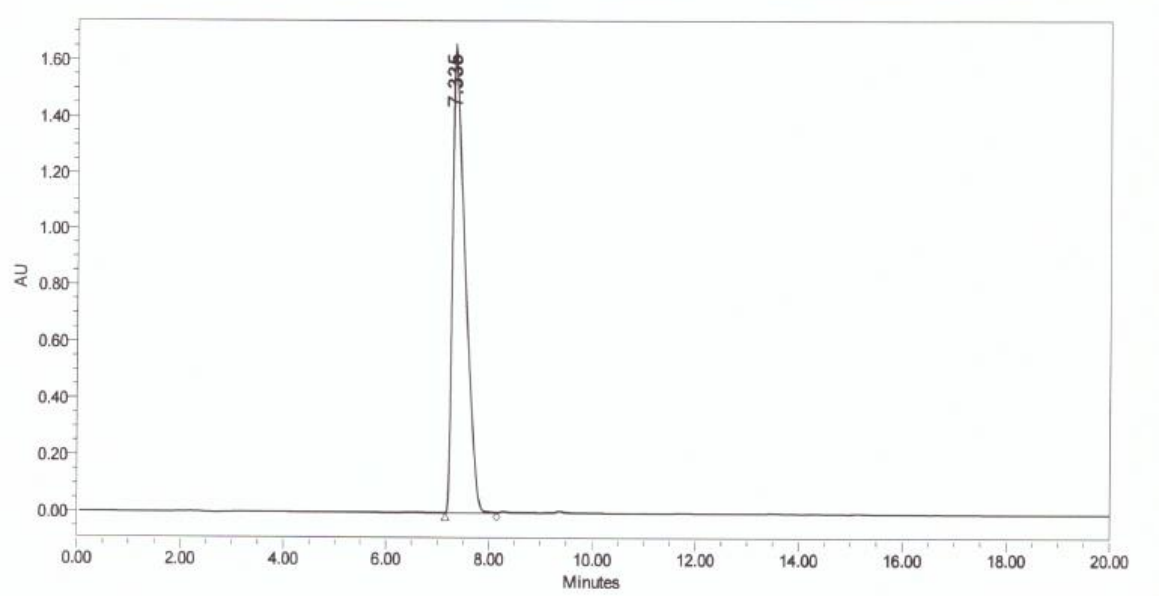

	RT	Area	% Area	Height
1	7.335	28492724	100.00	1658366

KDS2010

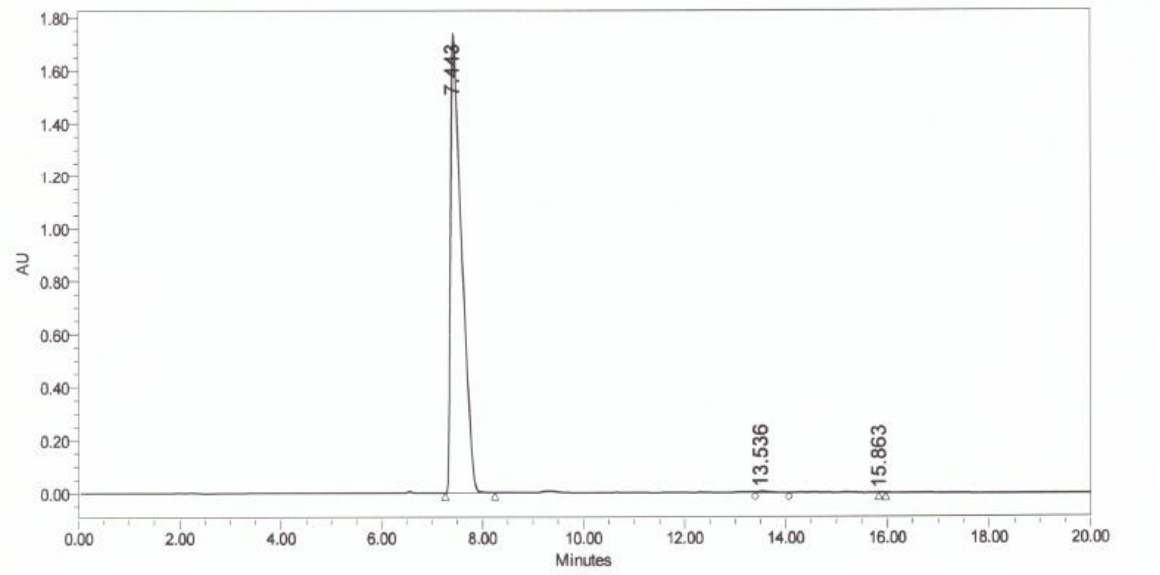

	RT	Area	% Area	Height
1	7.443	26628094	99.67	1752481
2	13.536	87208	0.33	5491
3	15.863	1497	0.01	354

KDS2002

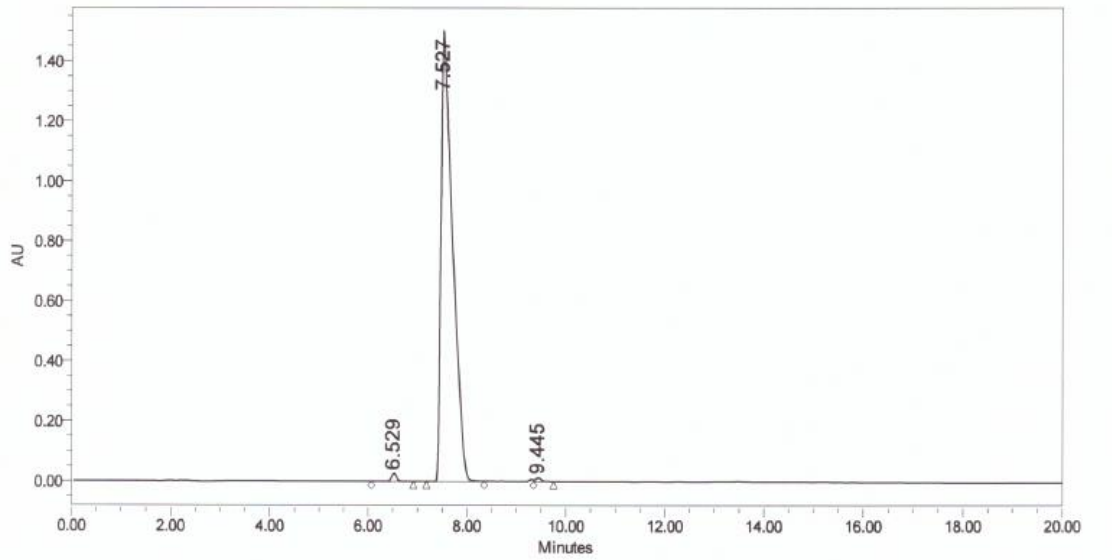

	RT	Area	% Area	Height
1	6.529	203982	0.80	26899
2	7.527	25272367	98.80	1518799
3	9.445	103765	0.41	12471

KDS2001

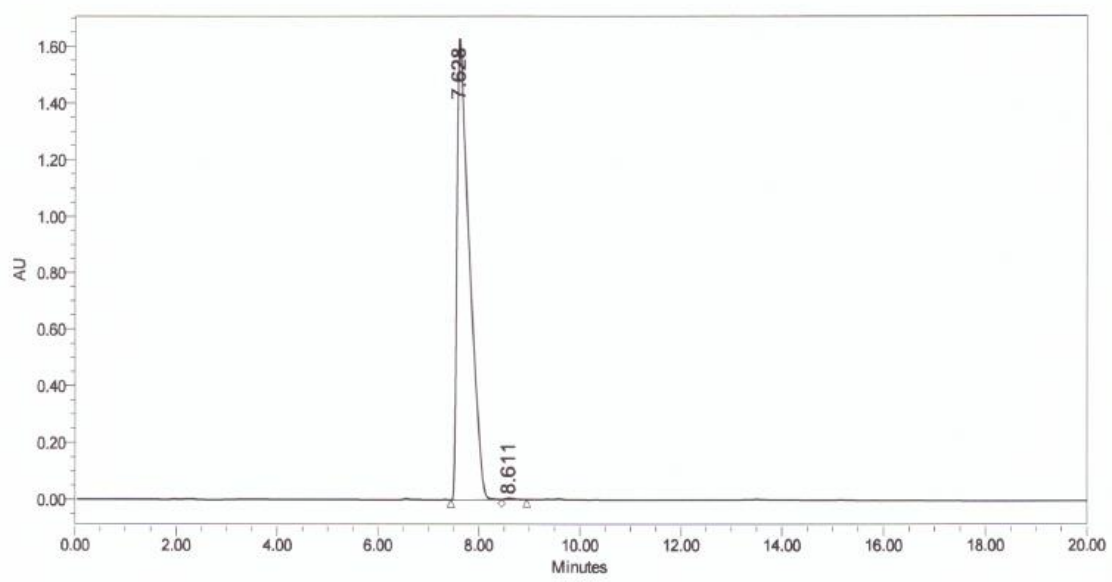

	RT	Area	% Area	Height
1	7.628	28245195	99.78	1645625
2	8.611	63682	0.22	4767

KDS2029

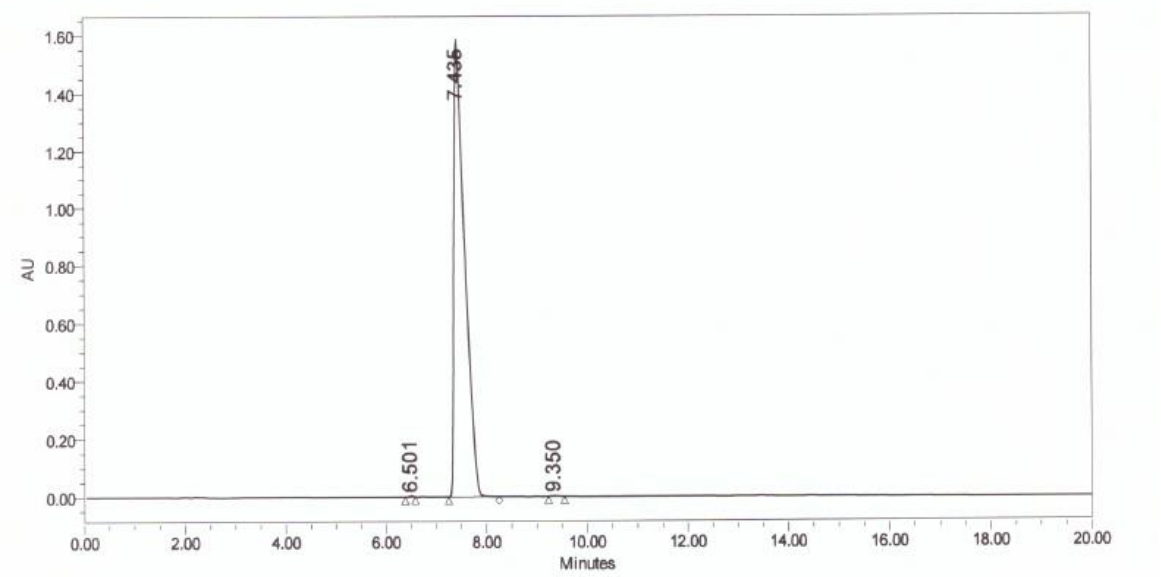

	RT	Area	% Area	Height
1	6.501	20639	0.09	3682
2	7.435	23930034	99.84	1587440
3	9.350	18797	0.08	1737

HR-MS spectra

KDS2051

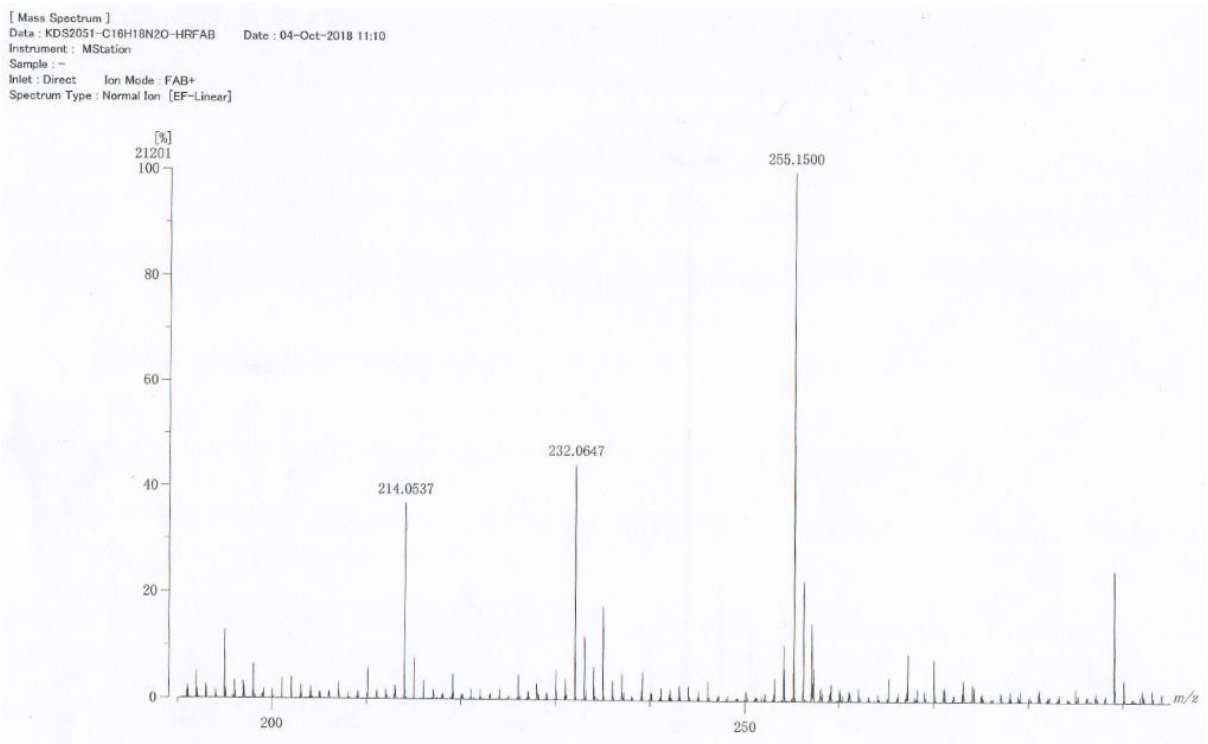

KDS0011

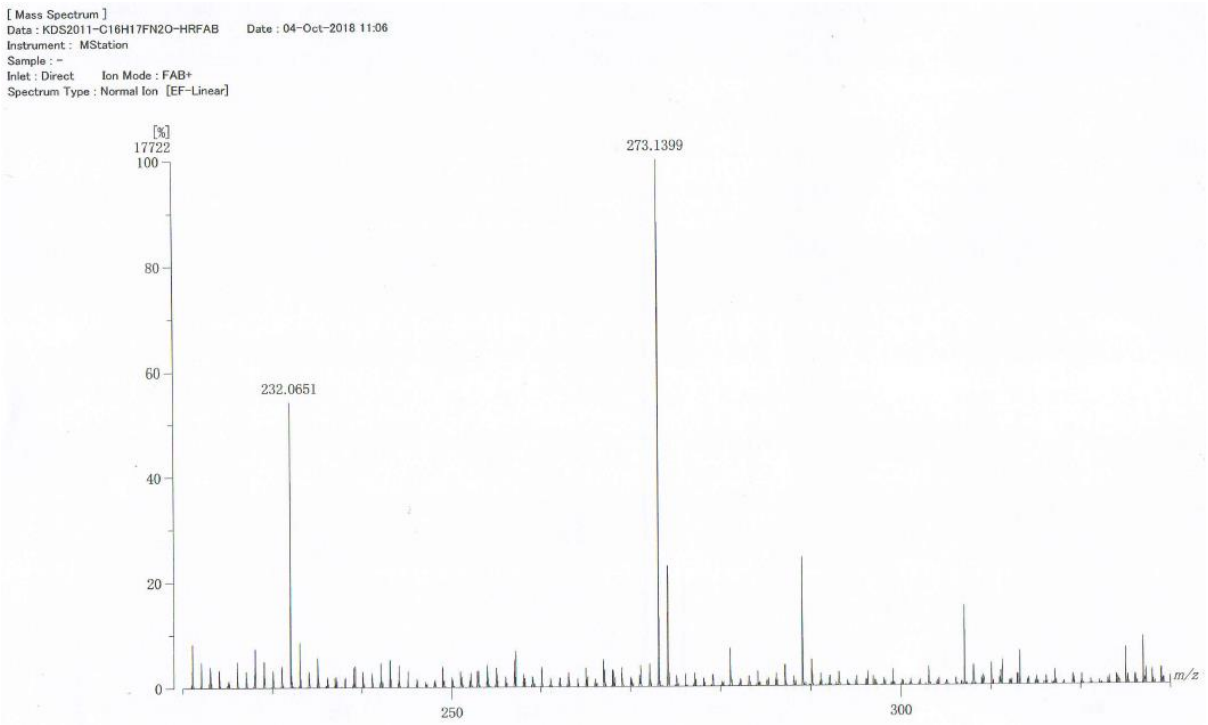

KDS0015

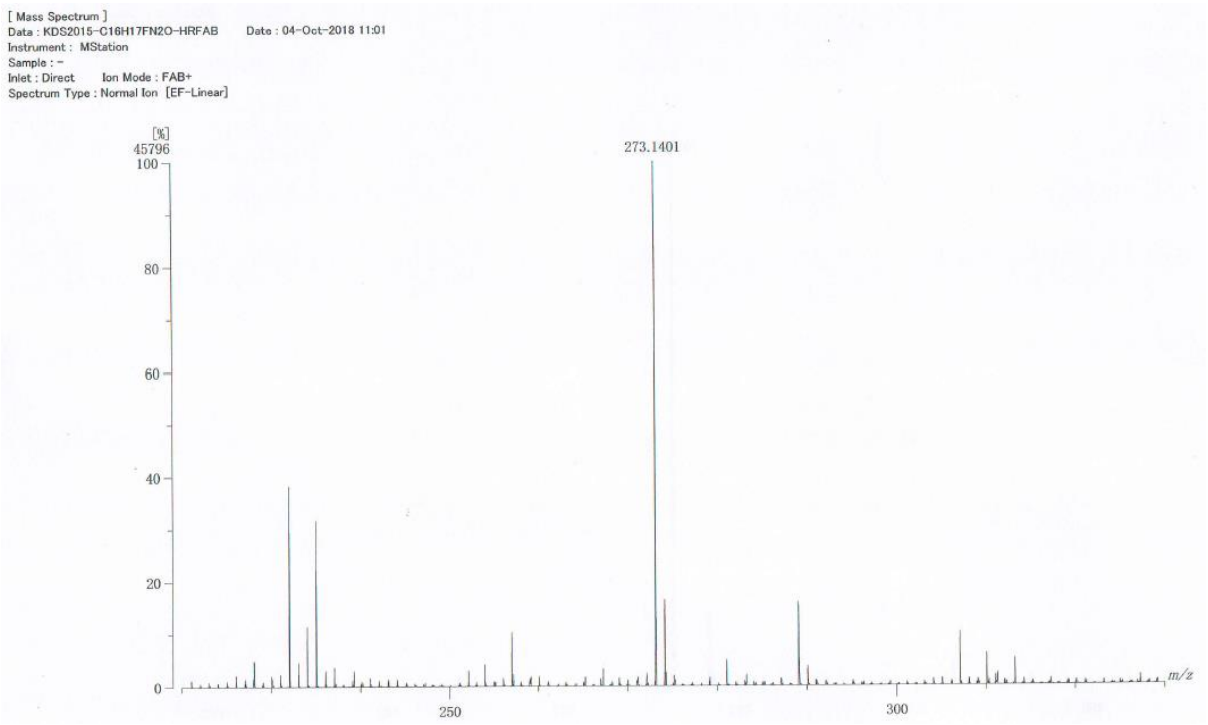

KDS2006

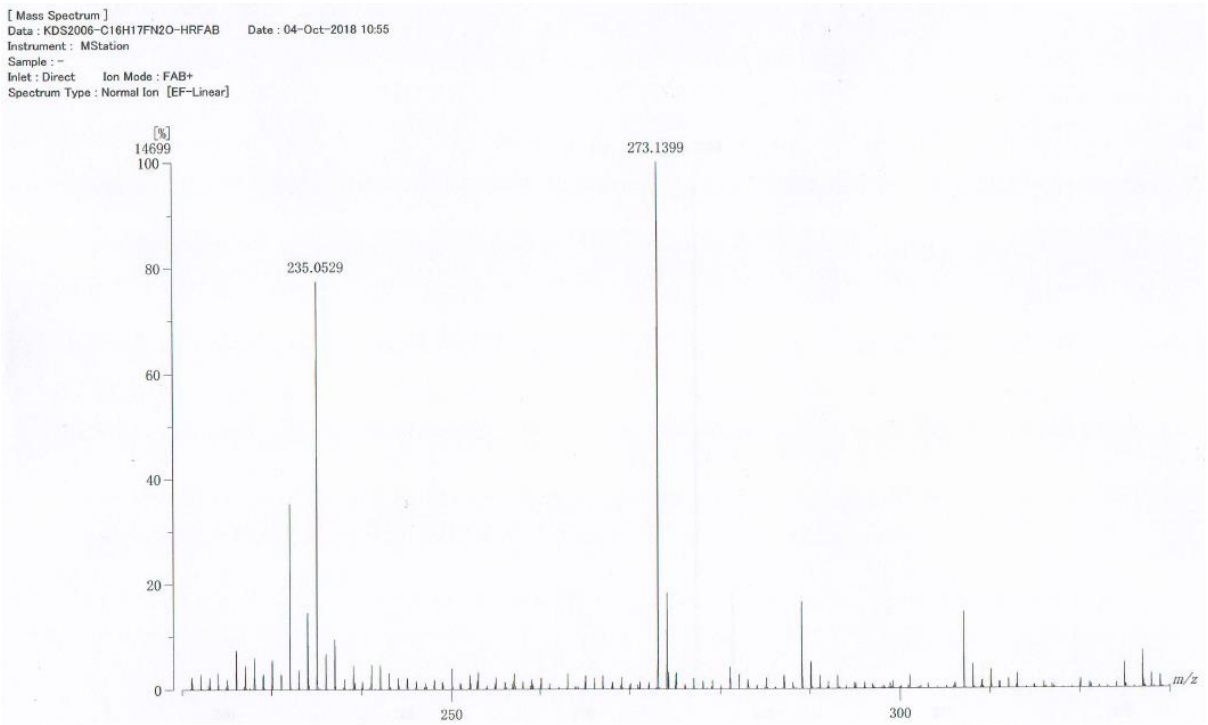

KDS2042

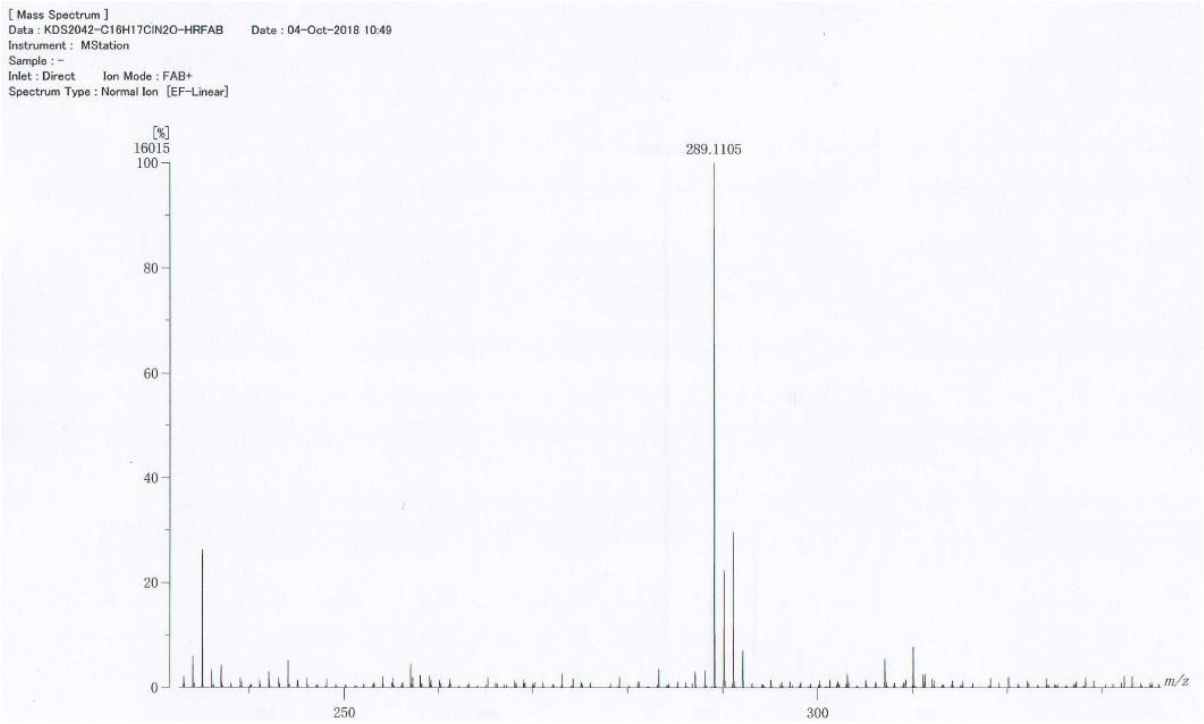

KDS0014

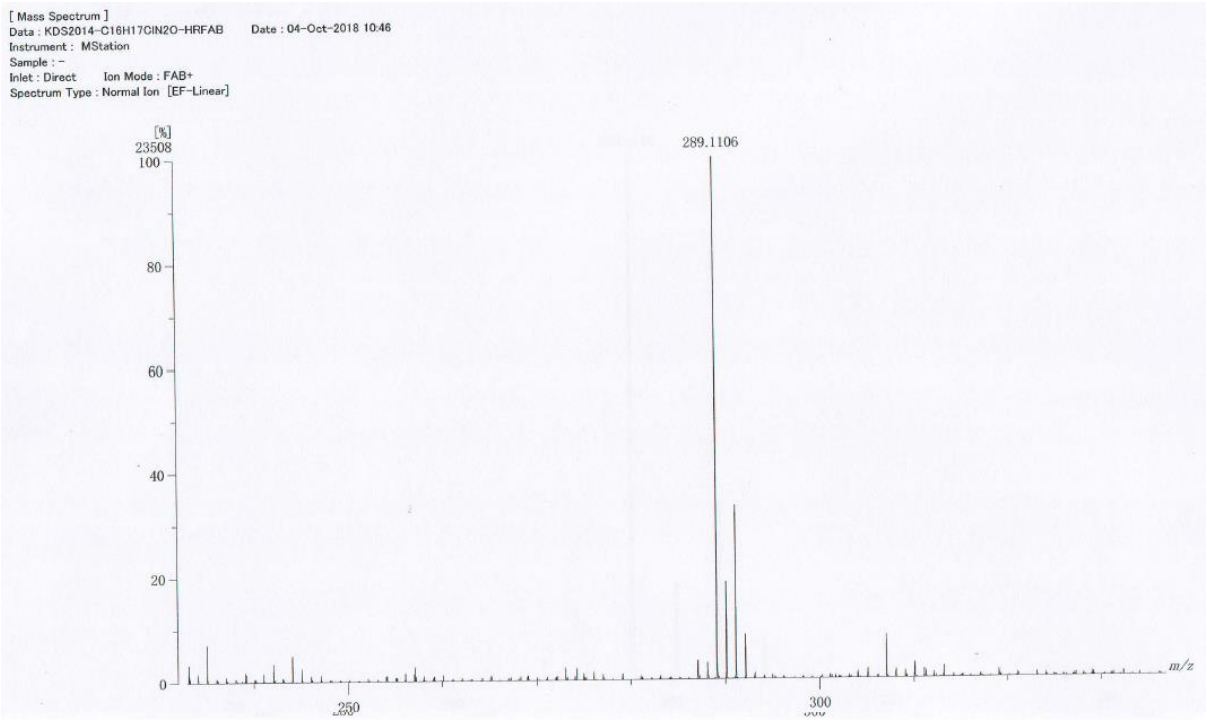

KDS2005

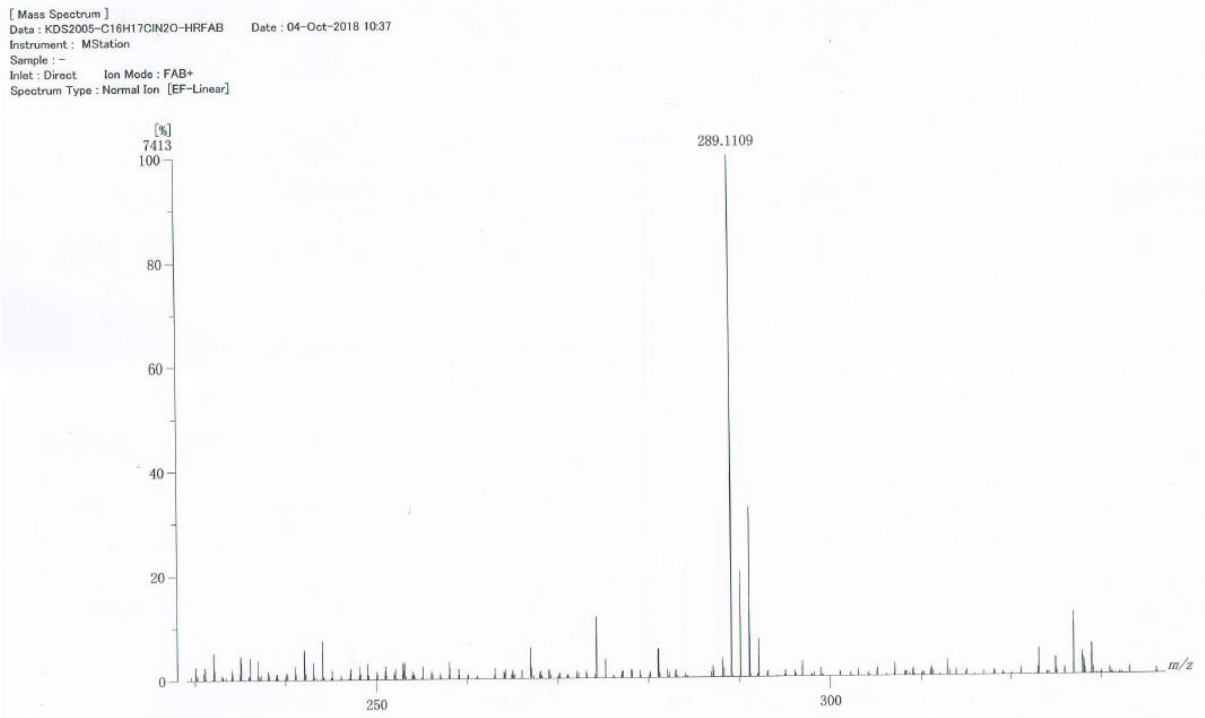

KDS2041

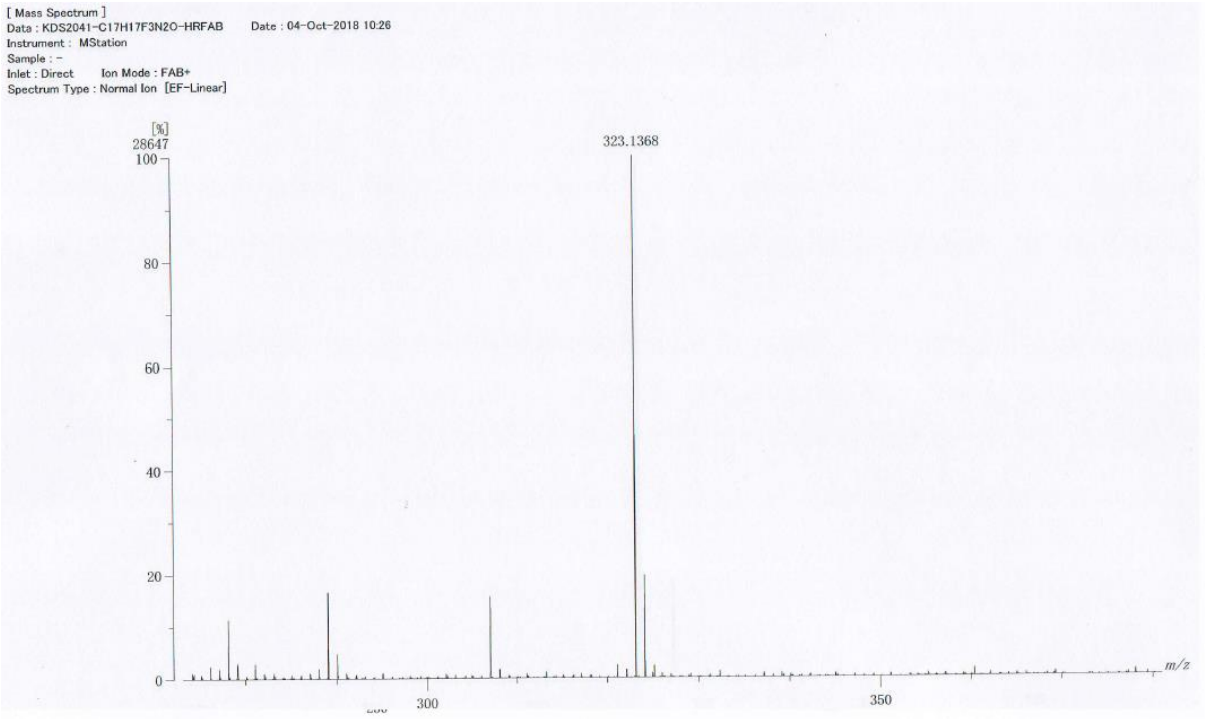

KDS0012

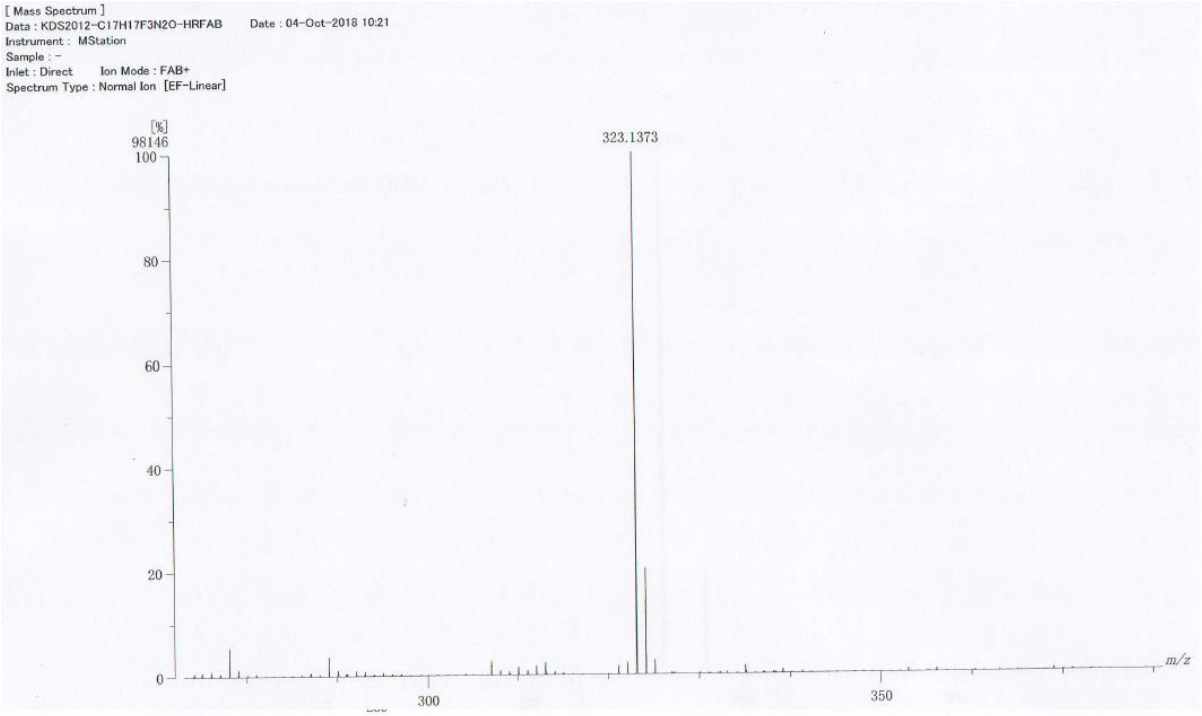

KDS2010

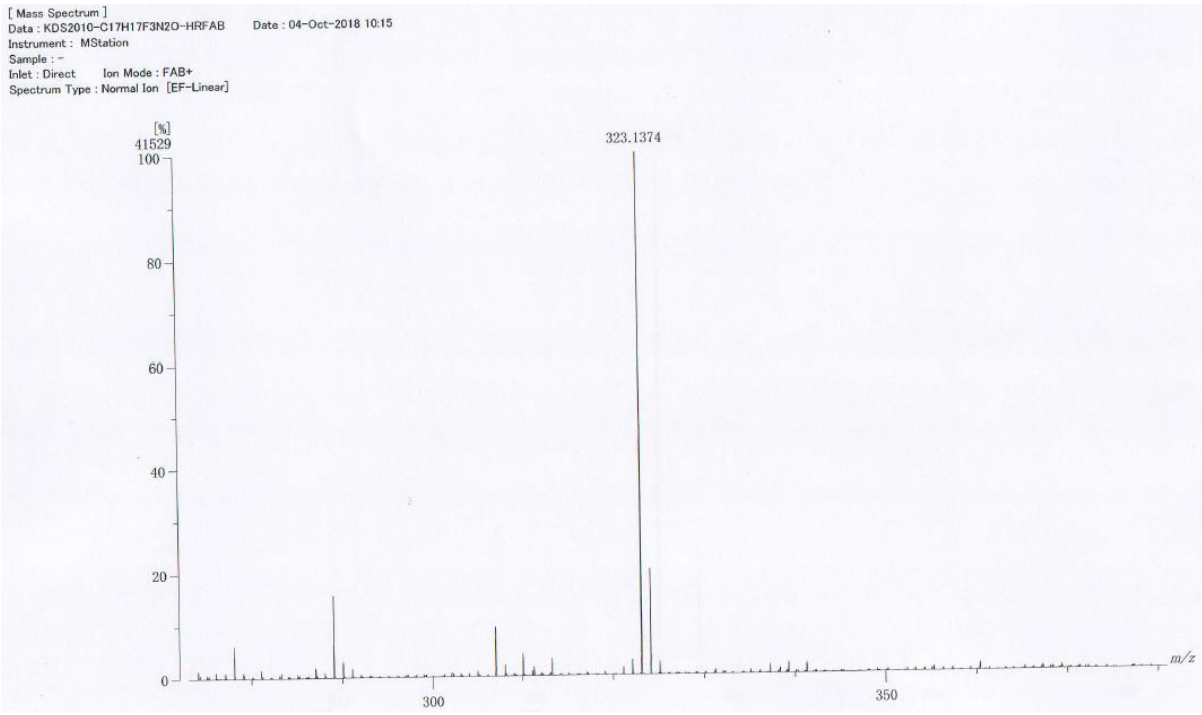

KDS2002

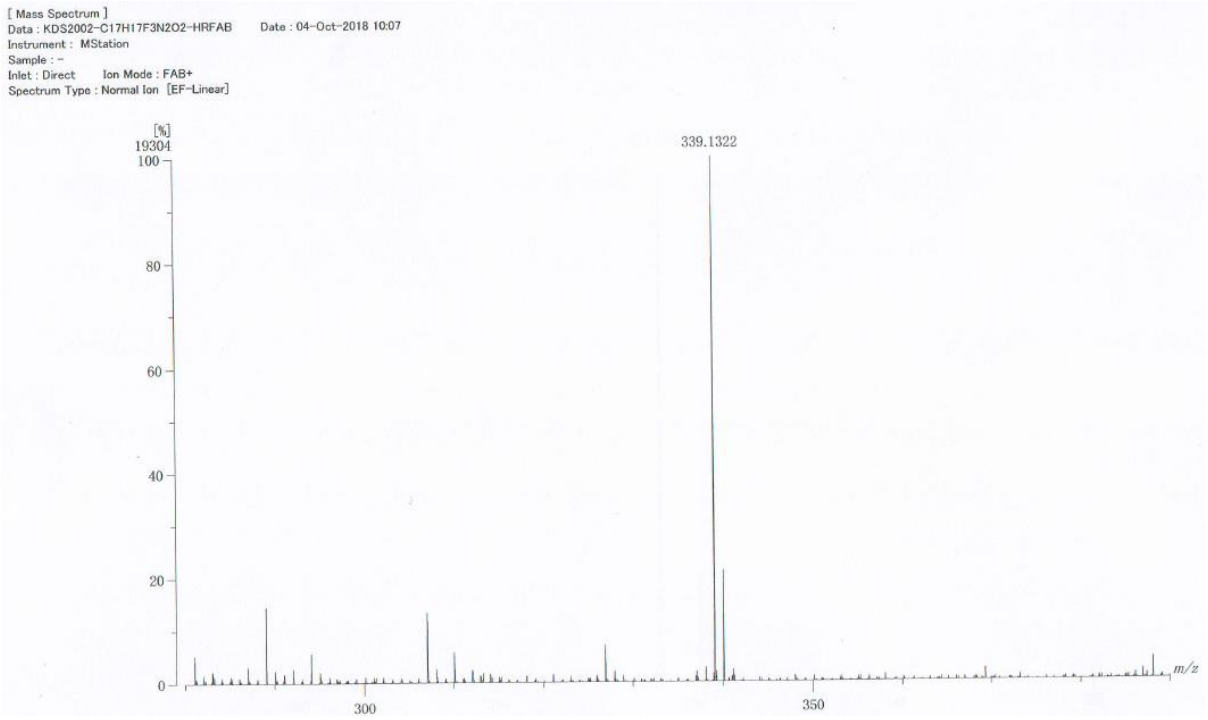

KDS2001

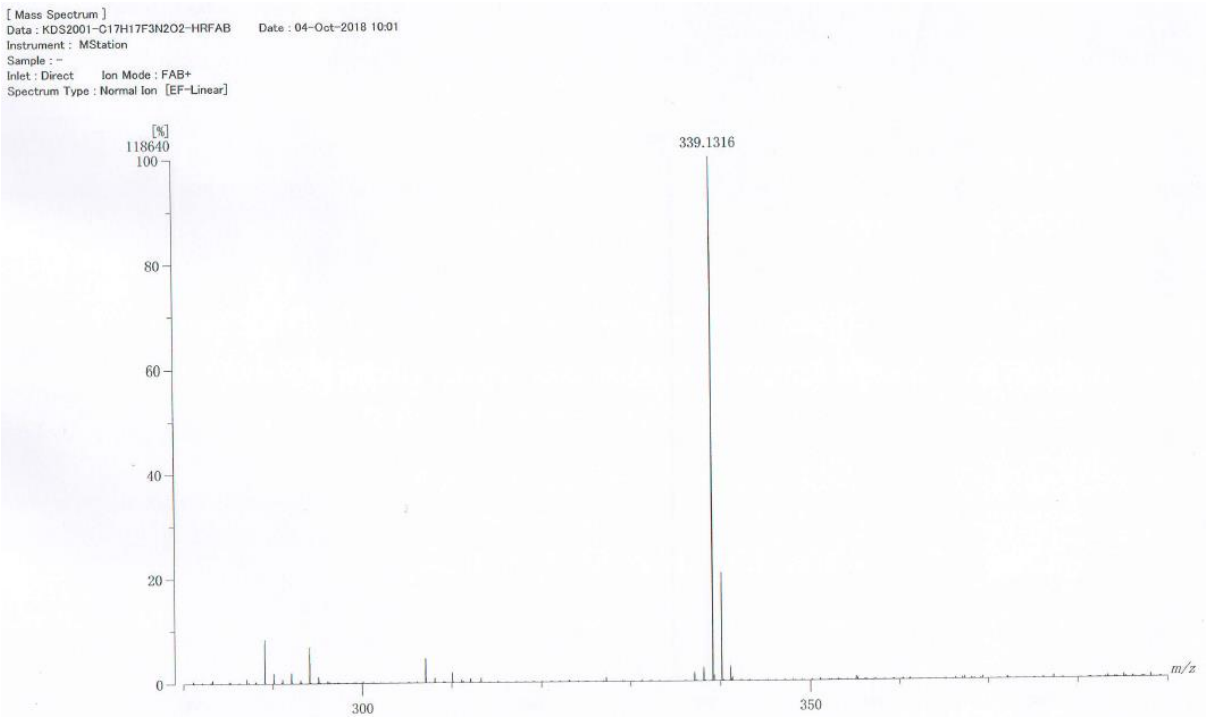

KDS2029

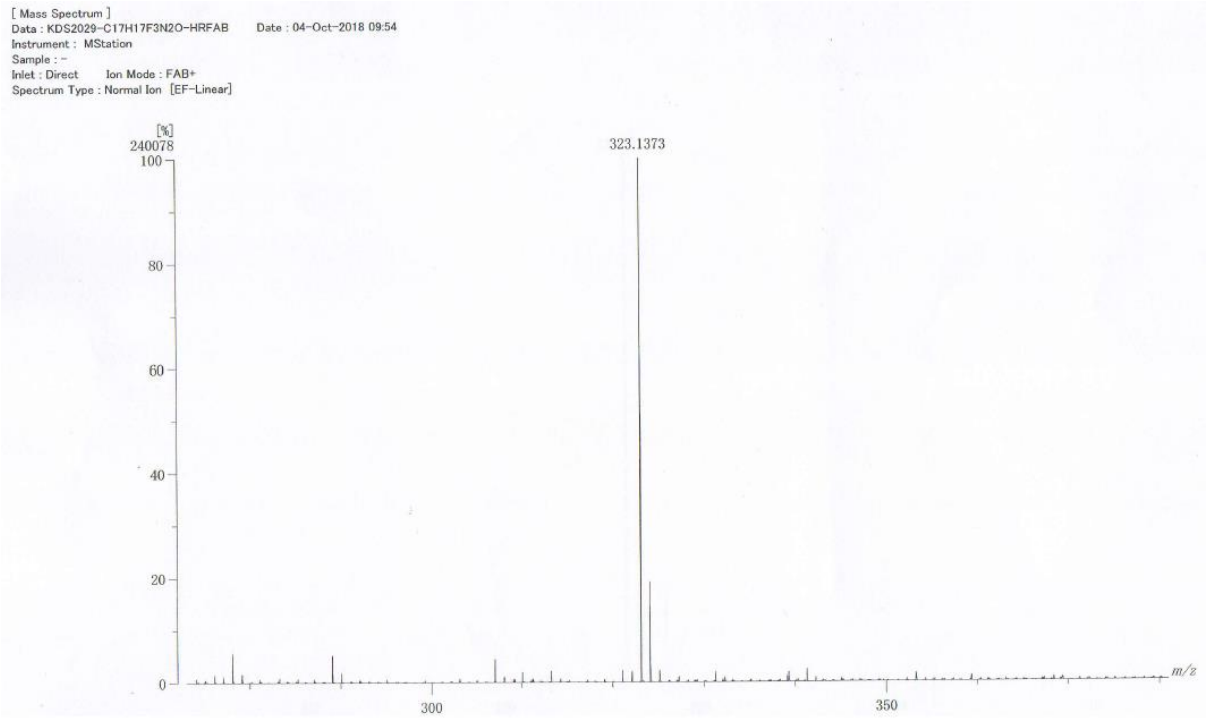
[Mass Spectrum]
Data : KDS2029-C17H17F3N2O-HRFAB
Date : 04-Oct-2018 09:54
Instrument : MStation
Sample : -
Inlet : Direct
Ion Mode : FAB+
Spectrum Type : Normal Ion [EF-Linear]
[%]
240078
323.1373
100
80
60
40
20
0
300
350
m/z